ΠΑΝΕΠΙΣΤΗΜΙΟ ΚΡΗΤΗΣ
ΣΧΟΛΗ ΕΠΙΣΤΗΜΩΝ ΥΓΕΙΑΣ
ΤΜΗΜΑ ΙΑΤΡΙΚΗΣ
ΤΟΜΕΑΣ ΒΑΣΙΚΩΝ ΕΠΙΣΤΗΜΩΝ
ΕΡΓΑΣΤΗΡΙΟ ΛΕΙΤΟΥΡΓΙΚΗΣ ΑΠΕΙΚΟΝΙΣΗΣ ΤΟΥ ΕΓΚΕΦΑΛΟΥ

Αναγνώριση και εκτέλεση κινήσεων σύλληψης τρισδιάστατων αντικειμένων με την άκρα χείρα παρουσία και απουσία οπτικής πληροφορίας. In vivo λειτουργική χαρτογράφηση των εμπλεκόμενων περιοχών του φλοιού εγκεφάλου πιθήκου με τη χρήση της ποσοτικής αυτοραδιογραφικής μεθόδου της 2-[^{14} C] δεοξυγλυκόζης.

Διδακτορική Διατριβή

Ευαγγελίου Ασημίνα

Επιβλέπουσα: καθ. Ε. Σαββάκη

Ηράκλειο, 2008

Στην οικογένειά μου

ΕΥΧΑΡΙΣΤΙΕΣ

Κατά το χρονικό διάστημα που εκπόνησα τη διδακτορική μου διατριβή ήρθα σε επαφή με ανθρώπους που είτε ως δάσκαλοι, είτε ως φίλοι, είτε κατέχοντες και τις δύο ιδιότητες φρόντισαν να με στηρίξουν. Σε όλους αυτούς τους ανθρώπους που για καλή μου τύχη ήταν πολλοί, χρωστώ ένα μεγάλο ευχαριστώ.

Ιδιαίτερα θα αναφερθώ στους ανθρώπους με τους οποίους ήρθα σε άμεση επαφή μέσω αυτού του διδακτορικού. Θα ήθελα να ευχαριστήσω πρώτα απ'όλα την επιβλέπουσά μου Ελένη Σαββάκη και το Ράο Βασίλη για την καθοδήγησή τους, την αμέριστη συμπαράσταση και τις εύστοχες παρατηρήσεις τους καθόλη τη διάρκεια αυτής της μελέτης. Επίσης θα ήθελα να ευχαριστήσω τον Αντώνη Μοσχοβάκη και το Γιάννη Δαλέζιο που σαν δάσκαλοι αλλά και σαν συνεργάτες ήταν πολύτιμοι καθώς και τα υπόλοιπα μέλη της επταμελούς εξεταστικής επιτροπής Κώστα Χριστάκο, Παναγιώτη Τραχανιά και Αντώνη Αργυρό για τον κόπο και την ευθύνη που ανέλαβαν.

Ευχαριστώ τους φίλους και συμφοιτητές μου Μπακόλα Σοφία, Ερημάκη Σοφία, Χατζηδημητράκη Κώστα, Κάτουλα Μάνο, Θεοχάρη Παρασκευά, Καρδαμάκη Ανδρέα, Ειρήνη Θεοδώρου, Στάμο Αλέξη και Κιλιντάρη Μαρίνα για την συμπαράστασή τους σε αυτή μου την προσπάθεια, για το ότι έκαναν ευχάριστες τις ώρες μου εντός και εκτός εργαστηρίου και γιατί και αυτοί με τη σειρά τους ήταν εκεί όποτε τους χρειαζόμουν.

Ευχαριστώ τις Μαρίες του εργαστηρίου μας, την Κεφαλογιάννη Μαρία και την Παγωμένου Μαρία για την άριστη τεχνική και γραμματειακή υποστήριξη αλλά και την ηθική συμπαράσταση που μου έδιναν σε όλο αυτό το χρονικό διάστημα.

Τέλος, θα ήθελα να ευχαριστήσω την οικογένειά μου, γιατί χωρίς αυτούς αυτό το όνειρο δεν θα γινόταν πραγματικότητα και τους φίλους μου που αν και δεν κινούμασταν στους ίδιους χώρους μοιραζόμασταν και θα μοιραζόμαστε καλές και δύσκολες στιγμές μαζί.

Πηγή χρηματοδότησης: ΓΓΕΤ- 01ED111

TABLE OF CONTENTS

LIST OF ABBREVIATIONS

2DG	2-deoxy-D-glucose	2-δεοξυ-D-γλυκόζη
^{14}C-DG	2-deoxy-D-[^{14}C]-deoxyglucose	2-δεοξυ-D-[^{14}C]-δεοξυγλυκόζη
3-D	three-dimensional	τρισδιάστατο
AIP	anterior intraparietal area	πρόσθια ενδοβρεγματική περιοχή
As	arcuate sulcus	τοξοειδής αύλακα
Cd	dark-control monkey	πίθηκος ελέγχου στο σκοτάδι
Cgs	cingulate sulcus	αύλακα του προσαγωγίου
CIP	caudal part of IPs	οπίσθιο τμήμα της ενδοβρεγματικής αύλακας
Cm	motion-control monkey	πίθηκος ελέγχου για τη βιολογική κίνηση
Cs	central sulcus	κεντρική αύλακα
D	dorsal	ραχιαίο
DG-6-P	2-deoxyglucose-6-phosphate	2-δεοξυγλυκόζη-6-φωσφορική
DP	dorsal prelunate area	ραχιαία προμηνοειδής περιοχή
ED	grasping-execution in dark monkey	πίθηκος που εκτελούσε κίνηση σύλληψης στο σκοτάδι
EL	grasping-execution in light monkey	πίθηκος που εκτελούσε κίνηση σύλληψης στο φώς
EMG	electromyography	ηλεκτρομυογραφία
FEF	frontal eye field	πρόσθια οφθαλμικά πεδία
G-6-P	glucose-6-phosphate	γλυκόζη-6-φωσφορική
IPs	intraparietal sulcus	ενδοβρεγματική αύλακα
L	lateral	πλάγιο
lc POs	lateral crown of POs	πλάγιο χείλος της βρεγματοϊνιακής αύλακας
LCGU	local cerebral glucose utilization	τοπική κατανάλωση γλυκόζης στο φλοιό
LIP	lateral intraparietal area	πλάγια ενδοβρεγματική περιοχή
LIPv	lateral intraparietal area, ventral	πλάγια ενδοβρεγματική περιοχή, κοιλιακή
Ls	lunate sulcus	μηνοειδής αύλακα
mc POs	medial crown of POs	έσω χείλος της βρεγματοϊνιακής αύλακας
MIP	medial intraparietal area	έσω ενδοβρεγματική περιοχή
MIPv	medial intraparietal area,ventral	έσω ενδοβρεγματική περιοχή, κοιλιακή
MST	medial superior temporal area	έσω άνω κροταφική περιοχή
O	grasping-observation monkey	πίθηκος που παρατηρούσε κίνηση σύλληψης
Opt	part of caudal inferior parietal convexity, caudal to PG	τμήμα της οπίσθιας κάτω βρεγματικής επιφάνειας, οπισθίως της PG
P	posterior	οπίσθιο
PE	subdivision of area 5 (in rostral SPL)	υποδιαίρεση της περιοχής 5 (πρόσθιο τμήμα του SPL)
PEa	cytoarchitectonic area of the medial bank of IPs	Κυτταροαρχιτεκτονική περιοχή της έσω όχθης της ενδοβρεγματικής αύλακας
PEc	subdivision of area 5 (in caudal SPL)	υποδιαίρεση της περιοχής 5 (πίσω τμήμα του SPL)
PG	subdivision of area 7 in inferior parietal lobe	υποδιαίρεση της περιοχής 7 στον κάτω βρεγματικό λοβό
PGm/7m	medial parietal area	έσω βρεγματική περιοχή
PIP	posterior intraparietal area	οπίσθια ενδοβρεγματική περιοχή
PO	parietoccipital area	βρεγματοϊνιακή περιοχή
POa	part of the lower bank of intraparietal sulcus	τμήμα της κάτω όχθης της ενδοβρεγματικής αύλακας

POm	medial parietoccipital sulcus	έσω βρεγματοϊνιακή αύλακα
POs	parietoccipital sulcus	βρεγματοϊνιακή αύλακα
RF’s	receptive fields	υποδεκτικά πεδία
RSC	retrosplenial cortex	οπισθοσπλήνιος φλοιός
SD	standard deviation	σχετική απόκλιση
SEF	supplementary eye fields	συμπληρωματικά οφθαλμικά πεδία
SII	secondary somatosensory cortex	δευτεροταγής σωματαισθητικός φλοιός
SMA	supplementary motor area	συμπληρωματική κινητική περιοχή
SPL	superior parietal lobe	άνω βρεγματικός λοβός
SSA	supplementary somatosensory area	συμπληρωματική σωματαισθητική περιοχή
TPO	temporal parietoccipital area	κροταφική βρεγματοϊνιακή περιοχή
Tpt	temporoparietal area	κροταφοβρεγματική περιοχή
TSA	transitional sensory area (upper bank of Cgs)	Μεταβατική αισθητική περιοχή (άνω όχθη της αύλακας του προσαγωγού)
V	ventral	κοιλιακό
V6	visual area 6	οπτική περιοχή 6
V6A	area V6A	περιοχή V6A
V6Ad	area V6A, dorsal	περιοχή V6A, ραχιαία
V6Av	area V6A, ventral	περιοχή V6A, κοιλιακή
VIP	ventral intraparietal area	κοιλιακή ενδοβρεγματική περιοχή
VP	ventral posterior area, visual cortex	κοιλιακή οπίσθια περιοχή, οπτικός φλοιός
A	anterior	πρόσθιο
M	medial	έσω
MT/V5	middle temporal/visual area 5	μέση κροταφική περιοχή/οπτική περιοχή 5

INTRODUCTION

In normal, everyday life conditions, humans and primates continuously interact manually with objects of interest. This interaction entails two partially distinct processes; the transport phase (reaching) in which the arm moves towards the object to be grasped and the grasping phase in which the hands' shape and orientation adapts to the form and orientation in space of the object to be grasped. Specifically, during that interaction there is a progressive opening of the hand with straightening of the fingers which is followed by a closure of the grip until it matches the size of the object and finally grasps it. Reaching requires spatial information about object location and involves proximal muscles of the arm, whereas grasping involves distal muscles and is based on information relative to the intrinsic attributes of the object. Grasping an object seems like a simple behavior which in most cases becomes rather "automatic" by experience, in the sense that we do not think about the way our hand would approach and grasp an object, where is this object located, which are the special characteristics of it, if there are enough visual cues to successfully guide us towards the object, what kind of configuration our hand must have in order to successfully grasp it etc.

When the object is visible, reaching-to-grasp behavior is accomplished by utilization of a) visual input, which provides information about the location of the target-object in the extrapersonal space and its relative distance from the agent's hand, and b) somatosensory (proprioceptive) input, that provides information about the current position of the moving hand. During reaching-to-grasp in darkness, there are different inputs useful to correctly guide the hand towards the target-object; a) somatosensory information about the current position of the hand, and b) sensory-motor memories of an internal representation of the object location and the motor act. The numerous parameters that have to be taken into account for the successful execution of this movement involve the activation of numerous brain areas contributing to the grasping behaviour.

When there is no previous experience of grasping certain objects, we normally resort to the following options; either we make the movement towards them and learn by trial and error or we learn by observing another person executing the same movement. According to the second option, the "previous experience" of observing that action helps us execute it more successfully, compared with executing that action without any relevant prior experience. It seems that the human motor system during observation of action in novel environments, incorporates the actions of others in building the motor repertoir of the individual (Mattar and Gribble, 2005).

Observation of an action is not only important for acquisition of motor skills but also for understanding the actions of others. According to the Mental Simulation Theory, our ability to explain and predict human behaviour and to attribute mental states to other agents, depends on our ability to simulate cognitive processes presumably taking place in somebody else's' brain. This would be demonstrated, according to this theory, by the finding that common cortical circuits are engaged during the execution of an intelligent behaviour and the comprehension of intelligently executed behaviour. There are already published data from our laboratory (Raos et al., 2004, 2007) and from other (Hari et al., 1998; Strafella and Paus, 2000; Grezes and Decety, 2001), showing common cortical areas subserving action observation and action execution.

In order to elucidate the cortical regions that are activated during grasping execution in the presence or absence of visual information, as well as the ones implicated in grasping observation, we employed the [^{14}C]-deoxyglucose quantitative autoradiographic method. This method gives us the ability to obtain robust quantitative data on brain activity based on glucose consumption (direct assessment), has the highest, up to date, known cortical resolution (20μm) and allows us to identify by means of cytoarchitectonic criteria the cortical areas activated in sections adjacent to the autoradiographic ones.

The cortical areas that have been examined in this study are areas lying at the anterior bank of parietoccipital sulcus and the adjacent cortex as well as areas at the medial cortical convexity. A brief summary about the location, connections and functional properties of the areas examined in this study, is described below.

Cortical areas in the anterior wall of the parietoccipital sulcus

Area PO was first described by Covey, as a region containing a complete representation of the contralateral visual field (Covey et al., 1982). It was reported that PO lacked the expanded representation of central vision (in contrast to most visual cortical areas) and received inputs from the parts of V1 and V2 of where the periphery was represented (Colby et al., 1983; Gattass et al., 1985).

Later Gattass and his colleagues, taking into account the discontinuities in the visual field representation and complex topography, advanced the hypothesis that what was first named as area PO might in fact contain more than a single visual area (Gattass et al., 1985).

In 1986 Zeki (Zeki et al., 1986), described a visual area in the anterior bank of the parieto-occipital sulcus, area V6, which probably corresponded to part of the previously described area PO. The borders of area V6 were defined by callosal connections.

Colby in 1988 redefined area PO using fluorescent tracers and injecting them into the so-far known area PO, which was first identified by single-neuron recordings. The "new PO" introduced by Colby, was a more restricted cortical region, roughly corresponding to the ventral part of what they had previously defined as area PO (Colby et al., 1988).

Area V6A was firstly distinguished from the "V6-complex" (or new PO) in 1996 by Galletti's group (Galletti et al., 1996). From 1996 and on areas V6 and V6A (dorsally to V6), are considered as separate areas.

Area V6

Location: Area V6 is a retinotopically organized visual area, located in the caudal aspect of the superior parietal lobule (SPL). It occupies a 'C'-shaped belt of cortex between the occipital and parietal lobes (and arranged in a roughly coronal plane). The upper branch of 'C' is located at the depth of POs and the lower one at the depth of POM with the mesial surface of the brain as a junction zone between the upper and the lower branch. V6 borders on area V3 posteriorly and area V6A anteriorly and dorsally.

Connections: Data collected from the use of retrograde fluorescent tracers and single-neuron recordings showed that area V6 receives retinotopically organized inputs from the striate cortex (V1) and several extrastriate areas (Colby et al., 1988;

Galletti et al., 2001). In specific, area V6 is connected reciprocally with areas V1, V2, V3, V3A, MT/V5, MST, MIP, VIP, LIP, (Colby et al., 1988; Galletti et al., 2001), V4T, $V6A_V$ (Galletti et al., 2001), FEF, MDP and PIP (Colby et al., 1988). Irrespective of whether the tracer (WGA-HRP) was injected into central or peripheral field representations in V6, the labeling was strong-to-moderate in areas V1,V2, V3, V3A, MT/V5, $V6A_V$, MIP and LIP_V, and weaker but consistent in areas V4T, MST and VIP. Very few labelled cells were found in V4 and DP (Galletti et al., 2001).

Another study by Shipp et al, has revealed that area V6, apart from being connected with areas V2, V3, V5 (MT),V6A, MST, LIP, VIP, MIP, 7m/PGm /MDP, as already reported, was also connected with areas 7a, PEc, PEci and area F7 of the dorsal premotor cortex (Shipp et al., 1998) .

In a previous study, Zeki reported that area V6 is connected with areas V5 (MT), V5A, V3A, and areas 6, 8 (FEF), 13 and 14 (Zeki et al., 1986).

Its subcortical connections include the pulvinar, caudate nucleus and pontine nuclei, superior colliculus (Shipp et al., 1998 ; Zeki et al., 1986) and claustrum (Shipp et al., 1998).

Visual topography: Area V6 contains a topographically organized representation of the entire contralateral hemifield up to an eccentricity of at least 80°. The lower visual field is represented in its upper branch (dorsally) and the upper visual field in its lower branch (ventrally). There is a prevailing representation of the lower visual field with respect to the upper one and the periphery is emphasized more with respect to the central visual field. The representation of the central visual field is not magnified with respect to the one of the periphery, in contrast to other visual areas. The central visual field representation (<20°) is located in the most lateral part of the posterior bank of POs. The vertical meridian is located at the border with area V6A (anteriorly) and the horizontal at the border with V3 (posteriorly) (Galletti et al., 1999a).

Electrophysiological data based on extracellular recordings and functional criteria, showed that all cells located in area V6 are visual in nature (Galletti et al., 1996; Galletti et al., 1999a). In V6, RFs ‘move’ coherently along the penetration, in a certain direction and with a physiological scatter. Their size increases with eccentricity (as in all other prestriate areas) and at any value of eccentricity RFs of V6 cells remain on average smaller than in V6A and larger than in V2 and V3. Also, RFs located in the upper visual field are on average fewer and larger than the ones in the lower visual field, at any value of eccentricity. The data mentioned above show higher representation of the lower visual field compared to the upper visual field.

Functional considerations: The nature of all V6 cells is visual. These visual neurons are sensitive to:

a) orientation

b) direction

c) the speed of movement of visual stimuli, and

d) sensitive to oculomotor activity (Galletti et al., 1999a).

In a previous study made by Galletti and his colleagues (Galletti et al., 1991), based on single cell recordings and with a total of 343 cells examined, it was found that 66% of V6 visual neurons were orientation-selective and 67% direction-selective. The mean range of orientation was ± 36.8º of the preferred orientation. Many of the cells tested were also influenced by oculomotor activity. In specific, 29 out of 156 neurons tested by saccades were affected by ocular movement. In 14/29 the initial burst of spikes preceded the onset of eye movement by periods of 0-150ms. 27 out of 29 cells also showed sensitivity to the direction of the saccadic movement with the majority of neurons preferring vertical downward directions and many others bottom contralateral directions. Although preferred directions turned out to be towards the hemifield mostly represented (lower), there was no fine correlation between the location of the center of the RF and the preferred direction of saccadic movement. Pursuit movements did not affect any of the neurons tested, whereas 102/174 neurons were affected by the direction of gaze, showing maximum discharge rate with gaze directions into the lower hemifield.

Area V6A

Location: Area V6A occupies a horseshoe-like region of cortex in the caudalmost part of the superior parietal lobule. It extends from the medial surface of the brain, through the anterior bank of the POs, up to the most lateral part of the fundus of POs. Its borders are on V6 ventrally, PEc dorsally, PGm/7m medially and MIP laterally (Galletti et al., 1999b).

Histological data based on labeling by use of neural tracers, revealed two different areas in V6A: the dorsal V6A (V6Ad), not receiving a direct input from area V6 and the ventral V6A (V6Av), receiving a direct input from V6 (Galletti et al., 2001).

Connections: Area V6A is connected with areas V3, V3A, V5/MT (regions of peripheral visual field representation), V6, MST (Shipp et al., 1998), MIP, VIP and LIP (Shipp et al., 1998; Caminiti et al., 1999; Marconi et al., 2001). The lack of

connectivity between V6A and visual area V2 can serve as a criterion in discriminating areas V6 and V6A, since V6 is strongly connected with V2. Also V6A connections with areas V3, V3A and V5 are less strong, compared to the ones of V6 with the earliest mentioned visual areas (Shipp et al., 1998). Parietal connections of V6A include AIP (Shipp et al., 1998), 7a (Shipp et al., 1998; Caminiti et al., 1999), PGm/7m, PEc (Shipp et al., 1998; Caminiti et al., 1999; Marconi et al., 2001), PE (Marconi et al., 2001), PEa (Caminiti et al., 1999; Marconi et al., 2001) and PEci (Shipp et al., 1998; Marconi et al., 2001). Also V6A is connected with area F2vr (Matelli et al., 1998; Shipp et al., 1998; Caminiti et al., 1999; Marconi et al., 2001) and F7 (Matelli et al., 1998; Shipp et al., 1998; Caminiti et al., 1999; Marconi et al., 2001; Tanne-Gariepy et al., 2002) of the dorsal premotor cortex. Light connections of V6A with areas F6 (Marconi et al., 2001) and F5 (Caminiti et al., 1999) have been observed.

Its subcortical connections include the pulvinar, caudate nucleus, superior colliculus, pontine nuclei (Shipp et al., 1998 ;Zeki et al., 1986) and claustrum (Shipp et al., 1998).

Visual Topography: While V6 is known to be a purely visual area which is retinotopically organized, V6A contains retino- and craniocentric visual neurons, together with neurons sensitive to gaze direction and/or saccadic eye movements, somatosensory stimulation and arm movements (Kutz et al., 2003).

Data from single cell recordings carried out on 1348 V6A neurons, revealed that 61% of neurons tested were visual and 39% non-visual in nature (Galletti et al., 1999b). These two types of neurons were not spatially segregated within area V6A. Visual neurons were sensitive to the orientation and direction of movement of visual stimuli, with the inferior (lower) contralateral quadrant most represented. Visual RFs were also found for inferior ipsilateral quadrant and upper visual field. The central visual field representation was located dorsally and the far periphery ventrally. The Rfs of the upper visual field were on average larger than those of the lower one. Furthermore large parts of the visual field were represented in small regions of V6A and the same regions of the visual field were re-represented many times in different parts of this area, without any apparent topographical order.

About 10% (28 of 290) of the visual neurons examined had RFs not organized in retinotopic coordinates. Their RFs remain anchored to the same spatial location, irrespective of eye movements, and change according to the changes of gaze direction. These so-called real-position cells were found only in area V6A, mainly in its ventral part.

As far as the visual topography in V6A is concerned, cells near one to another, could have RFs either in the same, or in completely different locations in the visual field. The existence of RFs jumping with unpredictable directions all over V6A means that in this area the visual field is not represented in an orderly way. In other words, the same part of the visual field is represented in many parts of the area. However, the central representation is predominantly represented dorsally whereas the far periphery is almost exclusively represented ventrally, near the border with area V6.

Functional considerations: Extracellular recordings in area V6A, showed that except from retino- and craniocentric visual neurons, there are also neurons sensitive to gaze direction and/or saccadic eye movements, somatosensory stimulation and arm movements (Galletti et al., 1991, , 1995; Galletti et al., 1997; Galletti et al., 1999b; Matelli and Luppino, 2001; Kutz et al., 2003).

In a recent study based on single-cell recordings in area V6A and in a total number of 597 neurons examined, 66 (11%) showed responses correlated with saccades, of which 26 responded also to visual stimulation and 31 did not (Kutz et al., 2003). Saccade neurons could respond before, during or after the saccade and they have been divided into two groups, one containing cells responding earlier than the earliest visual activity and one responding later on. Early-responding cells were active before and/or during the saccade (58%) and late-responding cells were active after the saccade. The responses to saccadic eye movements were directionally sensitive and varied with the amplitude of the saccade. Most of the preferred directions were towards the contralateral lower field or the ipsilateral upper field. Responses of late-responding cells disappeared in complete darkness and therefore could be attributed to visual responses due to retinal stimulation during saccades.

In another study on V6A neurons, it was suggested that there are 3 types of neurons in V6A (Nakamura et al., 1999) :

i) visual,

ii) eye-position and

iii) arm movement or position related neurons.

In eye-related neurons (48% of total examined), each cell had a preferred eye position field and 66% of them were significantly influenced by the direction of the saccade that preceded fixation. All responses were postsaccadic.

Area V6A also contains cells sensitive to somatosensory stimulation (Galletti et al., 1997; Breveglieri et al., 2002; Galletti and Fattori, 2003). The somatic representation of these cells is restricted to the upper limbs. Many of the

somatosensory cells are sensitive to the passive rotation of the joints of the upper contralateral limb (Galletti and Fattori, 2003). Arm and tactile-related neurons have also been reported in another study (Nakamura et al., 1999). The somatosensory receptive fields of the V6A cells (tactile) are located in the upper limbs (mostly on the contralateral side) and in regions of the body close to the arm (Galletti and Fattori, 2003). Tactile RFs are quite small, covering only restricted parts of the limb or body, being more frequent on proximal parts of the arm.

These neurons could provide information about position of arm or hand in space with respect to the trunk. This could be useful in recognizing the interaction between moving arm and peripersonal space, hence in confirming the actual location and status of the arm. Tactile RFs on the hand could provide information about the interaction between the hand and grasped object during grasping (Galletti and Fattori, 2003).

Many cells in V6A are modulated during arm movements aiming to reaching objects in the peripersonal space (Galletti et al., 1997; Nakamura et al., 1999; Galletti et al., 2001; Matelli and Luppino, 2001; Galletti and Fattori, 2003).

Forelimb related neurons in V6A:

i) are modulated during reaching towards visual targets and targets located outside the field of view and

ii) are able to encode the direction of arm movement .

Some of them:

i) show different rates of discharge according to the arm position in space

ii) do not discharge during the transport phase of reaching but only during grasping (Galletti and Fattori, 2003).

Arm-related neurons were located, according to Nakamura, more anteriorly with respect to the eye-related neurons (modulated by position or movement of the eyes) (Nakamura et al., 1999). This observation suggested that there may be a separate arm area, located at the anterior part of area V6A.

Arm-reaching neurons in V6A fire during active arm movements aiming to reach objects in the peripersonal space. Kinematically the same, but non-goal directed, movements, were unable to activate these cells. However, some V6A neurons that were not active during reaching under visual control became active when the animal's hand searched for pieces of food in the working space, outside its field of view (under somatosensory control) (Galletti and Fattori, 2003).

Moreover, about 50% of the neurons modulated by reaching in light continue to be modulated when the same movement is carried out in darkness (Galletti et al., 2001). This observation shows that arm reaching neurons in V6A receive

somatosensory in addition to the visual information. Many reaching cells in V6A were activated during the transport phase of reaching towards the object to be grasped. Some of these cells stopped firing or their discharge was strongly reduced when the animal touched the target. Another group of V6A arm-related neurons were not active during the transport phase of reaching, but discharged as soon as the animal's fingers touched a piece of food, continued to discharge during grasping and suddenly ceased firing, as soon as the hand with the grasped food returned back to the mouth.

The preliminary finding that both reaching and grasping modulate neuronal activity in V6A, was recently verified with extracellular recordings in monkeys who were either reaching to a point or grasping an object in darkness or they were reaching for food in a lit environment (Fattori et al., 2004). Results from the former experiment have shown that 45 out of 95 and 52 out of 84 neurons tested were modulated during reaching and grasping respectively. Results from the latter experiment showed that natural prehension movements modulate 30 out of 58 neurons tested, and in 8 of them only the last phase of prehension (grasping) was able to trigger neuronal response.

In a recent study, based on extracellular recordings in monkeys executing outward and inward reaching movements in darkness, it was revealed that reach-related activity modulated (excited or inhibited) V6A neurons either during inward or outward movements or even during the phase in which the monkey had to hold its hand on the selected target (Fattori et al., 2005). Each single V6A neuron exhibited a preference for movement direction and location of the arm in space but at a population level there was no such preference. The activity of some of the arm-reaching related neurons was additionally modulated by somatosensory inputs; by passive joint rotations, or skin light tactile stimulations, or deep pressure of subcutaneous tissues.

Lesions in area V6A resulted in deficits in reaching, wrist orientation and grasping (Battaglini et al., 2002; Battaglini et al., 2003). In specific, monkeys held their contralesional arm close to their bodies in an abnormal posture, were reluctant to use it, exhibited longer movement times during reaching, under- or overestimated the target position and rotated their hand abnormally during grasping; opening the grip laterally rather than downwards, resulting in difficulty in grasping and longer movement times. Those deficits have been also observed after posterior parietal lesions in monkeys (Faugier-Grimaud et al., 1978).

Clinical studies in human subjects tend to link V6A lesions with optic ataxia. Optic ataxia is characterized by impairment in reaching for and grasping visual objects with both hands in the contralesional visual field. Such impairment is not

described when subjects are allowed to orient their eyes and head towards the target of the reaching movement while reaching for it.

A relevant recent typical clinical study, dealing with 16 unilateral stroke patients exhibiting optic ataxia compared to 36 stroke patients without that disorder and by the use of MRI, revealed that the lesion responsible for optic ataxia included the lateral cortical convexity at the occipito-parietal junction, the junction between occipital cortex and SPL and the medial cortical aspect where it affected the precuneus close to the occipito-parietal junction, an area corresponding to monkey area V6A (Karnath and Perenin, 2005).

Taking into account the results shown above concerning neuronal properties, V6A contains:

i) visual cells
ii) real-position cells
iii) somatosensory cells
iv) arm-reaching /grasping related cells and
v) eye-related cells (oculomotor), that could be involved in the control of both reaching and grasping.

AREA PGm

Location: Area PGm (Pandya and Seltzer, 1982), or 7m (Cavada and Goldman-Rakic, 1989a), is part of the superior parietal lobule (SPL), located at the medial surface of the hemisphere. It corresponds to Von Bonin and Bailey's medial area PE (Von Bonin and Bailey, 1947).

Connections: Area PGm is connected with the dorsal premotor cortex, both its rostral (Petrides and Pandya, 1984; Cavada and Goldman-Rakic, 1989b; Johnson et al., 1993; Matelli et al., 1998; Caminiti et al., 1999; Leichnetz, 2001; Marconi et al., 2001; Tanne-Gariepy et al., 2002; Parvizi et al., 2006) and caudal parts (Caminiti et al., 1999; Tanne-Gariepy et al., 2002) (areas F7 and F2 respectively). PGm projections comprise the main parietal input into area F7 (Petrides and Pandya, 1984; Cavada and Goldman-Rakic, 1989b, , 1991; Johnson et al., 1993; Johnson et al., 1996; Matelli et al., 1998; Caminiti et al., 1999; Leichnetz, 2001; Marconi et al., 2001; Tanne-Gariepy et al., 2002; Parvizi et al., 2006) .There are also connections of

PGm with multiple frontal, association, somatosensory, visual, parietal, limbic and thalamic areas. These connections include: SMA (at the head and forelimb regions/representations) (Petrides and Pandya, 1984; Cavada and Goldman-Rakic, 1989b, , 1991), SEF (Cavada and Goldman-Rakic, 1989b, , 1991; Leichnetz, 2001), FEF (Cavada and Goldman-Rakic, 1989b, , 1991; Leichnetz, 2001) , dorsal bank of principal sulcus (Cavada and Goldman-Rakic, 1989b, 1991; Leichnetz, 2001) , anterior bank of inferior arcuate sulcus, area 45 (Cavada and Goldman-Rakic, 1989b, , 1991), shoulder above the superior ramus of arcuate sulcus (Leichnetz, 2001), area 46 (Parvizi et al., 2006), dorsal sector of posterior cingulate cortex and anterior cingulate cortex (Cavada and Goldman-Rakic, 1991), areas 23a/b, 23c (Leichnetz, 2001; Parvizi et al., 2006), 24c (Petrides and Pandya, 1984; Parvizi et al., 2006), posterior ventral bank of cingulate sulcus (Cavada and Goldman-Rakic, 1989a), area 31 (Parvizi et al., 2006) and area 8 (Petrides and Pandya, 1984; Parvizi et al., 2006). Area PGm is also connected with SII (Cavada and Goldman-Rakic, 1991), SSA (PEci) (Cavada and Goldman-Rakic, 1989b, 1991; Parvizi et al., 2006), V2 (Cavada and Goldman-Rakic, 1989a, 1991; Tanne-Gariepy et al., 2002), visual motion complex in the dorsal bank of STS (MST) (Cavada and Goldman-Rakic, 1989a, , 1991; Leichnetz, 2001; Tanne-Gariepy et al., 2002), posteriormost TPO (Parvizi et al., 2006), area 5 (Cavada and Goldman-Rakic, 1989a, , 1991; Leichnetz, 2001), MIP (Leichnetz, 2001), PG, PE (Parvizi et al., 2006), PEc (Marconi et al., 2001), V6A (Caminiti et al., 1999; Marconi et al., 2001), PO (Colby et al., 1988; Cavada and Goldman-Rakic, 1989a, 1991; Johnson et al., 1996; Leichnetz, 2001; Tanne-Gariepy et al., 2002; Parvizi et al., 2006), LIP (Tanne-Gariepy et al., 2002) , VIP (Leichnetz, 2001), area 7a (Leichnetz, 2001; Tanne-Gariepy et al., 2002), area 7ip, Opt (Leichnetz, 2001), granular retrosplenial cortex (Cavada and Goldman-Rakic, 1989a, 1991). Other connections include insular cortex (Cavada and Goldman-Rakic, 1991), basal forebrain (Parvizi et al., 2006), pulvinar (Leichnetz, 2001; Parvizi et al., 2006), presubiculum (Cavada and Goldman-Rakic, 1989a, 1991; Parvizi et al., 2006), parahippocampal cortex (Cavada and Goldman-Rakic, 1991), caudate nucleus (Cavada and Goldman-Rakic, 1991; Leichnetz, 2001; Parvizi et al., 2006), superior colliculus (Leichnetz, 2001), putamen (Cavada and Goldman-Rakic, 1991; Leichnetz, 2001; Parvizi et al., 2006), claustrum (Leichnetz, 2001; Parvizi et al., 2006), basis pontis (Parvizi et al., 2006) and zona incerta (Leichnetz, 2001; Parvizi et al., 2006).

Functional considerations: Little is known about the functional properties of PGm. However, connections of PGm with area 6; especially area F7 with which they seem to share common functional properties (Johnson et al., 1996; Wise et al., 1997;

Matelli et al., 1998; Matelli and Luppino, 2001; Parvizi et al., 2006), and with cingulate regions concerned with hand movements, has lead scientists to seek for reaching-related activity in this area.

Extracellular recordings applied in this area to elucidate if there is a relationship between neuronal activity in PGm and reaching, and the use of oculomotor, reaching and fixation tasks (for dissociating hand- from eye-related contributions) have revealed diverse types of reaching related cells (Ferraina et al., 1997b). These cells showed reaching-related activity (concerning hand movement and hand position). Activity in many of them was modulated by eye-position signals, and signals related to hand motor control, since their directional tuning was coherent in both oculomotor and reaching tasks.

In a neurophysiological study designed to elucidate the relative contribution of sensory, eye- and arm-related motor signals on PGm activity, preparatory, movement-related and postural activity for the control of reaching movements was found, activity which was strongly modulated by vision (Ferraina et al., 1997a). In particular, they found populations of neurons that displayed preparatory activity related with the direction of the oncoming movement, activity which was strongly modulated by the presence or absence of visual feedback from the hand, both during static posture and movement. Also the gaze-related activity of many neurons was combined with either visual or kinaesthetic signals about hand position in space. It is worthnoting that the activity of these cells was not modulated by pure visual stimuli.

In a recent electrophysiological study, examining the way PGm neurons relate to spatial parameters of smooth pursuit and/or saccades as well as to eye position, cells in PGm were found to be able to process both; smooth pursuit and saccadic eye movements, with eye position signal having a strong influence on both (Raffi et al., 2007) . The activity of smooth-pursuit neurons was modulated during or after the eye movement whereas saccade-related activity was mainly post-saccadic. Based on their results they concluded that PGm neurons which carry post-saccadic-eye-position tuned signals and possibly eye displacement information, may contribute to the transformation of coordinate frames for voluntary movements.

Area 31

***Location*:** Area 31 is located at the medial surface, between the posterior cingulate area 23c and medial parietal area PGm / 7m.

***Connections*:** Area 31 is connected with multiple cortical areas, including areas 6, 8, 9, 10, (Morecraft et al., 2004; Parvizi et al., 2006), 46 (Vogt and Pandya, 1987; Morecraft et al., 2004; Parvizi et al., 2006), areas 11, 12 and 13 of the orbital surface, medial portions of areas 1, 2, 3, area 4, pre-SMA and supplementary motor cortex (Morecraft et al., 2004), areas 29 (Vogt and Pandya, 1987; Kobayashi and Amaral, 2003; Morecraft et al., 2004; Parvizi et al., 2006; Kobayashi and Amaral, 2007) and 30 of the retrosplenial cortex (Kobayashi and Amaral, 2003; Morecraft et al., 2004; Parvizi et al., 2006; Kobayashi and Amaral, 2007), cingulate areas 23a, 23b, 23c (Vogt and Pandya, 1987; Morecraft et al., 2004; Parvizi et al., 2006), 24a, 24b, 24c (Morecraft et al., 2004; Parvizi et al., 2006), 24d, SSA, TSA (Morecraft et al., 2004) and area 32 (Parvizi et al., 2006). Area 31 is also connected with area PGm (Vogt and Pandya, 1987; Morecraft et al., 2004; Parvizi et al., 2006), PO, PG (Morecraft et al., 2004; Parvizi et al., 2006), PE (Parvizi et al., 2006), PEa (AIP, MIP, PIP), PEc (Morecraft et al., 2004), Opt (Vogt and Pandya, 1987; Morecraft et al., 2004), TPO (Vogt and Pandya, 1987; Morecraft et al., 2004; Parvizi et al., 2006), MST, Tpt ,rostral V3, Sylvian fissure, area 35, areas TH, TL, TF of the parahippocampal gyrus (Morecraft et al., 2004), the entorhinal cortex, thalamus, claustrum, basal forebrain, caudate/putamen, basis pontis and zona incerta (Parvizi et al., 2006). Intrinsic connections have also been observed (Morecraft et al., 2004).

Functional considerations: There are few studies in monkeys and humans dealing with the functional properties of this area.

A recent study based on recordings in monkeys, has revealed neuronal properties of area 31(Dean et al., 2004) . In this study, animals had either to fixate and make an immediate saccade towards a visual target, or to fixate and after an unpredictable delay period make a saccade towards a visual target. By comparing the results of the two tasks they concluded that: a) neurons in this area were activated both after the onset of small contralateral targets and after the onset of saccades to those targets, b) there was spatial selectivity for contralateral targets, present almost throughout the delay period, c) the overall neuronal responsiveness decreased during the delay period when both fixation and saccade targets were illuminated, irrespective of movement direction and amplitude and d) stronger

neuronal activity after target onset predicted more accurate saccades on delay-saccade trials. Given that overall responsiveness increased around the time of reward delivery, it was suggested that neuronal activity in this area may encode the motivational salience of visual and oculomotor events for orienting attention.

In an electrophysiological study, in which monkeys were trained to perform standard saccade tasks and smooth pursuit eye movements, it was found that neurons in posterior cingulate cortex and therefore in area 31, monitor eye movements and eye position, perhaps in service of the spatial analysis of visual input rather than the production of eye movements (Olson et al., 1996). The main findings of this study were the following: a) the neuronal discharge occurred almost exclusively during and after the eye movement, b) eye-movement-related activity was only partially dependent on visual feedback, since there were neurons whose activity persisted in total darkness, c) the neuronal direction selectivity was very broad, d) neuronal firing was dependent on the saccade amplitude and persisted but became attenuated postsaccadically, e) the postsaccadic level of activity was significantly dependent on orbital angle and saccade direction and f) the level of neuronal firing in some cases was modulated during smooth pursuit movements and varied as a function of both eye position and velocity.

Human studies based on fMRI methods revealed that area 31 among others could be involved in memory (Maddock et al., 2001) or self-evaluation processes (Johnson et al., 2002).

Maddock and his coworkers, used the BOLD fMRI method to investigate which areas participate in successful retrieval of autobiographical memories elicited by name-cued recall of family-members and friends (Maddock et al., 2001). Unfamiliar names which did not elicit any successful memory retrieval were used as control. Among other areas found to be activated by memory retrieval, the most strongly activated region which was significantly activated in all 8 subjects tested, was predominantly the caudal part of the left posterior cingulate cortex, part of which is area 31. These findings have led to the hypothesis that the posterior cingulate cortex (and area 31) plays an imporant role in successful memory retrieval.

In another BOLD fMRI study, investigating the neural correlates of self-reflection, subjects were asked to answer with a simple yes or no to questions about themselves concerning stable traits, attitudes and abilities (Johnson et al., 2002). The results showed that area 31 among others is involved in self-evaluation.

There are also other studies that correlate hypometabolism in area 31 with Alzheimer's disease (Minoshima et al., 1997, Choo et al., 2007).

Retrosplenial cortex (areas 29 and 30)

***Location*:** The retrosplenial cortex, which is comprised of areas 29 and 30, is located in the callosal sulcus.

According to cytoarchitectonic criteria, area 29 is subdivided into area 29 a-c with a granular layer directly adjacent to layer I and area 29d with differentiation of layers III and IV. Area 30 is characterized by a dysgranular layer IV. Based on their cytoarchitecture areas 29a-c and 29d constitute the granular retrosplenial cortex (RSC) and area 30 is the so called dysgranular or agranular subdivision of RSC (Vogt et al., 1987; Morris et al., 1999).

***Connections*:** The retrosplenial cortex is connected with several areas, including areas of the frontal, occipital, cingulate and parietal cortices as well as with subcortical areas.

In a recent study, where the cortical afferents of retrosplenial cortex and area 23 were investigated, it was demonstrated that the major inputs into the retrosplenial cortex derive from area 46, the hippocampal formation and the parahippocampal cortex (Kobayashi and Amaral, 2003). Additional inputs originate from areas 9, 10, 8, 11, 13 and 14, area V2, cingulate areas 23, 24, 31, the dorsal bank of STS (mainly area TPO), parietal areas 7a, PGm, LIP, DP and the entorhinal cortex, perirhinal cortex and subiculum. Intrinsic connections have also been reported.

Another study from the same group, focused on the cortical efferent projections of the macaque monkey retrosplenial and posterior cingulate cortices, by using ^{3}H-aminoacids as anterograde tracers (Kobayashi and Amaral, 2003). This study showed that the major projections of the retrosplenial cortex included areas 46, 9, 10, 11, the entorhinal and parahippocampal cortices as well as the hippocampal formation. Additional projections were found in areas 13, 12, 8, premotor area 6, area 23, area TPO of the superior parietal sulcus, parietal areas 7a, PGm, area V4 and association area caudal to 23v.

In another study, which focused on the connections of the posteromedial cortex in macaque monkeys, it was reported that the retrosplenial cortex projects to areas 23a/b and 31, periaquaductal gray matter, basis pontis, caudate, putamen and accumbens, receives input from areas 23a/b, 8, 11, 13, 25, basal forebrain, claustrum and amygdala, and is reciprocally connected with areas 9, 46, 24a/b,

superior temporal sulcus (area TPO), area PG, entorhinal cortex and thalamus (Parvizi et al., 2006) .

Connections of the retrosplenial cortex with prefrontal areas 9 and 10 have also been described in a previous study (Goldman-Rakic et al., 1984).

Studies that focused at the distinct connections of areas 29 and 30, revealed that area 30 is connected with area 46, 23, TPO (Vogt and Pandya, 1987; Morris et al., 1999), areas 9, 9/46,19, 29, 31, 8B, PGm, POa (Morris et al., 1999), Opt (Vogt and Pandya, 1987), areas TH, TF (Vogt and Pandya, 1987; Morris et al., 1999) and TL of the parahippocampal cortex (Vogt and Pandya, 1987), entorhinal cortex (Morris et al., 1999) and thalamus (Vogt et al., 1987; Morris et al., 1999). Area 29 is connected with areas 46 and 23, TPO, subiculum and with nuclei associated with limbic cortex, including anteroventral (AV), anterodorsal (AD) and laterodorsal (LD) nuclei (Vogt et al., 1987).

***Functional considerations*:** Very little is known about the function of this area in macaque monkeys. Its location has made it difficult to examine functional properties by means of neurophysiology.

Therefore, autoradiographic and imaging methods of the functional properties of RSC in animals and in humans are only available.

In a study, in which a delayed-response task was employed, the [^{14}C]-deoxyglucose (2DG) method was used, and revealed that the RSC of the monkey performing a visual tracking task with a delay (delayed-response task) consumed more [^{14}C]-deoxyglucose compared with the control monkeys who either sat quietly in a primate chair or were anesthetized (Matsunami et al., 1989). It was suggested that the RSC is involved in short-term memory functions, due to its connections with anterior thalamic nucleus, one of the main nuclei of the Papez circuit. Because of its connections with the visual association cortex or motor-related areas, such as anterior cingulate, SMA and premotor cortex, they suggested that activity in the RSC could be related to either “visual” or “motor” memory. Another suggestion based on their results was that elevated [^{14}C]-deoxyglucose consumption in the RSC could be due to “motor learning” processes. However, the lack of significant differences between the task-performing and the control monkeys indicates that the difference in 2-DG uptake reflected differences in the general arousal state of the monkeys.

Human studies based on imaging methods revealed that the retrosplenial cortex is implicated mostly in memory or topographic orientation processes.

In a case report, left retrosplenial hemorrhage resulted in topographic disorientation, i.e. the subject could not use directional information about familiar

places, encoded by past navigation, and he could not learn new directions to places beyond the range of visual surveillance (Ino et al., 2007). After recovery, an fMRI study on mental navigation demonstarted prominent activation in the retrosplenial area along the right POs and the circumference of the injured area on the left side. It was suggested that functional disturbance of bilateral retrosplenial area was related to the directional disorientation, and the recovery of this area improved directional orientation. In accordance with this perspective about the function of RSC was also a previous study (Takahashi et al., 1997).

In another fMRI study, based on navigation in a virtual-reality environment after acquisition of mental representation of the environment (cognitive map formation), it was revealed that the retrosplenial and hippocampal regions play a complementary role, both during formation of a cognitive map and during retrieval of information from it (Iaria et al., 2007). The RSC may mediate the transformation from one frame of reference (ground-level) to another (mental representation) regardless the direction of transformation.

In a recent fMRI study, employed to reveal the neural correlates of the use of visual information to ascertain the observer's location and to orient him in the world (spatial navigation), subjects made familiarity, location and direction judgments on photographs of real-world environments (Epstein et al., 2007). This study indicated that RSC is involved in retrieval of stored spatial representations by using the immediate scene as a cue, for situating oneself within a larger environment.

Finally, in another study, Bar and his coworkers used the fMRI method to examine the cortical events occurring during the analysis of visual context, by comparing the brain activity during perception of visual objects associated with a certain context, with activity during perception of objects not associated with any specific context (Bar and Aminoff, 2003). The activity in the RSC and the hippocampal cortex was significantly stronger for viewing objects with contextual information. They suggested that the parahippocampal and the RSC comprise a cortical "context network" that processes contextual associations during object recognition, and that the representation of contextual associations is not confined to spatial, place-related contexts.

PIP

***Location*:** Posterior intraparietal area (PIP, lies at the posterior end of intraparietal sulcus (IPs) where it joins the parietooccipital sulcus (POs). It is adjacent to area PO (Colby et al., 1988).

***Connections*:** Area PIP is connected with area PO (Colby et al., 1988), areas V3 (dorsal part) and VP (ventral posterior area) (Felleman et al., 1997), area V4 and especially its peripheral visual field representation (Ungerleider et al., 2008) and areas VIP lateral, LIPv, MSTdp and MT (Lewis and Van Essen, 2000).

***Visual Topography-Function*:** A study by Felleman et al, showed that the central visual field is represented ventroposteriorly and the periphery dorsoanteriorly (Felleman et al., 1997). The upper visual field is represented along the V3A-PIP border and the lower visual field in its medial part.

The functional properties of area PIP were recently investigated in fMRI experiments conducted both in humans and in monkeys.

A recent fMRI study (with MION contrast agent) performed in monkeys, investigated whether area PIP was sensitive to motion (Vanduffel et al., 2001). The task used the presentation of random dot and random line stimuli which were either coherently moving or stationary in front of monkeys that were fixating straight ahead. Area PIP, among others, was identified as motion sensitive to random moving lines.

A BOLD fMRI study, which was carried out in order to reveal the active brain areas during visually guided saccades in monkeys, showed that area PIP was activated by saccades (Baker et al., 2006). The cortical area which was mostly activated was located at the junction of the intraparietal and lunate sulci and represented either area PIP or the dorsal prelunate area DP.

Saito et al, conducted a human fMRI study to investigate the neural basis of tactile-visual cross-modal matching (Saito et al., 2003). The study employed four different tasks; a tactile-tactile (TT) matching task with no visual input, a tactile-tactile with visual input (TTv), a visual-visual matching task with tactile input (VVt) and a tactile-visual matching task (TV). Results indicate that area PIP, close to POs, is bilaterally activated more prominently during the TV task than either the TTv or VVt tasks and that the increase in PIP MR signal during the TV task was larger than the sum of those during each intra-modal matching task. Accordingly, it was suggested that area PIP may be involved in the integration of shape information from tactile-visual matching.

In a recent fMRI study, performed in behaving monkeys, it was examined whether the parietal cortex was involved in processing of stereoscopic (structural and/or positional) and 3D-shape-related information (Durand et al., 2007). It was found that area PIP along with CIP and MIP was sensitive to both structural and positional stereoscopic information, used in grasping and reaching respectively, whereas areas AIP and anterior LIP were more specifically engaged in extracting the 3D shape of objects.

METHODS

Subjects

Experiments were performed on ten adult female monkeys (*Macaca mulatta)*, weighing between 3.5 and 5 kg. The animals were purpose-bred by authorized suppliers (Deutches Primatenzentrum, Goettingen, Germany; R. Hartelust, Nederlands). All housing, experimental and surgical procedures were approved by the Greek Veterinary Authorities and the F.O.R.T.H animal use comittee, in accordance with European Council Directive 86/609/ECC. Monkeys had free access to food (Mucedola, Milan, Italy), while access to water was controlled and animals received adittional necessary fluids during daily experimental sessions, except for weekends during which access to water was free. Monitoring of the weight and well-being of the animals was regular and, if necessary, supplementary water was provided.

Animal preparation

The monkeys were accommodated in their cages (Crist Instrument Co, Hagerstown, MD, USA), immediately after their arrival, and were allowed to get used to their new environment for a month before any operation began. During this period, they had free access to food and water, were presented with toys and music for stimulation and were carefully monitored on a daily basis for normal behaviour and eating habits.

A month later, animals were prepared for behavioural training, by implanting a metal bolt for head immobilization. The metal bolt (Crist Instrument Co, Hagerstown, MD, USA), embedded in dental cement (Resivy, Vence, France), was surgically implanted on each monkeys' head with the use of mandibular plates (Synthes, Bettlach, Switzerland) which were secured on the bone by titanium screws (Synthes, Bettlach, Switzerland). All surgical procedures were performed under aseptic conditions and anesthesia (ketamine hydrochloride, Imalgene 1000, Merial, France, 20mg/kg, i.m and sodium pentobarbital 25mg/kg, i.m), with the aid of a stereo microscope. Systemic antibiotics (Rocephin, Roche, Switzerland, 60-70 mg/kg/day i.m) and analgesics (Apotel, Uni-Pharma, Hellas) were administered pre- and post-operatively. The animals were allowed to recover from surgery for at least three weeks before beginning of training sessions.

Experimental set-up

The behavioural apparatus contained a PC-controlled rotating turntable, into which six 3-D geometrical solids were accommodated. It was placed in front of the monkeys, at shoulder height, at a distance depending on whether the experimenter or the monkey performed the grasping movements; 50cm or 20cm respectively. Monkeys sat in a primate chair (Crist Instrument Co, Hagerstown, MD, USA), with their head fixed, hindlimbs immobilized and one or both forelimbs restrained depending on the special features of the task. The 3-D objects accommodated into the turntable were two plates, one horizontally and the other vertically oriented (25mm wide, 35mm deep and 3mm thick), a ring (15mm in diameter), a sphere (10mm in diameter), a cube (side of 10mm) and a cylinder (5mm diameter and 40mm length). The above objects were grasped in the following ways: the plates with the primitive precision grip (use of thumb and the radial surface of the second and third phalanxes of the index finger), the ring with the digging out grip (index finger inserted into a ring), the cube and the sphere with the side grip (thumb and the radial surface of the last phalanx of the index finger) and the cylinder with the finger prehension (use of the first three fingers). A sliding window located at the front of the behavioural apparatus allowed access to only one object at a time. Eye movements were recorded with an infrared oculometer (Dr. Bouis). EMG (gainx2000, band-pass filter 0.3-3000KHz) recordings were performed by using Ag-AgCl surface electrodes. The digitized electromyograms (1000Hz) were recorded from the biceps and wrist extensor muscles and were aligned at the end of the movement, rectified and averaged over 150 movements in each case. Monkeys were trained over a period of time ranging from 4-11 months (depending on the requirements of each task), on a daily basis for at least an hour, until they reached success rates of ~90%. During the ^{14}C-DG experiments, monkeys performed the tasks they were trained for and received water as reward through a water delivery tube attached close to their mouth.

Tasks

Execution in light (EL)

Two monkeys were trained to execute a grasping movement using their left forelimb and under visual guidance (Figure **1a**). Both monkeys had their right forelimbs as well as their hindlimbs restrained with Velcro® tapes during the task. These monkeys were required to fixate the illuminated odject behind the opened window (opening of the window in that task resulted in the illumination of the compartment, thus making the object visible) for 0.7-1sec, until dimming of the light which acted as a go-signal for the grasping movement. The grasping movement included reaching, grasping and pulling the ring with the left forelimb within 1sec, although the movement was usually completed within 500-600 msec. The monkeys had to maintain fixation (within the 8º diameter circular window) until the end of the movement. They were allowed to move their eyes outside the circular window only during the intertrial intervals ranging between 2 and 2.5 sec. The monkeys received water as reward after every successful trial.

Observation of grasping (O)

Three monkeys were first trained to perform grasping movements in the same conditions as in the EL task, and then to observe the same grasping movements executed by the experimenter. The reach-to-grasp training sessions took place months before the ^{14}C-DG experiment. In order to eliminate any possible side-to-side effects due to prior grasping training, the first monkey was trained to grasp with its left hand, the second with its right and the third one with both hands consecutively. During the observation of grasping task (O), the forelimbs of the monkeys were restricted both during the O sessions as well as during the ^{14}C-DG experiment. The O task was designed as follows: the behavioural apparatus was placed at 50cm distance in front of the monkey, at shoulder height. The experimenter was always performing the grasping behaviour by using her right hand, standing on the right side of the monkey, with only the reaching and grasping components of the movement visible to the monkey. All task conditions, object and movement parameters were similar to the ones described for the EL task, so that the mean movement rates were comparable.

Motion Control (Cm)

The motion control monkey was required to observe all components of the O task with the exception of the hand-object interaction that occurs while grasping an object. In specific, the monkey was trained to watch the opening of the window of the behavioural apparatus, the presentation of the object, the closure of the window and the experimenter's reaching movement towards the closed window with hand/fingers extended, for a total period of 2.7-3sec per trial. A schematic overview of the task is illustrated in Figure **1b**. Both hands of the monkey were restricted during this task. Furthermore, the monkey had to maintain fixation (within the 8º diameter circular window) throughout each trial and was allowed to move its eyes freely (outside the circular window) only during the intertrial intervals, which ranged between 2 and 2.5 sec. This monkey was used to control the effects imposed by the biological motion of the reaching arm and the visual stimulation by the 3-D object, in order to reveal the net effects of the goal-directed reaching-to-grasp components.

Execution in dark (ED)

Two monkeys were trained to execute grasping movements in the dark with their left forelimb, while the right forelimb and the hindlimbs were restrained and their heads fixed. The behavioural apparatus and the task parameters were almost identical with the execution in light task, to achieve the same number of movements during the experimental period (Figure **1c**).The illumination of the compartment which made the object visible and served as go-signal for the initiation of the grasping movement, was substituted by two auditory cues that signaled the onset of the trial and the go-signal for the initiation of the grasping movement. In each trial the sliding window opened and the low frequency auditory cue signaled the fixation period in which the monkeys were required to keep their gaze straight ahead. The high frequency cue signaled the onset of the grasping movement during which the monkeys were required to reach, grasp and pull a ring (3-D object) while they maintained their gaze straight ahead. The task took place in complete darkness and the monkeys were rewarded with water after every successful trial.

Dark control (Cd)

Two monkeys served as control animals for the ED task. The first was presented with auditory stimuli, similar to the ones used in the ED task, which were used as the go-signals for fixation (low frequency) and onset of the grasping movement (high frequency). This monkey was allowed to move its eyes freely throughout the experiment and received water as reward. Water was delivered randomly to prevent association of the auditory cues with reward expectancy. The second control monkey was exposed to the same conditions, was also able to move its eyes freely, but did not receive reward. Both tasks were held in complete darkness and animals were alert for the whole duration of the ^{14}C-DG experiment (45min).

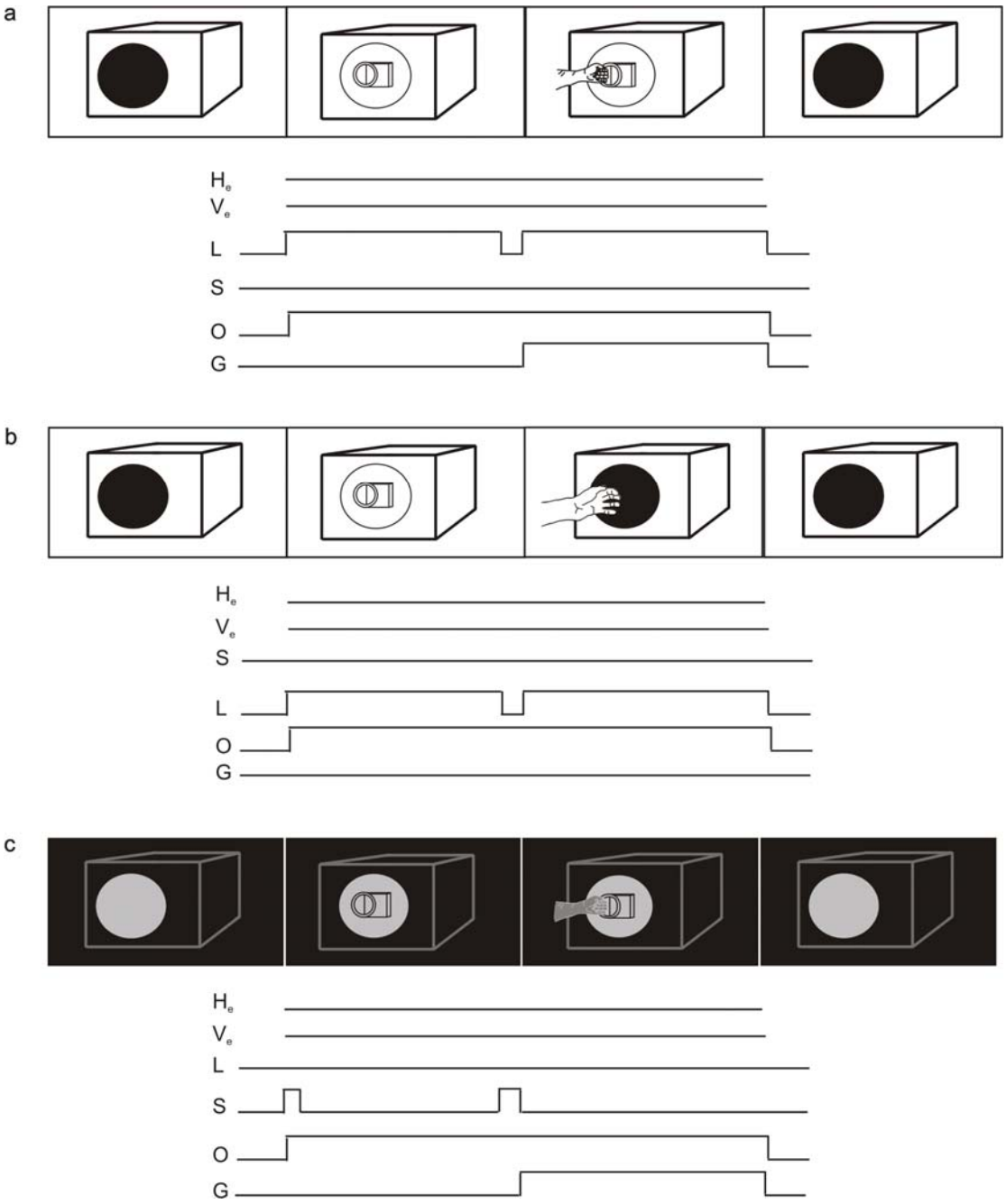

Figure 1: *Schematics of behavioural paradigms and task events during the* ***(a)*** *grasping-execution in light (EL) task,* ***(b)*** *Motion-control (Cm) task and* ***(c)*** *grasping-execution in dark (ED) task.* H_e *and* V_e *represent the horizontal and vertical eye position, respectively. L represents the illumination of the compartment of the behavioural apparatus that made the object visible. S represents the auditory cues that signaled either the onset of the trial or the go-signal for the initiation of grasping during the ED task, O stands for observation and G for execution of grasping.*

The [^{14}C]- Deoxyglucose ([^{14}C-DG]) Method

The [^{14}C]-deoxyglucose autoradiographic method was applied to measure the metabolic activity simultaneously in all components of the central nervous system. This method was designed by Sokoloff et al (Sokoloff et al., 1977) and uses radioactive deoxyglucose (Figure **2a**) an analog of glucose (Figure **2b**) in order to trace glucose consumption and therefore local functional activity, since glucose is the main source of energy for brain cells.

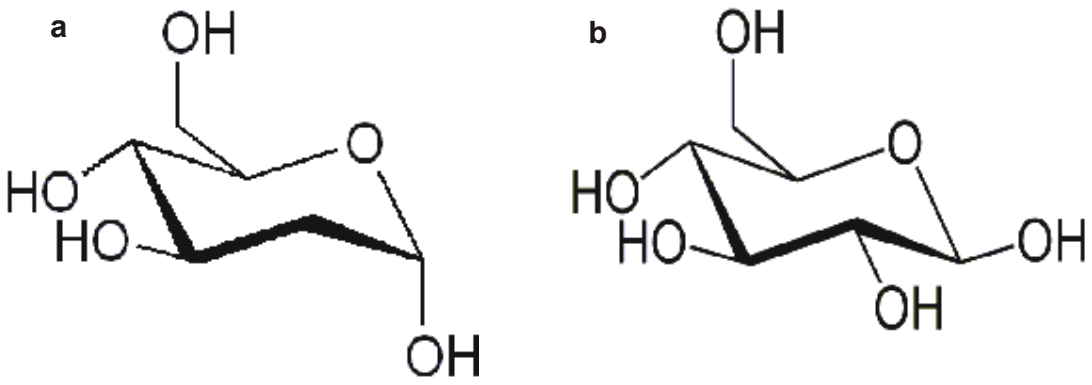

Figure 2: *Chemical structure of 2-deoxy-D-[^{14}C] glucose (**a**) and glucose (**b**).*

Theoretical basis of the method

This method is based on the notion that functionally active cells use glucose as their basic source of energy in normal conditions; therefore, metabolically active cells would utilize glucose for energy production.

The use of radiolabelled substrates for energy metabolism is crucial in order to have pictorial representations of functionally active brain structures, by means of autoradiography. In Sokoloff's method, 2-deoxy-D-[^{14}C] glucose acts as a tracer of metabolic activity simultaneously in all components of the brain. The method is designed in such a way that the radioactivity concentration is proportional to the rate of glucose consumption.

The 2-deoxy-D-[^{14}C] glucose (2DG) was selected for this method because its biochemical properties make it the most appropriate substrate for tracing glucose metabolism and measuring local cerebral glucose utilization by autoradiography.

2DG is bidirectionally transported between blood and brain and shares with glucose the same carrier that transports them through the blood-brain barrier. Therefore they compete for blood-brain transportation. Then, both 2DG and glucose undergo phosphorylation by hexokinase and are transformed into 2-deoxyglucose-6-phosphate (DG-6-P) and glucose-6-phosphate (G-6-P), respectively. Glucose-6-phosphate is further metabolized to fructose-6-phosphate and eventually to CO_2 and water. Unlike glucose-6-P, 2-deoxyglucose-6-phosphate cannot be converted to fructose-6-phosphate and consequently does not follow the glycolytic pathway. This is due to the structural difference between 2DG and glucose. 2DG (Figure **2a**) differs from glucose (Figure **2b**) in a substitution of OH^- by hydrogen. Deoxyglucose-6-phosphate can be converted into deoxyglucose-1-phosphate, then into UDP-deoxyglucose and eventually into glycogen, glycolipids and glycoproteins. However, only a very small fraction proceeds to these products in mammalian tissues (Nelson et al., 1984). In any case these compounds are secondary, stable products of DG-6-P and altogether represent the products of deoxyglucose phosphorylation. Therefore, deoxyglucose-6-phosphate remains trapped in the cerebral tissue, at least for the duration of the experimental period. Radiolabelled substrates other than 2DG, which could be used for measuring energy metabolism, are oxygen and glucose, which display stoichiometric utilization related to oxygen consumption. However, oxygen and its metabolic products are volatile with short physical half-life and the metabolic products of glucose are lost rapidly from brain tissues. Therefore, in contrast with the 2DG, radioactive oxygen or glucose cannot be used for measuring local cerebral glucose utilization by autoradiography.

When the duration of the experimental period is kept short enough (less than an hour), the quantity of [^{14}C]DG-6-P accumulated in any cerebral tissue at any given time following the introduction of 2DG into the circulation, equals the integral of the rate of 2DG phosphorylation by hexokinase in that tissue during that interval of time. This integral is related to the amount of glucose that has been phosphorylated over the same interval, depending on the time courses of the relative concentrations of 2DG and glucose in the precursor pools and the Michaelis-Menten kinetic constants for hexokinase with respect to both glucose and 2DG. When cerebral glucose is in a steady state, then the amount of phosphorylated glucose during the interval of time equals the steady state flux of glucose through the hexokinase-catalyzed step times the duration of the interval, and the net rate of flux of glucose through this step equals the rate of glucose utilization. All the aforementioned relationships can be thoroughly combined into the model depicted in Figure **3**.

This model can be mathematically analyzed to derive an operational equation (Figure **4**), provided that: a) glucose metabolism is in a steady state throughout the experimental period, i.e. constant plasma glucose concentration and constant rate of glucose consumption, b) the concentrations of both glucose and 2DG are homogeneous in the compartments and c) 2DG concentrations are low compared to their glucose counterparts i.e. tracer kinetics apply. The operational equation defines R_i, the rate of glucose utilization/unit mass of tissue, i. Inspite of its complex appearance, this equation is a general statement of the standard relationship by which rates of enzyme-catalyzed reactions are determined from measurements made with radioactive tracers. The numerator of the equation represents the amount of radioactive product formed in a given time interval; it is equal to C_i^*, the combined concentrations of 2DG and [^{14}C]DG-6-P in the tissue at time T, measured by the quantitative autoradiographic technique, less a term that represents the free unmetabolized 2DG still remaining in the tissue. The denominator represents the integrated specific activity (i.e. ratio of labeled to total molecules) of the precursor pool times a factor, the lumped constant, which is equivalent to a correction factor for an isotope effect (i.e. kinetic differences between the labeled and natural compound). The term with the exponential factor in the denominator, takes into account the lag in the equilibration of the tissue precursor pool with the plasma.

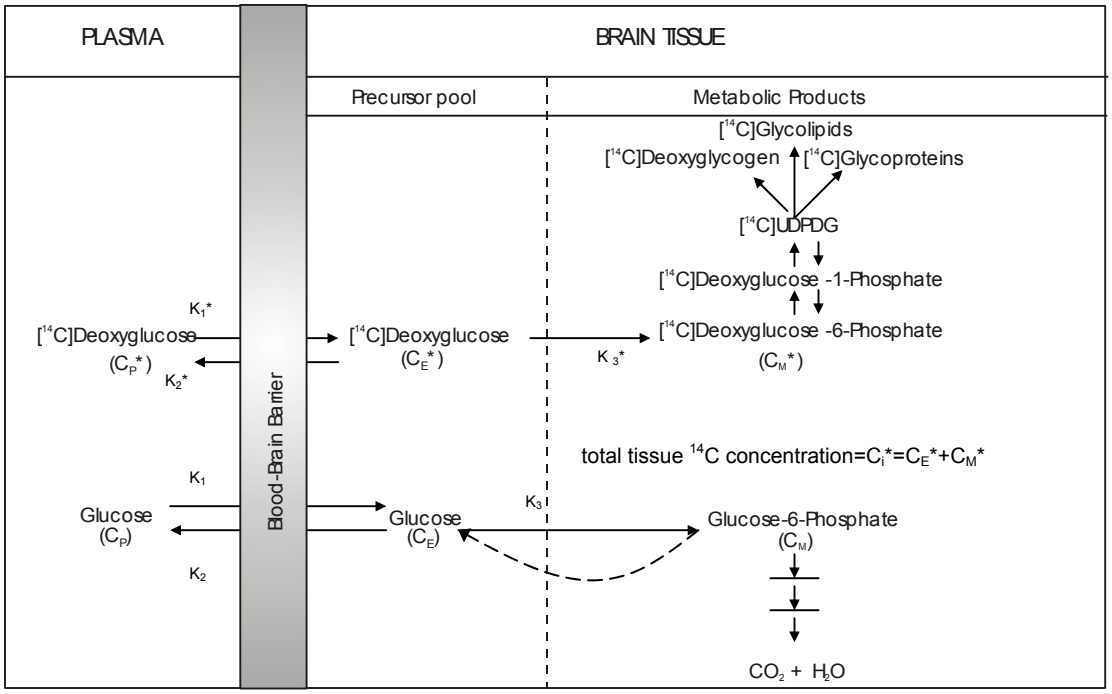

Figure 3: *Diagrammatic representation of the theoretical basis of [^{14}C]-deoxyglucose method for measurement of local cerebral glucose utilization (Sokoloff et al, 1977). C_i* represents the total 2DG concentration in a single homogeneous tissue of the brain. C_P^* and C_P represent the concentrations of 2DG and glucose in the arterial plasma respectively; C_E^* and C_E represent their respective concentrations in the tissue pools that serve as substrates for hexokinase. C_M^* represents the concentration of 2DG-6-phosphate and C_M the concentration of glucose-6-phosphate in the tissue. The constants K_1^*, K_2^* and K_3^* represent the rate constants for carrier-mediated transport of 2DG from plasma to tissue, for carrier-mediated transport back from tissue to plasma and for phosphorylation by hexokinase respectively; K_1, K_2 and K_3 are the equivalent glucose rate constants. The dashed arrow represents the glucose-6-phosphate hydrolysis by glucose-6-phosphatase activity, which is low.*

Operational equation of the [^{14}C] Deoxyglucose Method

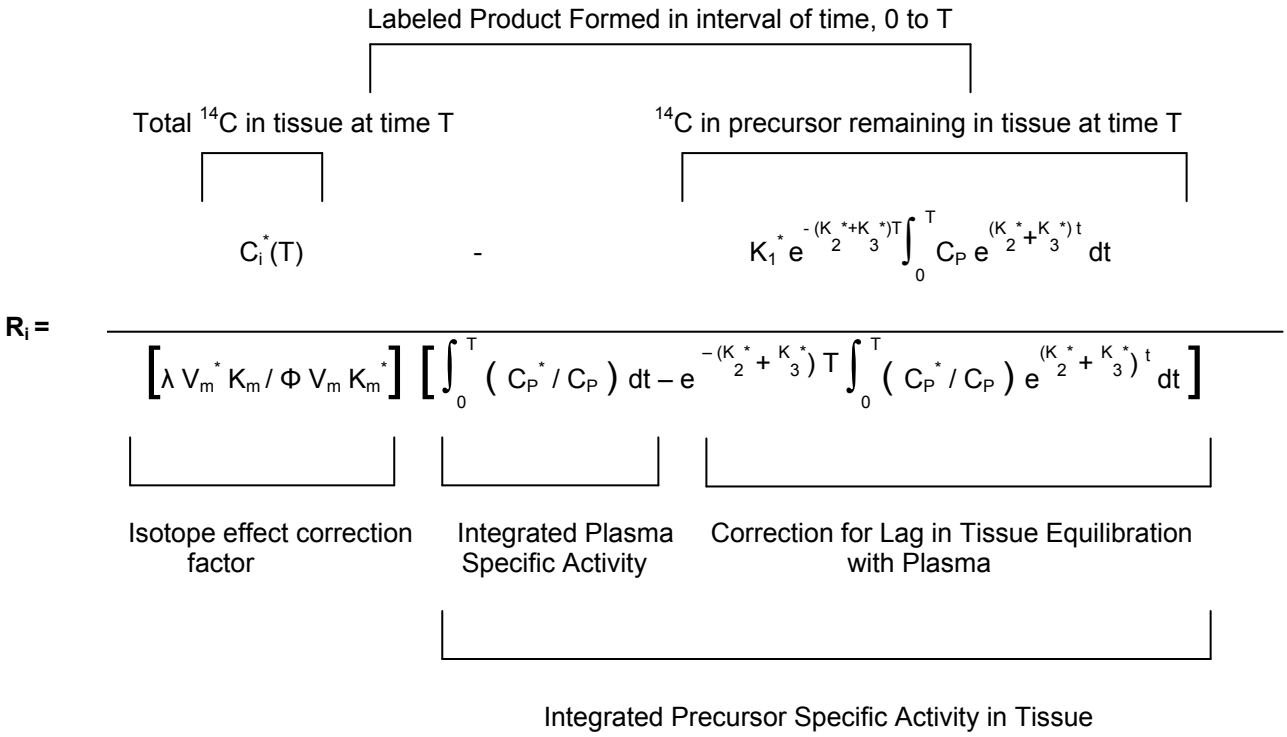

Figure 4: *Operational equation of the [^{14}C]-deoxyglucose method. T represents the time of termination of the experimental period; λ equals the ratio of the distribution space of deoxyglucose in the tissue to that of glucose; Φ equals the fraction of glucose that once phosphorylated continues down the glycolytic pathway; and K_m^* and V_m^* and K_m and V_m represent the Michaelis-Menten kinetic constants of hexokinase for deoxyglucose (asterisks) and glucose (no asterisks) respectively. The other symbols are the same as those defined in figure 3.*

[^{14}C]-Deoxyglucose experiment (2DG experiment)

All experiments were performed on awake behaving monkeys. During the experimental session, each monkey was subjected to femoral vein and artery catheterization under general anesthesia (ketamine hydrochloride, 20mg/kg, i.m.). The catheters were filled with dilute heparin solution (1000U/ml) and were plugged at one end. The length of both catheters (45cm) minimized extensive flushing of dead space during the sampling period. After catheterization the animals were allowed to recover from anesthesia for 4-5 hours, restrained in the primate chair used for the experiments. When the animals recovered from anesthesia, they started the behavioural tasks they were trained for and 5 minutes later the experimental period was initiated by the infusion of 2DG as a pulse, through the venous catheter, over a period of 30 s. A dose of 100μCi/kg of 2DG (specific activity 55mCi/ml, ARC, St. Louis, MO, USA) was used, and since the 2DG was supplied in ethanol solution, it was first evaporated to dryness and then re-dissolved in 1ml of saline. With zero time marking the start of the infusion, arterial blood samples were collected in heparinized tubes at predetermined time intervals: 0s, 15s, 30s, 45s, 1min, 2min, 3min, 5min, 7.5min, 10min, 15min, 25min, 35min and 45min in order to monitor the entire time course of the 2DG concentration in plasma. Care was taken to clear the dead space of the arterial catheter prior to the collection of each sample. The samples were immediately centrifuged after collection in a high speed Beckman centrifuge and kept on ice until used for the analyses. Immediately after the collection of the last sample (45min), the monkey was sacrificed by an intravenous infusion of 50mg sodium thiopental in 5ml saline, followed by a saturated solution of KCl for cardiac arrest. Plasma glucose levels, blood pressure, hematocrit and blood gases ranged within normal values in all monkeys and remained constant throughout all [^{14}C]-DG experiments.

Analysis of arterial plasma 2DG and glucose concentrations

The concentration of deoxyglucose was calculated by its ^{14}C content. Twenty μl of plasma and 3ml of scintillation liquid (Insta-Gel, Packard Co., Illinois, USA) were placed into a counting vial and measured in a liquid scintillation counter (Beckmann Coulerton Inc., Foullerton, CA, USA). The efficiency (E) of the counting was estimated by internal standardization (calibrated [^{14}C]-toluene) and the obtained counts (cpm) were transformed into disintegrations per minute (dpm), according to

the equation dpm=cpm/E. The plasma glucose concentration was assayed in a Spotchem dry glucose analyzer (Spotchem, Menarini, Italy), to establish the required steady state for plasma glucose levels throughout the experimental period and to obtain the glucose level values required by the equation.

Processing of brain tissue-Preparation of autoradiographs

Immediately after the end of the experiment, the cerebral hemispheres, the cerebellum and the spinal cord were removed, frozen by immersion in isopentane maintained between -45ºC and -50ºC with dry ice, and kept in there for at least 15min to ensure full and even freezing. When completely frozen, the tissue was covered with embedding medium (M1, Lipshaw Manufacturing Co, Detroit, MI, USA) in order to avoid dehydration, and stored at -80ºC until sectioning. About 2500 serial horizontal brain sections, 20μm thick, were obtained from each hemisphere in a cryostat (Cryopolycut, Reichert Jung) at -20ºC. One section in every 500μm was collected on a slide and stained with thionine for the identification of the cytoarchitectonic borders of cortical areas of interest. Each section was collected on coverslips and immediately transferred on a hot plate maintained at 60ºC for drying. Immediate transfer of the coverslips to the hot plate prevented movement of the label by diffusion. After remaining on the hot plate for 30min, coverslips were glued on cardboards and exposed to X-ray medical films (EMC1 Kodak, MR Kodak) for a period of 3-14 days depending on the films used and plasma glucose levels, along with a set of precalibrated ^{14}C standards (Amersham plc, Little Chalfont, Buckinghamshire, UK). Films were developed in a Kodak X-OMAT 1000 automatic processor.

Analysis of autoradiographs

The autoradiographs provide a pictorial representation of the relative ^{14}C concentrations among cerebral structures; the darker the region, the higher the rate of glucose utilization. The quantitative densitometric analysis of the autoradiographs was carried out with a computerized image-processing system (MCID, Imaging Research, Ontario, Canada), which allowed integration of the local cerebral glucose

utilization (LCGU) values over the area of interest. LCGU values (in μmol/100g/min) were calculated by using the same method as in previous experiments held by our laboratory (Savaki et al., 1993; Raos et al., 2004). In specific, a calibration curve of the relationship between optical density and tissue ^{14}C concentration for each film was obtained by measuring the optical density corresponding to all different standards. Local tissue concentrations were dtermined from the calibration curve and the optical densities of the cortical areas of interest. LCGU values were obtained from the local tissue concentrations of ^{14}C (C_i^* (T)) which were densitometrically determined from the autoradiographs and the plasma [^{14}C] DG (C_P^*) and glucose concentration (C_P) according to the original operational equation (Sokoloff et al., 1977) illustrated in Figure **4** and the appropriate kinetic constants for the monkey (Kennedy et al., 1978).

Two-Dimensional reconstructions

Two-dimensional reconstructions (2D maps) of the spatio-intensive pattern of metabolic activity (LCGU) within the rostrocaudal and the dorsoventral extent of the cortical areas of interest (parietoccipital cortex and medial parietal cortex) in each hemisphere, were generated according to a method developed in our laboratory (Dalezios et al., 1996; Savaki et al., 1997). A schematic description of the 2D maps is illustrated in Figure **5b**. In the rostrocaudal extent of each section, the distribution of activity was determined by measuring LCGU values pixel by pixel (spatial resolution of anteroposterior sampling: 50μm/pixel) along a line parallel to the surface of the cortex, covering all cortical layers as shown in Figure **5c**. Data arrays of 5 adjacent horizontal sections (in the dorsoventral dimension of the brain) of 20 μm each, were averaged and plotted to produce one line in the 2D maps (spatial resolution of plots: 100μm). Adjacent data arrays were aligned at the intersection of the anterior bank of the POs with the medial surface of the cortical hemisphere (medial crown of POs), to produce the 2D maps of POs. About 650 serial horizontal sections were used for the 2D reconstructions in order to cover the full extent of the parietoccipital cortex. An example of 6 horizontal sections at different dorsoventral levels is depicted in Figure **5c**, as well as their approximate location in the monkey brain figurine illustrated in Figure **5a**. Occasional missing data arrays in the dorsoventral dimension were filled using linear interpolation between neighbouring values. Normalization of LCGU values was based on the average unaffected gray matter value, pooled across all

hemispheres of all monkeys. The statistical significance of differences in LCGU values in areas of interest was determined by the Student's unpaired t-test. Only differences exceeding 7% were considered for statistical analysis, given that homologous areas of the two hemispheres of a normal resting monkey can differ by up to 7% (Savaki et al., 1993).

Geometrical normalization

For a direct comparison of areas between hemispheres of different monkeys and given that each monkey could have differences in its sulcal morphology pattern when compared to another, we applied geometrical normalization to the 2D maps generated for each monkey. For this reason, first section by section rostrocaudal distances were measured. Then the average of each one of these measures was computed to produce a reference map of landmarks. The distances used were those between the surface landmarks of the medial (POm) and the medial and lateral crowns of POs, as well as those between the cytoarchitectonic borders of V6 and V6A. For the latter, one section every 500μm was stained with thionine. The cytoarchitectonic boundaries of areas V6 and V6A were based on criteria established by Luppino et al (Luppino et al., 2005). Each individual reference map, with its own landmarks, was linearly transformed in MATLAB (Mathworks Inc) to match the reference map.

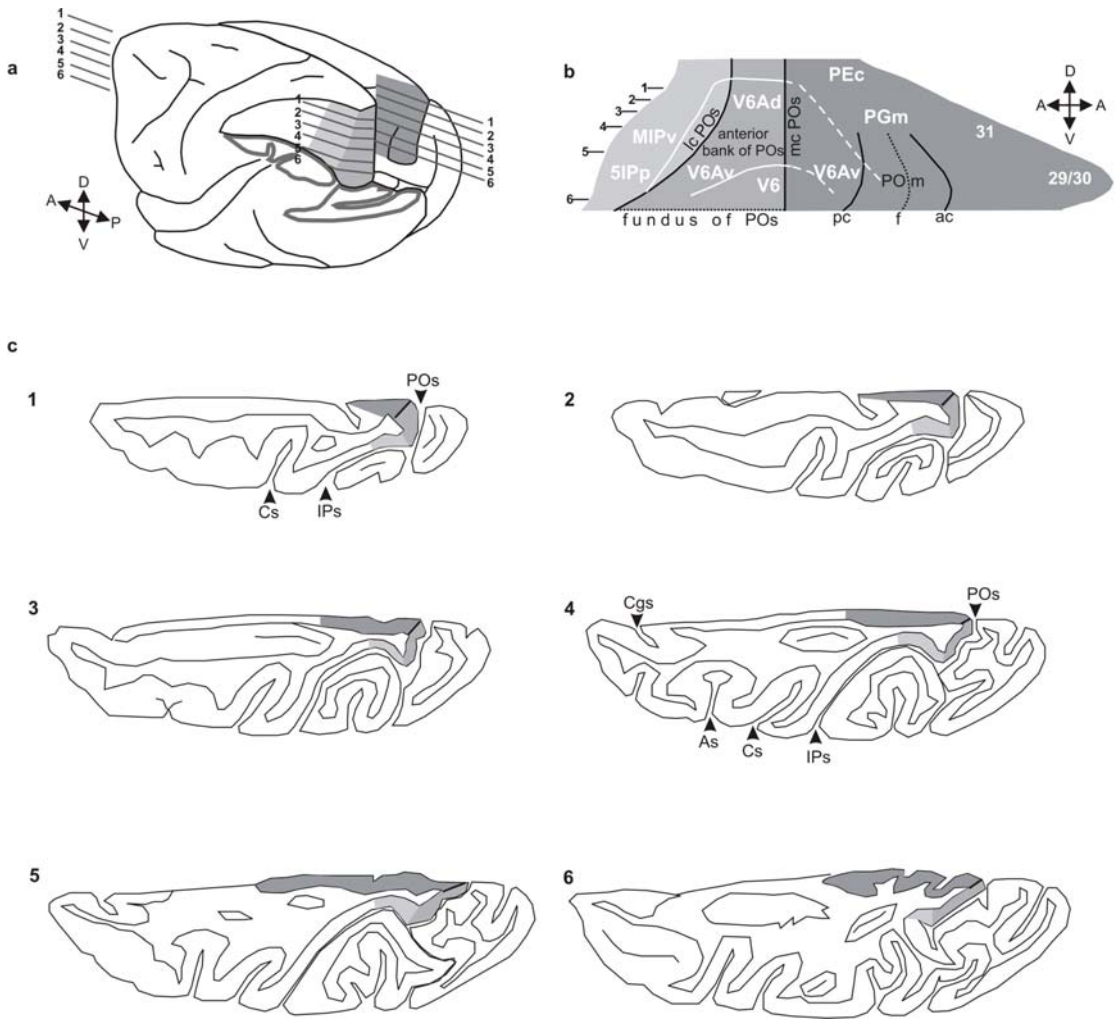

Figure 5: *Reconstruction of medial parietal and parietoccipital cortices. (**a**) Illustration of the posterolateral view of a partly dissected left hemisphere of a monkey, with partial view of its mesial surface. The inferior parietal and the occipital lobules were cut at the levels of the fundi of IPs and POs respectively, to reveal the medial bank of IPs and the anterior bank of POs cortices. Shaded area represents the reconstructed cortex, which includes part of the medial bank of IPs (light gray shaded areas, MIPv and 5IPp), the anterior bank of POs (medium gray shaded area) and the adjacent part of the medial parietal cortex (dark gray shaded areas); areas V6, V6Ad, V6Av. (**b**) Schematic illustration of the reconstructed cortex. Different shades of gray correspond to those in panel **a**. Black lines represent surface landmarks, while solid and interrupted white lines represent cytoarchitectonically and functionally identified borders respectively, of the cortical areas indicated. The vertical black line in the middle of the reconstruction, represents the point of alignment of the serial horizontal sections; medial crown of the anterior bank of POs (mc POs). The black line located at the left of the alignment point, represents the lateral crown of POs (lc POs). The black lines located at the right side of the point of alignment (two solid and one interrupted), represent the posterior crown (pc), fundus (f) and anterior crown (ac) of the medial parietoccipital sulcus (POm). (**c**) Schematic illustrations of six (1-6) horizontal sections through the left hemisphere of a monkey brain at different dorsoventral levels (1 corresponds to the dorsalmost section and 6 to the ventralmost section), which are indicated both at the brain view (panel **a**) and the schematic illustration of the reconstructed cortex (panel **b**). Shaded areas depict the cortical region measured and unfolded in the reconstruction (2D) maps and different shades of gray, correspond to those in panel **a** and **b**. Cs; central sulcus, IPs; intraparietal sulcus, As; arcuate sulcus, Cgs; cingulate sulcus, POs; parietoccipital sulcus.*

RESULTS

To map the cortical regions activated during grasping execution either in the presence or in absence of visual guidance, as well as those activated during grasping observation, we employed the [^{14}C]-deoxyglucose quantitative autoradiographic method. This method provides direct quantitative assessment of the brain activity based on glucose consumption, has the highest spatial resolution (20μm) as compared to other imaging methods and allows the identification of the affected cortical areas by means of cytoarchitectonic criteria.

In this study we focused on the cortical areas located in the medial parietal convexity, the anterior bank of the parietooccipital cortex and the posterior part of the medial intraparietal bank namely V6, V6A, 5IPp, PGm/7m, area 31 and retrosplenial cortex (areas 29 and 30).

All monkeys were trained for several months before the ^{14}C-DG experiment to perform their tasks continuously for at least 1 hour per day. On the day of the ^{14}C-DG experiment, monkeys performed their tasks for the entire experimental period (45 min) without any breaks, and successful completion of each trial was rewarded with water. Success rate remained roughly constant (>90%) throughout the experiment. The mean rate of movements was similar for the execution and the observation tasks, as well as for the arm-motion control. Given that 85% of the radiolabeled deoxyglucose is taken up by cells during the first ten minutes of the ^{14}C-DG experiment, we report the performance of the animals during this critical period. The amount of time that the monkeys spent fixating within the window of the behavioral apparatus during the critical ten first minutes of the ^{14}C-DG experiment ranged between 6 and 7 min. For the rest of the time, the animals did not display any systematic oculomotor behavior that could account for false-positive effects in oculomotor related areas. In other words the line of sight of all the experimental monkeys was at random positions throughout the entire oculomotor space.

During the critical ten first minutes of the ^{14}C-DG experiment, the Cm monkey observed 9 movements of the experimenter's arm per min and fixated within the window of the behavioral apparatus for 6 min (Figure **7a**). Given that the side-to-side difference in glucose consumption in the Cm monkey was not significant, an average of the two hemispheres of the Cm monkey was used to produce the 2D map shown in Figure **6c**. The Cm monkey was used to take into account the effects of (i)

the biological motion of the purposeless (non-goal-directed) reaching arm and (ii) the

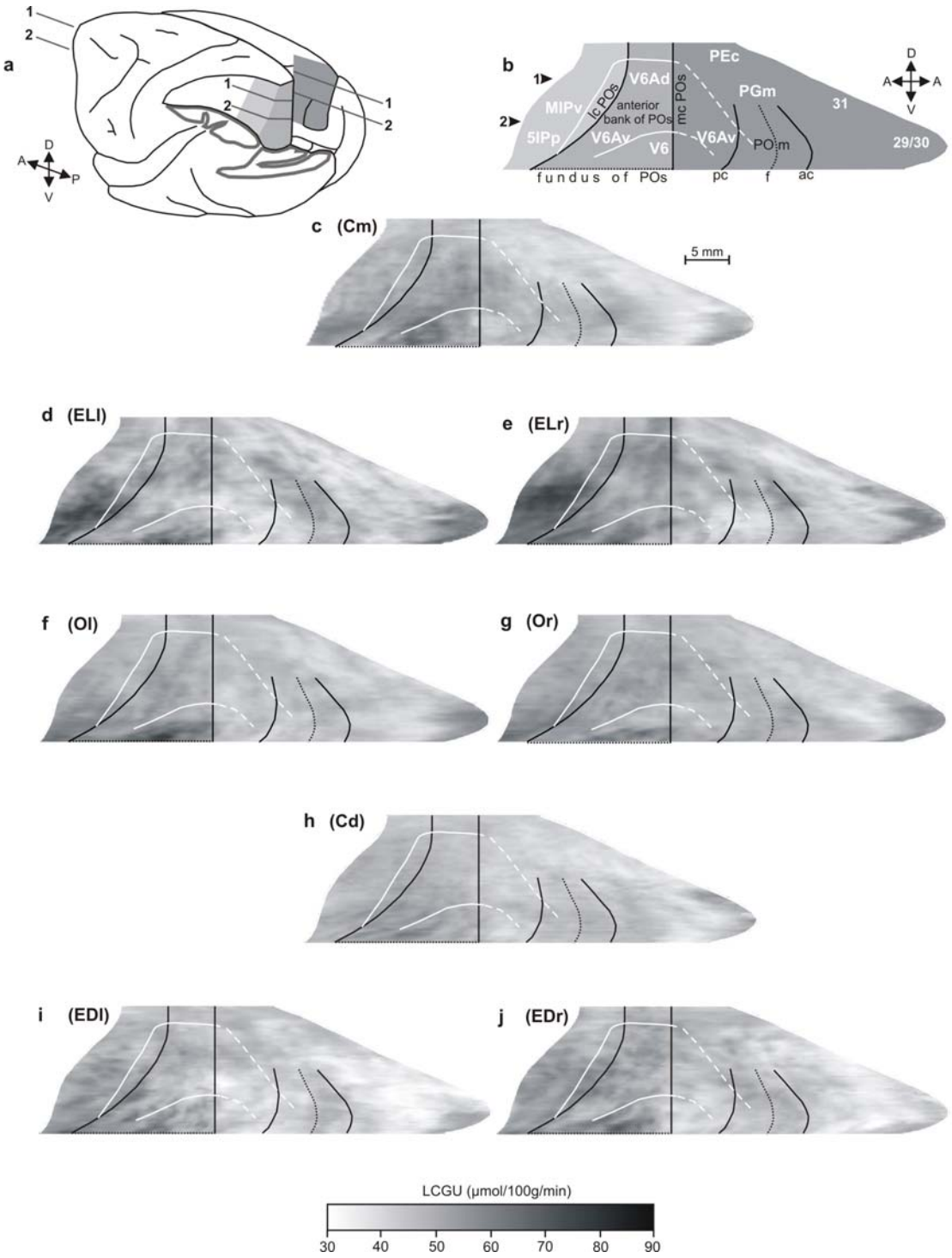

Figure 6: *2D maps of the spatio-intensive pattern of metabolic activity (LCGU) in the medial parietal and parietoccipital cortex. (**a**) Postero-lateral view of the partly dissected left hemisphere of a monkey brain with partial view of its mesial surface. The inferior parietal lobule was cut away at the level of the fundus of the IPs to show the cortex of the medial bank of this sulcus. The occipital lobe of the same hemisphere was also cut away at the level of the fundus of the POs and the lunate sulcus (Ls) to show the cortex of the anterior bank of POs. Shaded area represents the reconstructed cortex including part of the medial bank of IPs, the anterior bank of POs and the adjacent part of the medial parietal cortex. (**b**) Schematic illustration of the geometrically normalized reconstructed cortical field. Different shades of gray correspond to those in panel **a**. Black lines represent surface landmarks, solid and interrupted white lines represent cytoarchitectonically and functionally identified borders,*

*respectively, of the labeled cortical areas. The vertical black line in the middle of the reconstructed field depicts the point of alignment of the serial horizontal sections, which lies at the intersection of the anterior bank of the POs with the medial crown of POs (mc POs). The black line on its left demarcates the lateral crown of POs (lc POs) which corresponds to the intersection of the three sulci: IPs, POs and Ls. The two solid black lines on the right of the alignment point represent the crowns (pc and ac) and the interrupted black line the fundus (f) of POm. (**c**) Averaged map from the two hemispheres of the motion-control monkey. (**d**) Averaged map from the left hemispheres of the two EL monkeys. (**e**) Averaged map from the right hemispheres (contralateral to the moving forelimb) of the two EL monkeys. (**f**) Averaged map from the left hemispheres of the three O monkeys. (**g**) Averaged map from the right hemispheres of the three O monkeys. (**h**) Averaged map from the hemispheres of the two Cd monkeys. (**i**) Averaged map from the left hemispheres of the two ED monkeys. (**j**) Averaged map from the right hemispheres of the two ED monkeys. Gray-scale bar indicates local cerebral glucose utilization (LCGU) values in µmol/100g/min. Other conventions as in Figure 5.*

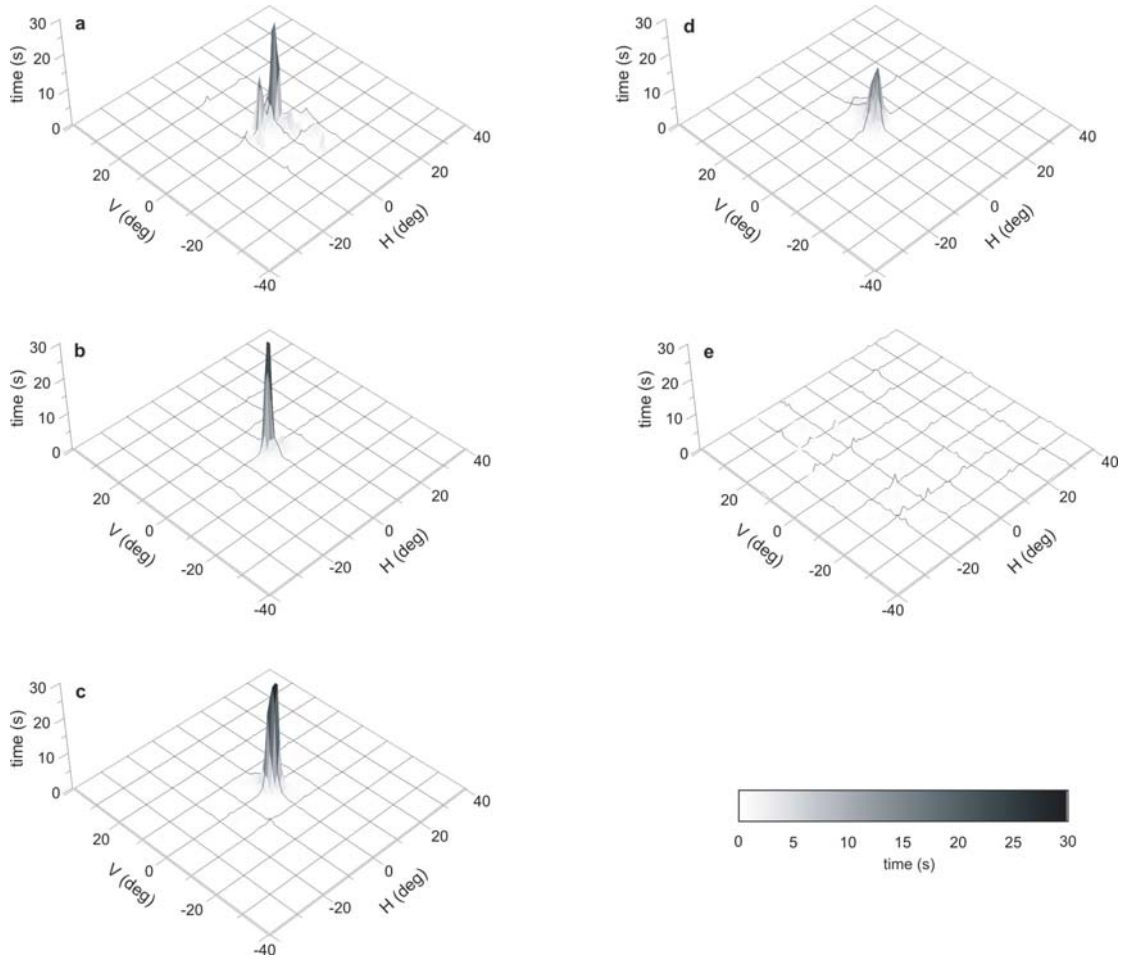

***Figure 7:** Three-dimensional histograms of the dwell time of the line of sight as a function of eye position during the critical ten first min of the ^{14}C-DG experiment. (**a**) Motion-control monkey. (**b**) Averaged oculomotor behaviour from the two grasping-execution monkeys. (**c**) Averaged behaviour from the three grasping-observation monkeys. (**d**) Averaged oculomotor behaviour from the two grasping-execution in dark monkeys. (**e**) Averaged behaviour from the three dark-control monkeys. Horizontal axis (X) and vertical axis (Y) in degrees, Z axis in s. Gray-scale bar indicates time in s.*

visual stimulation by the 3D object, and served as control for the EL and the O monkeys.

The EL monkeys performed 10 grasping movements per min, during the critical ten first minutes of the ^{14}C-DG experiment and fixated within the window of the behavioral apparatus for 7 min (Figure **7b)**. The average map of the left hemispheres (ipsilateral to the moving forelimb) and the average map of the right hemispheres (contralateral to the moving forelimb) of the two EL monkeys are presented in figures **6d** and **6e**, respectively.

During the critical ten first minutes of the ^{14}C-DG experiment, the O monkeys observed 12 grasping movements per min performed by the experimenter and fixated within the window of the behavioral apparatus for 7 min (Figure **7c)**. The average map of the left hemispheres and the average map of the right hemispheres of the three O monkeys are presented in figures **6f** and **6g**, respectively.

The line of sight of the Cd monkeys was at random positions throughout the entire oculomotor space (Figure **7e**).The average map of the hemispheres of the two Cd monkeys is presented in figure **6h**. Cd monkeys served as a control for the ED ones.

The ED monkeys performed 11 grasping movements per min, during the critical ten first minutes of the ^{14}C-DG experiment and fixated within the window of the behavioral apparatus for 7 min (Figure **7b)**. The average map of the left hemispheres (ipsilateral to the moving forelimb) and the average map of the right hemispheres (contralateral to the moving forelimb) of the two ED monkeys are presented in figures **6i** and **6j**, respectively.

The geometrically normalized maps presented in figure **6** were used (i) to obtain average-LCGU maps out of control or experimental hemispheres and (ii) to subtract control from experimental averaged maps. The average LCGU values were calculated in sets of five adjacent sections (20 μm thick) throughout each cortical area of interest in each hemisphere. Experimental to control LCGU values were compared for statistical significances by the Student's unpaired t-test. Given that ipsilateral to contralateral LCGU values in normal control monkeys range up to 7% (Savaki et al., 1993), only differences higher than 7% were considered for statistical treatment. To illustrate the percent LCGU differences between the experimental (E) monkeys and their corresponding controls (C), we generated images of the spatio-intensive pattern of distribution of the metabolic activations, using the formula (E-C)/C*100.

ACTIVATIONS INDUCED BY GRASPING-EXECUTION IN LIGHT

When the averaged maps of the parieto-occipital and medial parietal cortex in the left or in the right hemispheres of the EL monkeys (Figures **6d** and **6e**, respectively) are compared with the corresponding averaged map of the Cm monkey (Figure **6c**), increased metabolic activity (net activation) is apparent in several cortical regions (Figure **8**, see also Table **1**).

Grasping-execution in light, activated area 5IPp in the medial bank of the intraparietal sulcus (by 23% ipsilaterally and 26% contralaterally), area PGm/7m in the medial parietal convexity, (by 14% ipsilaterally and 19% contralaterally), area 29/30 of the retrosplenial cortex RSC (by 17%), and area V6 in the anterior bank of the parieto–occipital sulcus (by 9%), bilaterally. Area V6Ad in the anterior bank of the parieto–occipital sulcus was activated only contralaterally by 13%. Area 5IPp is reported for the first time from our laboratory and does not correspond to any region previously described in the literature. It is ventrally demarcated by the fundus of IPs and borders areas MIP dorsally, 5VIP rostrally and V6A caudally. It is located rostral to area PIP, which has been described in the most anterior and lateral part of POs (Colby et al 1988).

ACTIVATIONS INDUCED BY GRASPING-OBSERVATION

When the averaged maps of the parieto-occipital and medial parietal cortex in the left or in the right hemispheres of the O monkeys (Figures **6f** and **6g**, respectively) are compared with the corresponding averaged map of the Cm monkey (Figure **6c**), increased metabolic activity (net activation) is apparent in several cortical regions (Figure **9**, see also Table **2**).

Areas activated for grasping-observation in the medial parietal convexity include PGm/ 7m (by 10% bilaterally), 31 (by 8% bilaterally) and 29/30 (left hemisphere 10%, right hemisphere 12%). Moreover, the same part of area V6 in the anterior bank of the parieto-occipital sulcus that was activated for grasping-execution in light was also activated for grasping-observation (left hemisphere 17%, right hemisphere 11%).

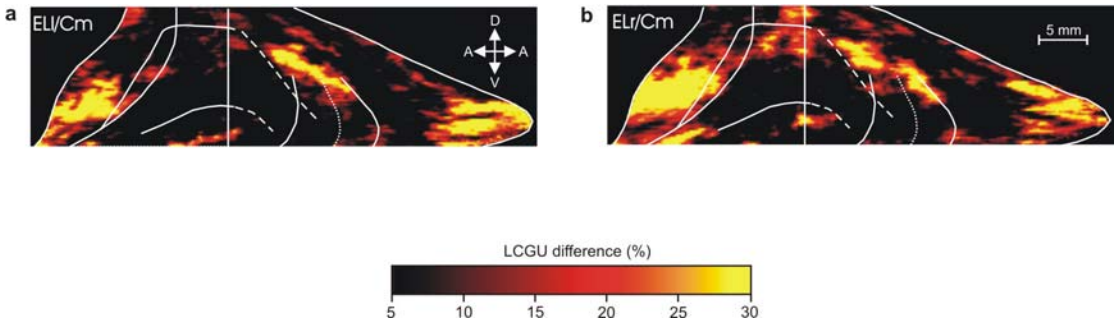

Figure 8: *Medial parietal and parietoccipital cortical maps of percent LCGU differences from the motion-control (Cm). Percent differences were calculated by using the formula (EL-Cm)/Cm*100. (**a**) Map of net execution-induced activations averaged from the left hemispheres of the two EL monkeys. (**b**) Map of corresponding activations averaged from the right hemispheres (contralateral to the moving forelimb) of the two EL monkeys. White lines correspond to surface landmarks and cytoarchitectonic borders illustrated in figure 5.*

Table 1. Metabolic effects induced by grasping execution in light (EL) in the parieto-occipital and medial parietal cortical areas of the monkey brain.

Cortical area	**n**	**Cm** LCGU±SD	**ELl** LCGU±SD	**ELr** LCGU±SD	**ELl/Cm** (%)	**ELr/Cm** (%)
Medial intraparietal bank						
5IPp	53	53±4	65±4	67±4	**23**	**26**
Anterior parieto-occipital areas						
V6Ad	34	48±2	49±1	54±2	2	**13**
V6Av	80	51±1	47±2	52±2	-8	2
V6	38	52±2	49±5	52±2	-6	0
V6 (max)	18	47±2	51±4	51±2	**9**	**9**
Medial parietal areas						
PGm/7m (max)	66	42±3	48±3	50±3	**14**	**19**
31 (max)	72	39±1	40±2	41±1	3	5
Retrosplenial cortex (29/30)	69	41±3	48±8	48±3	**17**	**17**

*n, number of sets of five adjacent horizontal sections used to obtain the mean local cerebral glucose utilization (LCGU) values (in µmol/100g/min) for each region. Cm values represent the average LCGU values from the two hemispheres of the motion-control monkey. ELl and ELr values represent the average LCGU values from the two left and the two right hemispheres of the grasping-execution monkeys, respectively. SD, standard deviation of the mean. ELl/Cm, ELr/Cm; percent differences between ELl, ELr, and Cm, respectively, calculated as (experimental-control)/control*100. Values in bold indicate statistically significant differences by the Student's unpaired t test at the level of P < 0.001.*

ACTIVATIONS INDUCED BY GRASPING-EXECUTION IN DARK

When the averaged maps of the parieto-occipital and medial parietal cortex in the left or in the right hemispheres of the ED monkeys (Figures **6i** and **6j**, respectively) are compared with the corresponding averaged map of the Cd monkey (Figure **6h**), increased metabolic activity (net activation) is apparent in several cortical regions (Figure **10**, see also Table **3**).

Grasping-execution in dark induced activations in area 5IPp (by 13%) and part of V6 (by 14% for the left and 22% for the right hemisphere) bilaterally, as well as in areas V6Ad (by 11%) and PGm/7m (by 12%) contralaterally to the grasping hand.

SPATIAL DISTRIBUTION OF THE EFFECTS INDUCED BY GRASPING EXECUTION IN LIGHT AND GRASPING OBSERVATION

When spatially compared by superimposition, the observation-induced activations were found to overlap the execution-in-light-induced ones considerably (Figure **11**). In the above mentioned figure, red, green and yellow correspond to execution-in-light-induced, observation-elicited, and common activations, respectively. It is evident that area 5IPp in both hemispheres and V6Ad in the hemisphere contralateral to the moving forelimb are activated solely for grasping-execution in light, area 31 is activated bilaterally only for grasping-observation, while areas PGm/7m and the RSC are activated for both observation and execution of grasping.

To illustrate quantitatively the distribution of metabolic activity within the affected regions we plotted the differences between the experimental monkeys (either EL or O) and the control monkey (Cm) (as % LCGU values and 95% confidence intervals per 100 μm), across the rostro-caudal extent of the ribbon highlighted in the schematic representation of the reconstructed cortex above the graph in Figure **12**. The plots in this figure represent the percent differences between the EL and the Cm monkeys (red lines, solid for right and interrupted for left hemispheres), as well as between the O and the Cm monkeys (green lines, solid for right and interrupted for left hemispheres). The ribbon, along which differences were measured, included areas 5IPp, MIPv, V6Ad, PGm/7m, 31 and RSC. The plots in Figure **12** show bilateral activation of area 5IPp and contralateral activation of area V6Ad in the EL monkeys, bilateral activation of area 31 mainly in the O monkeys, and bilateral activation of PGm/7m and RSC in both EL and O monkeys.

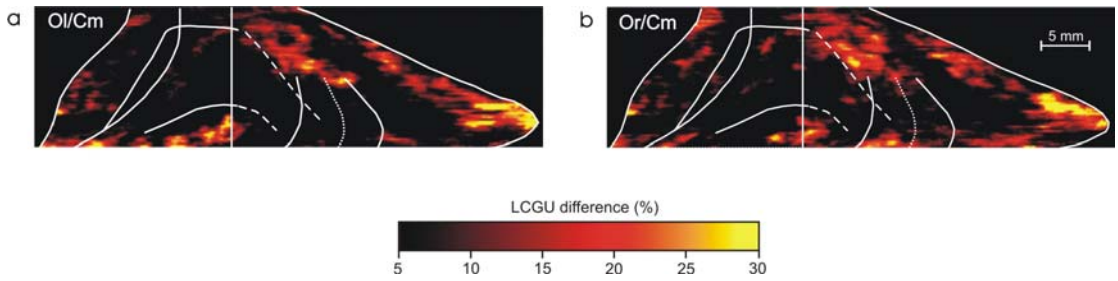

Figure 9: *Medial parietal and parietoccipital cortical maps of percent LCGU differences from the motion-control (Cm). Percent differences were calculated by using the formula (O-Cm)/Cm*100. (**a**) Map of net observation-induced activations averaged from the left hemispheres of the three O monkeys. (**b**) Map of corresponding activations averaged from the right hemispheres of the three O monkeys. Colour bar indicates % LCGU differences from the Cm. White lines correspond to surface landmarks and cytoarchitectonic borders illustrated in figure 5.*

Table 2. Metabolic effects induced by grasping observation (O) in the parieto-occipital and medial parietal cortical areas of the monkey brain.

Cortical area	**n**	**Cm** LCGU±SD	**Ol** LCGU±SD	**Or** LCGU±SD	**Ol/Cm** (%)	**Or/Cm** (%)
Medial intraparietal area						
5IPp	53	53±4	56±4	56±4	6	6
Anterior parieto-occipital areas						
V6Ad	34	48±2	47±1	49±1	-2	2
V6Av	80	51±1	49±2	51±1	-4	0
V6	38	52±2	53±5	50±4	2	-4
V6 (max)	18	47±2	55±3	52±3	**17**	**11**
Medial parietal areas						
PGm/7m (max)	66	42±3	46±2	46±2	**10**	**10**
31 (max)	72	39±1	42±1	42±1	**8**	**8**
Retrosplenial cortex (29/30)	69	41±3	45±4	46±4	**10**	**12**

*n, number of sets of five adjacent horizontal sections used to obtain the mean local cerebral glucose utilization (LCGU) values (in µmol/100g/min) for each region. Cm values represent the average LCGU values from the two hemispheres of the motion-control monkey. Ol and Or values represent the average LCGU values from the three left and the three right hemispheres of the grasping-observation monkeys, respectively. SD,standard deviation of the mean. Ol/Cm, Or/Cm, are percent differences between Ol, Or and Cm, respectively, calculated as (experimental-control)/control*100. Values in bold indicate statistically significant differences by the Student's unpaired t test at the level of P < 0.001.*

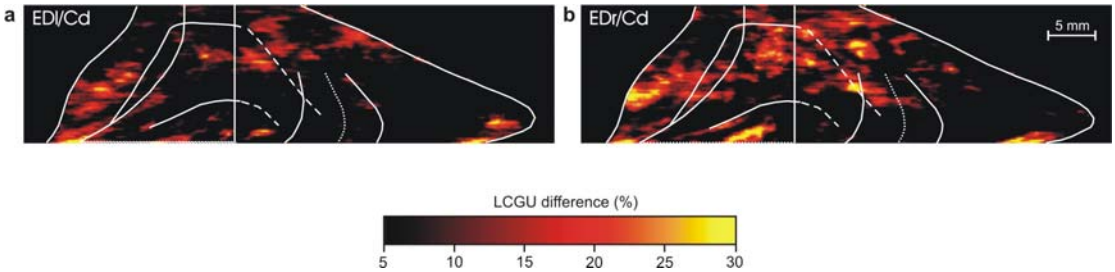

Figure 10: *Medial parietal and parietoccipital cortical maps of percent LCGU differences of the hemispheres of the ED monkeys from the dark-control monkey (Cd). Percent differences were calculated by using the formula (ED-Cd)/Cd*100. (**a**) Map of net execution-induced activations averaged from the left hemispheres of the two ED monkeys. (**b**) Map of corresponding activations averaged from the right hemispheres of the two ED monkeys. Colour bar indicates % LCGU differences from the Cd. White lines correspond to surface landmarks and cytoarchitectonic borders illustrated in figure 5.*

Table 3. Metabolic effects induced by grasping execution in dark (ED) in the parieto-occipital and medial parietal cortical areas of the monkey brain.

Cortical area	**n**	**Cd** LCGU±SD	**EDl** LCGU±SD	**EDr** LCGU±SD	**EDl/Cd** (%)	**EDr/Cd** (%)
Medial intraparietal area						
5IPp	53	48±2	54±3	54±3	**13**	**13**
Anterior parieto-occipital areas						
V6Ad	35	45±1	46±2	50±1	2	**11**
V6Av	80	47±2	47±2	49±1	0	4
V6	38	48±1	48±3	48±3	0	0
V6 (max)	18	49±1	56±2	60±1	**14**	**22**
Medial parietal areas						
PGm/7m (max)	66	41±1	44±1	47±1	7	**12**
31 (max)	72	39±1	38±5	38±2	-3	-3
Retrosplenial cortex (29/30)	69	41±4	38±4	39±3	-7	-5

*n, number of sets of five adjacent horizontal sections used to obtain the mean local cerebral glucose utilization (LCGU) values (in µmol/100g/min) for each region. Cd values represent the average LCGU values from the hemispheres of the dark-control monkeys. EDl and EDr values represent the average LCGU values from the two left and the two right hemispheres of the grasping-execution in dark monkeys, respectively. SD; standard deviation of the mean. EDl/Cd and EDr/Cd are percent differences between EDl, EDr and Cd, respectively, calculated as (experimental-control)/control*100. Values in bold indicate statistically significant differences by the Student's unpaired t test at the level of P < 0.001*

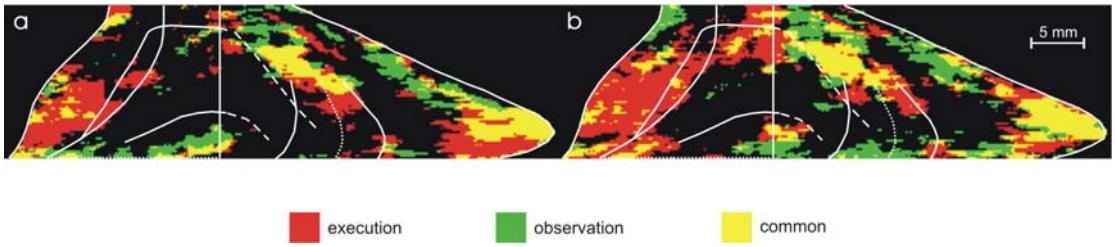

Figure 11: *Superimpositions of figures **8a** and **9a**. (**f**) Superimposition of figures **8b** and **9b**. In panels **a** and **b**, red and green represent activations higher than 10%, induced by grasping-execution in light and grasping observation respectively. Yellow stands for common activations, induced by both execution (under visual guidance) and observation of grasping. White lines correspond to surface landmarks and cytoarchitectonic borders illustrated in figure 5.*

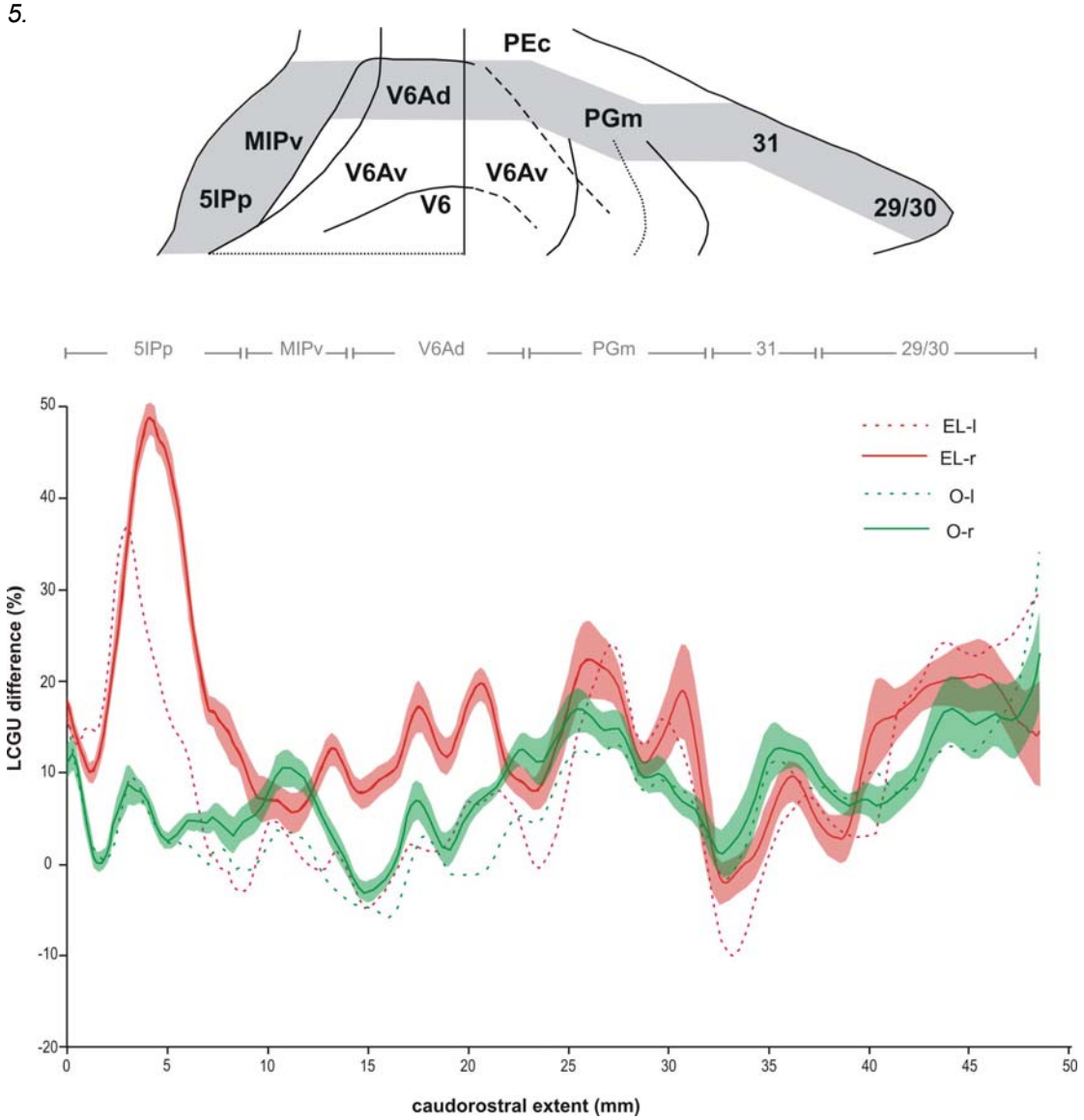

Figure 12: *Plots of percent LCGU differences along the reconstructed cortex of part of the medial bank of IPs, the dorsal part of the anterior bank of POs and its adjacent medial parietal cortical field (along the ribbon highlighted in the drawing above the plots) including area 5IPp, part of medial intraparietal area (MIPv), the dorsal part of V6A, areas PGm/7m, 31 and the retrosplenial cortical areas 29/30. Red plots illustrate the differences between the two execution monkeys and the Cm. Green plots illustrate the differences between the three observation monkeys and the Cm. Plots with solid and dotted lines correspond to the right and the left hemispheres, respectively. Red and green shaded areas indicate 95% confidence intervals. Baseline corresponds to 0% LCGU difference from the Cm. Zero rostrocaudal extent represents the ventral border of area 5IPp.*

SPATIAL DISTRIBUTION OF THE EFFECTS INDUCED BY GRASPING EXECUTION IN LIGHT AND GRASPING EXECUTION IN DARK.

In figure **13**, red, blue and violet correspond to execution-in-light-induced, execution-in-dark-elicited, and common activations, respectively. It is evident that RSC and the ventral portion of PGm/7m are activated bilaterally only for grasping execution-in-light, while 5IPp bilaterally, as well as, V6Ad and the dorsal portion of PGm/7m contralaterally, are activated by grasping in both conditions.

To illustrate quantitatively the distribution of metabolic activity within affected regions by grasping-execution either in light or dark, we plotted the differences between the experimental monkeys (EL and ED) and the corresponding control monkeys (Cm and Cd, respectively) (as % LCGU values and 95% confidence intervals per 100 μm), across the rostro-caudal extent of the ribbon highlighted in the schematic representation of the reconstructed cortex above the graph in Figure **14**. The plots in this figure represent the percent differences between the EL and the Cm monkeys (red lines, solid for right and interrupted for left hemispheres), as well as between the ED and the Cd monkeys (blue lines, solid for right and interrupted for left hemispheres). The ribbon, along which differences were measured, included area 5IPp, MIPv, V6Ad, PGm/7m, 31 and RSC. It is evident that area 5IPp bilaterally, V6Ad contralaterally, the dorsal portion of PGm/7m (bilateral in the EL, contralateral the ED) are activated in both EL and ED monkeys, while the ventral portion of PGm/7m bilaterally and area 29/30 (in both hemispheres) are activated only in EL monkeys (Figure **14**).

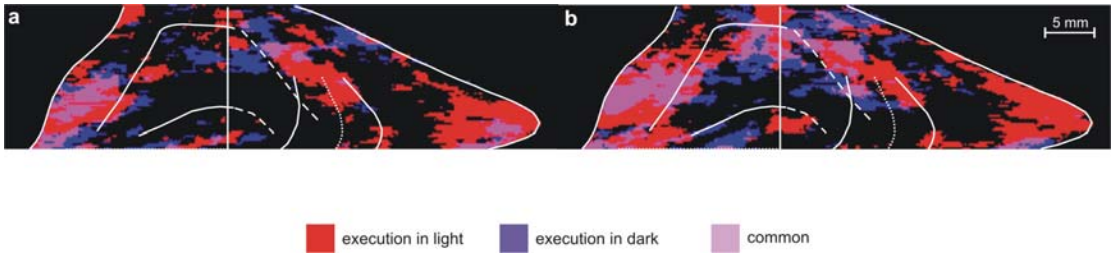

Figure 13: *(**a**) Superimpositions of figures **8a** and **10a**. (**b**) Superimposition of figures **8b** and **10b**. In panels **a** and **b**, red and blue represent activations higher than 10%, induced by grasping-execution in light and grasping-execution in dark respectively. Purple stands for common activations, induced by both execution in light (under visual guidance) and execution in dark (under somatosensory guidance). White lines correspond to surface landmarks and cytoarchitectonic borders illustrated in figure 5*

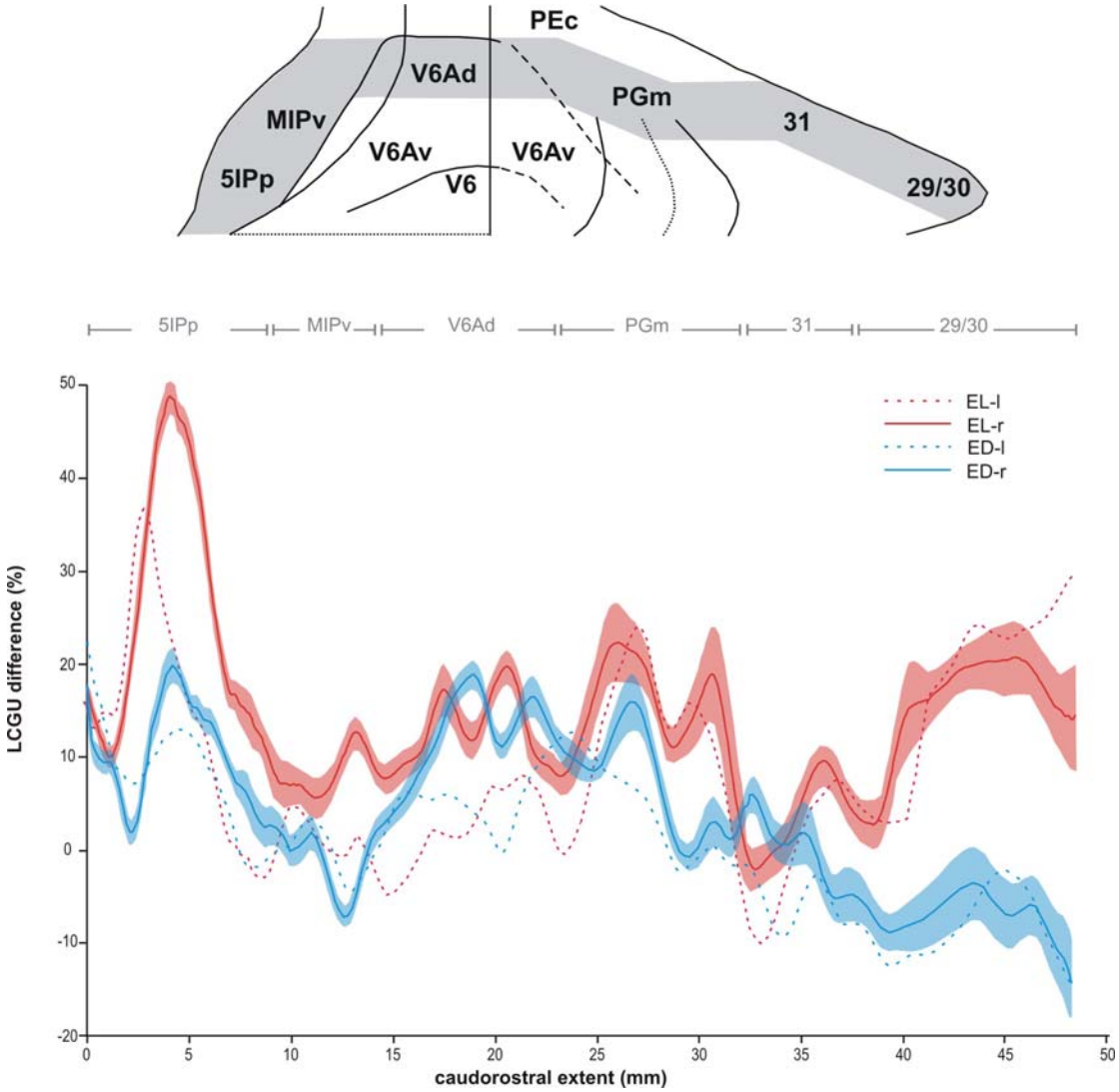

Figure 14: *Plots of percent LCGU differences along the reconstructed cortex described in figure **12** and depicted as a ribbon in the drawing above the plots. Red plots illustrate the differences between the two EL monkeys and the Cm monkey, while blue plots illustrate the differences between the two ED monkeys and the Cd monkeys. Plots with solid and dotted lines correspond to the right and the left hemispheres respectively. Red and blue shaded areas indicate 95% confidence intervals. Baseline corresponds to 0% LCGU differences from the control in each case (Cm for EL monkeys and Cd for ED monkeys). Zero rostrocaudal extent represents the ventral border of area 5IPp.*

DISCUSSION

The present study was carried out to investigate the cortical regions involved in grasping-execution behaviour and was focused on areas of the medial parietal and parietoccipital cortices. In order to clarify the distinct contribution of each area, 5 tasks were employed; a) grasping-execution in light (EL), b) grasping-execution in dark (ED), c) grasping-observation (O), d) motion control (Cm) and e) dark control (Cd).

We used the [^{14}C]-DG quantitative method to map the metabolic activity in the brain of the monkeys employed in the aforementioned tasks and produce high resolution 2D maps of the medial parietal and parietoccipital cortex and subsequently of areas V6, V6A, PGm/7m, 31, RSC and 5IPp.

This is the first time that quantitative 2D-maps of the spatio-intensive distribution of metabolic activity are generated for these areas, assessing their special contribution in visual and somatosensory guidance of grasping behaviour, as well as in observation/recognition of the same behaviour.

Area V6

Area V6 occupies a “C”-shaped belt of cortex between the occipital and parietal lobes. Portion of V6 was found to be activated for both grasping-execution in light and observation of the same action performed by the experimenter. In specific, the percent LCGU differences of monkeys performing grasping movements from the motion-control have been calculated as 9% for both hemispheres and the ones between monkeys observing this action and the motion-control were 17% for the left and 11% for the right hemispheres.

The engagement of this area, both in observation and execution of visually guided grasping movements presented in this study, is consistent with previous findings reporting that this area receives form- and motion- related visual signals from the striate and extrastiate cortices and projects to arm-related areas as MIP and V6A (Colby and Duhamel, 1991; Duhamel et al., 1997; Galletti et al., 2001; Galletti and Fattori, 2003). V6 may analyze fast form and motion signals originating from visual areas, and through its connections with bimodal areas such as a) MIP and V6A representing the arm (Colby and Duhamel, 1991; Galletti et al., 1997) and b) V6A related to spatial locations of the objects to be grasped (Galletti et al., 1993, 1995)

and via their projections to premotor area 6 (Tanne et al., 1995; Matelli et al., 1998; Shipp et al., 1998) may participate to the visual guidance of grasping.The bilateral involvevement of part of V6 also during grasping execution in dark, suggests that area V6 may be involved in the somatosensory quidance of grasping as well.

It is also reported from previous studies (Galletti et al., 1999a) that area V6 is a topographically organized area and contains a representation of the entire contralateral hemifield up to an eccentricity of at least 80°, with the periphery represented medially and the central field laterally (Galletti et al., 1999a). Our data show that portions of both the peripheral and the central fields of V6 are implicated in grasping-execution and grasping-observation, something that indicates that the animals were attending their approaching arm or the experimenter's arm from the visual periphery to the center, while fixating the object straight ahead. It is interesting to note that in V6 real-motion (Galletti and Fattori, 2003) and direction-selective cells (Galletti et al., 1996) have been reported. The stronger activation demonstrated in the O task (17% for the left and 11% for the right hemispheres) compared to the EL task (9% in both hemispheres), indicates that the animals were more attentive to the experimenter's approaching arm during the O task, than to their own during the EL task. Activity related to the vision of arm biological-motion and to oculomotion is annuled by the subtraction of the Cm monkey.

Area V6A

Area V6A is a visual/somatosensory area that occupies a horseshoe-like region of the superior parietal lobule and borders with area V6 ventrally, PEc dorsally, PGm/7m medially and MIP laterally. It has been divided into two functionally different areas, V6Ad which is not connected with area V6 and V6Av which receives a direct input from area V6 (Galletti et al., 2001). The part of V6A found to be significantly activated during the tasks employed in our study was V6Ad. The tasks that affected the metabolic activity in area V6Ad was the EL (13% difference from Cm) and the ED (11% difference from Cd). It is worth noting that only the contralateral hemispheres to the moving forelimb showed increased metabolic activity. Grasping-observation, as such, did not have any effect on the activity of this area. This demonstrates that V6A is related with the execution of grasping only, and not with the observation/execution of actions.

Our data are in agreement wih previous findings that area V6A and especially its dorsal counterpart (V6Ad) contains arm-related cells (Fattori et al 1999). In specific, it

has been reported that both reaching (Fattori et al., 2001; Fattori et al., 2005) and grasping (Fattori et al., 2004) modulate the activity of neuronal populations in V6A and this modulation could not be attributed neither to visual input nor to eye movements (Fattori et al., 2004).

In addition, it has been recently demonstrated (Raos et al., 2003) that in area F2 of the premotor cortex, an area strongly connected with area V6A as already mentioned in the introduction, there is a representation of both proximal and distal complex movements.

Moreover in V6A, there exist somatosensory cells with their somatic receptive fields located on proximal and distal parts of the contralateral arm (Breveglieri et al., 2002).

Lesion studies in monkeys and clinical studies in human subjects, tend to link deficits in reaching or grasping and optic ataxia with lesions in area V6A (Faugier-Grimaud et al., 1978; Battaglini et al., 2002; Battaglini et al., 2003; Karnath and Perenin, 2005).

Taken into account the aforementioned reports, it is obvious that the activation of area V6A and especially its dorsal part in our study reflects control of reaching to grasp movements. Presumably, arm-movement related neurons in V6A integrate motor-signals related to arm movements with somatosensory signals evoked by these movements to online guide reaching-to-grasp behaviour.

Area PGm/7m

Area PGm/7m which occupies the medial wall of the SPL and comprises the alternative visuomotor relay station receiving visual input and projecting to the PMd (Petrides and Pandya, 1984; Cavada and Goldman-Rakic, 1989b; Johnson et al., 1996; Matelli et al., 1998), has been found to be bilaterally activated at the hemispheres of both EL and O monkeys. In specific, the % LCGU differences from the Cm was 10% for both hemispheres in the O task and 14% and 19% for the left and the right hemispheres respectively in the EL task. The ED task also affected the metabolic activity of area PGm/7m significantly, as compared to the Cd monkey. More specifically, the % LCGU differences from the Cd, were 7% and 12% for the left and the right hemispheres respectively.

The above results are in accordance with previous studies, reporting that cells in PGm/7m displayed activity related to hand movement and hand position (Ferraina et al., 1997a; Ferraina et al., 1997b). This activity was strongly influenced by eye-position signals and was not modulated by pure visual stimuli, suggesting that neurons in this area combine visuomanual and oculomotor signals, possibly leading

from target localization to movement generation with the composition of motor commands based on kinesthetic and visual control signals (Ferraina et al., 1997a).
The higher metabolic activity observed in the monkeys who performed movements as compared to those who observed the grasping behaviour (14% and 19% vs 10%), indicates the stronger involvement of this area in execution than in recognition of actions.
Also our findings are in aggrement with a previous study which demonstrated that an area between the parietoccipital sulcus and the posterior end of the cingulate sulcus (apparently corresponding to area PGm/7m), was activated both during execution and observation of action (Binkofski et al., 1999) .
Finally, it is interesting to note that areas such as the Supplementary Somatosensory Area (SSA) or the cingulate cortex, which are heavily connected with area PGm/7m, have also found to be activated for grasping-execution and grasping-observation (Raos et al., 2007).

Retrosplenial Cortex (RSC)

The RSC, which consists of areas 29 and 30 and is located in the callosal sulcus, was found to be bilaterally activated both during grasping-execution (EL task ; 17% LCGU difference from Cm for both hemispheres) and grasping-observation (10% LCGU difference for the left and 12% for the right hemispheres, compared to Cm) tasks.
The RSC has been reported to be involved in aspects of working memory (Matsunami et al., 1989; Petrides et al., 1993; Epstein et al., 2007), topographic orientation (Takahashi et al., 1997; Epstein et al., 2007; Iaria et al., 2007; Ino et al., 2007), and the perception of visual objects associated with a specific context, forming in conjunction with other areas a cortical “context network” that processes contextual associations during object recognition (Bar and Aminoff, 2003).

The bilateral involvement of RSC both in the EL and O tasks, combined with the lack of activity in this area during the ED task, suggests that vision of the object-hand interaction during grasping and the immediate scene in front of the monkey plays a crucial role in the activation of this area. Therefore, the RSC could possibly be implicated in processing of contextual associations during object recognition and in encoding of the current salience of objects in the immediate (visual) scene for orienting and navigating towards them. Also it may be involved in topographic spatial

navigation, for situating oneself within a larger environment, using the immediate scene as a cue.

The involvement of this area in short-memory functions cannot be excluded, since it is connected with the Papez circuit, the visual association cortex or motor-related areas such as the anterior cingulate, SMA and the premotor cortex. However, the lack of increased metabolic activity during the ED task, suggests that this kind of activity could be related to “visual” and not “motor” memory.

Area 31

Area 31 which is located between area 23c of the cingulate sulcus and area PGm/7m, has been found to be bilaterally activated only during grasping-observation. Previous reports tend to link activity in this area with oculomotor activity in the service of spatial analysis of the visual input (Olson et al., 1996) and with the motivational salience of visual and oculomotor events for orienting attention (Dean et al., 2004). If that was the case, then increased metabolic activity would have been observed not only in the O task but also in the E tasks.

There are also other reports relating the activity in area 31 with different functions. According to Johnson et al, area 31 is an important region for accessing a sense of self (Johnson et al., 2002). Also there are reports linking the activity in area 31 with memory retrieval (Minoshima et al.,1997; Choo et al., 2007). These studies reported sustained hypometabolism in area 31 in patients with very early-stage Alzheimer’s disease, in which difficulty with memory was the most prominent symptom. Our data are consistent with the aforementioned reports. The animals employed in the O tasks were previously trained to execute the same grasping movements they were asked to observe. Thus, area 31 may be involved in the retrieval of memories, if any, relative to the event occuring in the immediate scene (i.e. monkeys retrieve memories of themselves performing grasping movements, while observing them) and in the atribution of action to another agent and not to the self. It is also interesting to note that area F7 of the dorsal premotor cortex which is connected with area 31 (Morecraft et al., 2004), has also been found to be activated only in the observation and not in the execution tasks (Raos et al., 2007).

Similarly, the activation of area V6A only in the execution and not in observation tasks, could contribute in attributing the action of grasping to the self and not to another agent (the experimenter).

Area 5IPp

Area 5IPp is an area which we report for the first time in the literature. It is located in the caudalmost part of the medial bank of the IPs, adjacent to the fundus. It only partially corresponds to area PIP which lies at the posterior part of the IPs where it joins the POs.

Area PIP, is considered a motion sensitive area (Vanduffel et al., 2001), integrating shape information by cross modal (tactile and visual) matching (Saito et al., 2003) and providing crucial object information useful in reaching and grasping (Durand et al., 2007).

Our results demonstrate bilateral activation of area 5IPp during the grasping-execution tasks, performed either under visual guidance (23% LCGU difference from Cm for the left and 26% from Cm for the right hemispheres of the EL monkeys), or in complete darkness (13% difference for both hemispheres of the ED monkeys compared to Cd).

These data are in accord with the aforementioned reports and it is suggested that area 5IPp participates in the visual and somatosensory quidance of the reaching-to-grasp behaviour, by integrating object shape and object positional information from different sensory modalities.

The involvement of 5IPp only in grasping-execution and not in grasping-observation, as similarly observed in area V6Ad, imply that these areas may also contribute in attributing the action to the self (monkey) and not to another agent (the experimenter).

"Observation and execution of grasping of three dimensional objects in presence and in absence of visual information. In vivo functional mapping of the monkey brain cortical areas involved, by the use of the quantitative autoradiographic method of 2 [^{14}C]-deoxyglucose".

Laboratory of Functional Brain Imaging, Department of Basic Sciences, Faculty of Medicine, School of Health Sciences, University of Crete

SUMMARY

The aim of the present study was to elucidate the cortical regions that are activated during grasping execution in the presence or absence of visual information, as well as the ones implicated in grasping observation. For this reason, we employed the quantitative autoradiographic method of 2 [^{14}C]-deoxyglucose (2DG). This method uses radioactive deoxyglucose, an analog of glucose, to trace glucose consumption and therefore local functional activity, since glucose is the main source of energy for brain cells. Furthermore, it provides direct quantitative assessment of the brain activity based on glucose consumption, has the highest spatial resolution (20μm) as compared to other imaging methods and allows the identification of the affected cortical areas by means of cytoarchitectonic criteria.

The 2DG method was applied in *Macaca mulatta* monkeys, trained at the following tasks:

a) execution of grasping in light (EL),
b) execution of grasping in dark (ED),
c) observation of grasping performed by the experimenter (O),
d) observation of the experimenter's hand reaching towards the behavioural apparatus with hand/fingers extended (Cm), and
e) exposure to experimental conditions similar to the ED task, without grasping execution (Cd).

In this study we focused on the cortical areas located in the medial parietal convexity, the anterior bank of the parietooccipital cortex and the posterior part of the medial intraparietal bank namely V6, V6A, 5IPp, PGm/7m, area 31 and retrosplenial cortex (areas 29 and 30).

The net activations induced by the EL task, involve areas 5IPp, PGm/7m, RSC and V6 at both hemispheres, and area V6Ad at the hemisphere contralateral to the moving forelimb. The ED task influenced the metabolic activity in areas V6Ad and

PGm/7m contralaterally and 5IPp and V6 bilaterally. The O task increased the metabolic activity of areas PGm/7m, 31, RSC and V6 at both hemispheres.
Common activations for the EL and the O tasks were observed in RSC and PGm/7m at both hemispheres. Execution of grasping in light or in dark (EL and ED tasks), induced common activations in areas V6Ad and PGm/7m at the contralateral hemispheres and in area 5IPp and part of area V6 at both hemispheres.

As far as area V6 is concerned, it could be involved in the visual and somatosensory quidance of grasping movements. In support with this view are its connections with arm-related areas such as MIP and V6A which in turn project to premotor area 6.

The contralateral activation of area V6A only in the grasping-execution tasks, demonstrates that V6A is related with the execution of grasping only and not with the observation of the same action. Presumably, the arm-movement related activity observed in the dorsal part of V6A, corresponds to neurons that integrate motor-signals related to arm movements with somatosensory signals evoked by these movements, in the service of online quidance of the reaching-to-grasp behaviour.

Area PGm/7m which was found bilaterally activated during the EL and O tasks and contralaterally activated during the ED tasks, may be involved in the combination of visuomanual and oculomotor signals for the composition of motor commands (based on kinesthetic and visual signals) for movement generation. The higher metabolic activity observed in this area for the execution tasks as compared to the observation task, may be an indication for the stronger involvement of this area in execution than in recognition of actions.

Area 31, which was activated only during observation and not during execution of grasping, may contribute to memory proccesses and in attribution of an action (i.e. grasping) to another agent and not to the self. Similarly, area V6A which was activated during execution and not during observation of the reaching-to-grasp behaviour, could also be involved in the attribution of grasping to the performer (self) and not to another agent.

The RSC which was bilaterally activated during the EL and the O tasks, may process contextual associations during object recognition, encoding the current salience of objects in the immediate (visual) scene for orienting and navigating towards them. Also it may be involved in topographic spatial navigation, for situating oneself within a larger environment, using the immediate scene as a cue.

Area 5IPp is an area which is reported for the first time in the literature and only partially corresponds to area PIP. The strong bilateral involvement of area 5IPp in the grasping execution tasks performed either in light or in darkness, suggests that

this area could participate in the visual and somatosensory quidance of the reaching-to-grasp behaviour. More specifically, it could be implicated in providing object positional information, useful for reaching, and object feature/shape information by cross modal (visual and tactile) matching, useful for grasping. The involvement of area 5IPp only in execution and not in observation tasks, implies a possible role of this area in the attribution of an action to the performer (i.e. the monkey) and not to another agent (i.e. the experimenter).

«Αναγνώριση και εκτέλεση κινήσεων σύλληψης τρισδιάστατων αντικειμένων με την άκρα χείρα παρουσία και απουσία οπτικής πληροφορίας. In vivo λειτουργική χαρτογράφηση των εμπλεκόμενων περιοχών του φλοιού εγκεφάλου πιθήκου με τη χρήση της ποσοτικής αυτοραδιογραφικής μεθόδου της 2-[^{14} C] δεοξυγλυκόζης».

Εργαστήριο Λειτουργικής Απεικόνισης του Εγκεφάλου, Τομέας Βασικών Επιστημών, Τμήμα Ιατρικής, Σχολή Επιστημών Υγείας, Πανεπιστήμιο Κρήτης

ΠΕΡΙΛΗΨΗ

Η αλληλεπίδραση των χεριών μας με αντικείμενα που βρίσκονται στον εξωπροσωπικό χώρο αποτελεί συνηθισμένη καθημερινή μας συμπεριφορά. Η αλληλεπίδραση αυτή άλλοτε είναι φαινομενικά απλή και άλλοτε δύσκολη, ειδικά όταν περιλαμβάνει συγκεκριμένες αλληλουχίες επιμέρους κινήσεων και δεξιότεχνες κινήσεις των δακτύλων ώστε να εκτελεστεί σωστά. Και στις δυο παραπάνω περιπτώσεις, η κίνηση προσαρμόζεται ανάλογα με τις τρέχουσες ανάγκες και τις συνθήκες του περιβάλλοντος έτσι ώστε να είναι ακριβής και αποτελεσματική.

Είναι γνωστό ότι η πραγματοποίηση κινήσεων με την άκρα χείρα περιλαμβάνει δυο διακριτές διαδικασίες, τη φάση προσέγγισης του χεριού προς το αντικείμενο-στόχο και τη φάση σύλληψης του αντικειμένου-στόχου, κατά την οποία ο προσανατολισμός και η διαμόρφωση του χεριού προσαρμόζονται ανάλογα με τη φόρμα και την θέση του αντικειμένου στο χώρο, ώστε η κίνηση να εκτελεστεί με επιτυχία.

Η καθοδήγηση του χεριού προς το αντικείμενο-στόχο γίνεται ανάλογα με τις συνθήκες του περιβάλλοντος. Πιο συγκεκριμένα, όταν η εκτέλεση της κίνησης σύλληψης αντικειμένου με την άκρα χείρα πραγματοποιείται υπό οπτική καθοδήγηση, τότε τόσο οπτικά ερεθίσματα που παρέχουν πληροφορίες για τη θέση του αντικειμένου-στόχου στον εξωπροσωπικό χώρο και για τη σχετική απόσταση αυτού από το χέρι, όσο και σωματαισθητικά ερεθίσματα που παρέχουν πληροφορίες για την τρέχουσα θέση του κινούμενου χεριού, συνεπικουρούν ώστε η κίνηση αυτή να εκτελεστεί με ακρίβεια. Όταν η εκτέλεση της παραπάνω κίνησης πραγματοποιείται σε περιβάλλον από το οποίο απουσιάζουν οπτικά δεδομένα, όπως όταν η κίνηση πραγματοποιείται στο σκοτάδι, τότε είναι προφανές ότι θα υπάρξει μερική διαφοροποίηση στο είδος των ερεθισμάτων που θα συμβάλλουν στην σωστή καθοδήγηση του χεριού προς το αντικείμενο-στόχο. Στην περίπτωση αυτή, η συμβολή σωματαισθητικών δεδομένων και κιναισθητικών απομνημονευμάτων (proprioceptive memories) της θέσης του αντικειμένου στο χώρο και της κίνησης

σύλληψης προς αυτό, είναι καθοριστική στην επιτυχή εκτέλεση αυτής της κινητικής συμπεριφοράς.

Ένας ακόμη παράγοντας που συντελεί στην επιτυχή εκτέλεση μιας κίνησης σύλληψης είναι και η πρότερη εμπειρία. Είναι γνωστό ότι μια κινητική συμπεριφορά π.χ. μια κίνηση σύλληψης αντικειμένου, είναι πιο ακριβής και επιτυχημένη στην εκτέλεσή της όταν έχει υπάρξει πρότερη εμπειρία αυτής, είτε μέσω εκτέλεσής της, είτε μέσω παρατήρησης της ίδιας κίνησης επιτελούμενης από άλλο υποκείμενο. Κατά την άποψη πολλών ερευνητών, το ανθρώπινο κινητικό σύστημα μέσω της παρατήρησης χρησιμοποιεί της εμπειρίες άλλων για να κατασκευάσει το δικό του κινητικό ρεπερτόριο.

Από τα παραπάνω φαίνεται ότι η πραγματοποίηση μιας φαινομενικά απλής συμπεριφοράς, όπως είναι η κίνηση σύλληψης με την άκρα χείρα, επιτυγχάνεται με την ενεργοποίηση πολυάριθμων εγκεφαλικών περιοχών που η καθεμιά ξεχωριστά θα συμβάλλει ώστε η κίνηση ανάλογα με τις τρέχουσες συνθήκες να επιτελεστεί επιτυχημένα και με ακρίβεια.

Για την αποκάλυψη φλοιικών περιοχών εγκεφάλου πιθήκου που εμπλέκονται στην παρακολούθηση και εκτέλεση κινήσεων σύλληψης με την άκρα χείρα, παρουσία και απουσία οπτικής πληροφορίας, χρησιμοποιήσαμε την ποσοτική αυτοραδιογραφική μέθοδο της [^{14}C]-δεοξυγλυκόζης.

Η συγκεκριμένη μέθοδος επιτρέπει την άμεση εκτίμηση της μεταβολικής δραστηριότητας μιας εγκεφαλικής περιοχής, υπολογίζοντας ποσοτικά την τοπική κατανάλωση δεοξυγλυκόζης (DG), ραδιενεργού χημικού αναλόγου της γλυκόζης, η οποία ως γνωστό αποτελεί τη βασική πηγή ενέργειας για τα μεταβολικά δραστήρια νευρικά κύτταρα. Επίσης η μέθοδος αυτή, σε σχέση με όλες τις άλλες σύγχρονες νευρο-απεικονιστικές μεθόδους, διαθέτει την υψηλότερη χωρική διακρισιμότητα των εγκεφαλικών περιοχών (20μm) και δίνει τη δυνατότητα ταυτοποίησης των εμπλεκόμενων σε κάθε συνθήκη περιοχών με κυτταροαρχιτεκτονικά κριτήρια.

Η παραπάνω μέθοδος εφαρμόστηκε σε πιθήκους Macaca mulatta, οι οποίοι είχαν εκπαιδευτεί στις παρακάτω δοκιμασίες:

α) Εκτέλεση κίνησης σύλληψης τρισδιάστατων αντικειμένων με την άκρα χείρα στο φώς (EL),

β) Εκτέλεση κίνησης σύλληψης με την άκρα χείρα στο σκοτάδι (ED) και

γ) Παρατήρηση κίνησης σύλληψης τρισδιάστατου αντικειμένου, πραγματοποιούμενης από τον πειραματιστή (O),

δ) Παρατήρηση κίνησης προσέγγισης του άνω άκρου του πειραματιστή με τεντωμένα τα δάκτυλα του χεριού χωρίς να πραγματοποιείται κίνηση σύλληψης (control of biological motion, Cm) και

ε) Παραμονή στο σκοτάδι σε συνθήκες όμοιες με εκείνες της δοκιμασίας ED με δυνατότητα κίνησης των οφθαλμών ελεύθερα στο χώρο (control dark, Cd). Ο ένας από τους πιθήκους αναφοράς της ομάδας αυτής προσλάμβανε νερό ως ανταμοιβή σε τυχαία χρονικά διαστήματα, ενώ ο άλλος δεν έπαιρνε καμία ανταμοιβή.

Όλες οι διαδικασίες χειρισμού των πειραματοζώων, ήταν σύμφωνες με τις ισχύουσες νομοθεσίες τόσο των ελληνικών όσο και των ευρωπαϊκών αρμόδιων αρχών.

Στις δοκιμασίες EL, ED, O και Cm, το βλέμμα των πειραματοζώων ήταν εστιασμένο ευθεία μπροστά, σε ένα νοητό κυκλικό παράθυρο διαμέτρου 8 deg.

Ο αριθμός των κινήσεων σύλληψης που είτε πραγατοποιήθηκαν είτε παρατηρήθηκαν από τα πειραματόζωα κατά τη διάρκεια της πειραματικής διαδικασίας ήταν παρόμοιος, ώστε τα συγκριτικά αποτελέσματα των διαφορών στη μεταβολική δραστηριότητα ανά εγκεφαλική περιοχή και ανά δοκιμασία να είναι αξιόπιστα και με στατιστικώς σημαντική βαρύτητα. Μόνο διαφορές άνω του 7% ελήφθησαν υπόψη ως στατιστικώς σημαντικές στην παρούσα μελέτη, με δεδομένο ότι η διαφορά στη μεταβολική δραστηριότητα μεταξύ ομολόγων περιοχών των δύο ημισφαιρίων εγκεφάλου πιθήκου σε κατάσταση ηρεμίας μπορεί να φτάσει έως και 7%.

Μετά το τέλος της πειραματικής διαδικασίας, τα εγκεφαλικά ημισφαίρια, η παρεγκεφαλίδα και τμήμα του νωτιαίου μυελού αφαιρέθηκαν, πάγωσαν με τη χρήση διαλύματος ισοπεντανίου σε θερμοκρασία κυμαινόμενη μεταξύ -45^0C και -50^0C και διατηρήθηκαν στους -80^0C. Οι σειριακές οριζόντιες εγκεφαλικές τομές πάχους 20μm που συλλέχθηκαν, εκτέθηκαν σε αυτοραδιογραφικά φιλμ και στη συνέχεια ψηφιοποιήθηκαν με τη βοήθεια υπολογιστικά υποστηριζόμενου συστήματος ανάλυσης εικόνας.

Ακόλουθα, μετρήθηκε η τοπική κατανάλωση της δεοξυγλυκόζης (LCGU) στις περιοχές που αφορούσαν την παρούσα μελέτη, τομή προς τομή και pixel προς pixel και δημιουργήθηκαν δισδιάστατοι χάρτες που καλύπτουν ολόκληρη την ραχιαιοκοιλιακή και προσθιοπίσθια έκταση των αναλυόμενων περιοχών και αναπαριστούν τη χωρική κατανομή της μεταβολικής δραστηριότητας σε αυτές.

Λόγω ανατομικών διαφοροποιήσεων που υπάρχουν μεταξύ των εγκεφαλικών ημισφαιρίων διαφορετικών πιθήκων, ακολούθησε γεωμετρική κανονικοποίηση των χαρτών αυτών με βάση ένα χάρτη αναφοράς. Ο χάρτης αναφοράς προέκυψε από το μέσον όρο κυτταροαρχιτεκτονικών και ανατομικών σημείων αναφοράς που συλλέχθησαν από το σύνολο των ημισφαιρίων των ζώων που έλαβαν μέρος στη μελέτη αυτή. Με την κανονικοποίηση όλων των δισδιάστατων χαρτών με βάση το χάρτη αναφοράς, μπορεί να γίνει άμεση σύγκριση της μεταβολικής δραστηριότητας όλων των προς μελέτη φλοιϊκών περιοχών σε όλα τα εγκεφαλικά ημισφαίρια και να εξαχθούν ασφαλή συμπεράσματα.

Οι εγκεφαλικές περιοχές που αναλύθηκαν στην παρούσα μελέτη, είναι εκείνες που βρίσκονται στην πρόσθια όχθη της βρεγματοϊνιακής αύλακας (POs) και στον γειτνιάζοντα φλοιό, όπως επίσης και σε περιοχές της έσω επιφάνειας του εγκεφάλου. Πιο συγκεκριμένα, οι περιοχές που αναλύθηκαν είναι οι V6, V6A, PGm/7m, η περιοχή 31, οι περιοχές 29 και 30 και η περιοχή 5IPp η οποία περιγράφεται για πρώτη φορά και καταλαμβάνει μέρος της οπίσθιας ενδοβρεγματικής περιοχής (PIP).

Όσον αφορά την περιοχή V6, τα αποτελέσματα δείχνουν ότι υπάρχει αμφίπλευρη ενεργοποίησή της, τόσο κατά την εκτέλεση κινήσεων σύλληψης, όσο και κατά την παρακολούθηση της ίδιας κίνησης όταν πραγματοποιείται από τον πειραματιστή. Με δεδομένο ότι αυτή η περιοχή συνδέεται με οπτικές εγκεφαλικές περιοχές και προβάλλει σε περιοχές σχετιζόμενες με την κίνηση των άνω άκρων, όπως η έσω ενδοβρεγματική περιοχή (MIP) και η V6A, καθώς και σε άλλες οι οποίες κωδικοποιούν τη θέση των αντικειμένων-στόχων στο χώρο, όπως η V6A και η κοιλιακή ενδοβρεγματική περιοχή (VIP), θα μπορούσε να συμβάλλει στην οπτική αλλά και στην σωματαισθητική καθοδήγηση των κινήσεων σύλληψης.

Στην περιοχή V6A, και ειδικά στο ραχιαίο τμήμα της (V6Ad), παρατηρήθηκε αντίπλευρη (στο κινούμενο χέρι) ενεργοποίηση, κατά την εκτέλεση κινήσεων σύλληψης τόσο στο φώς όσο και στο σκοτάδι. Το γεγονός ότι δεν παρατηρήθηκε αυξημένη μεταβολική δραστηριότητα στην περιοχή αυτή κατά την παρατήρηση εκτέλεσης κινήσεων σύλληψης από τον πειραματιστή, δείχνει ότι η V6Ad συμβάλλει στην εκτέλεση της κίνησης. Το παραπάνω εύρημα είναι σύμφωνο με προγενέστερα βιβλιογραφικά δεδομένα που αναφέρουν ότι η κίνηση σύλληψης αντικειμένου επηρεάζει την δραστηριότητα των νευρωνικών πληθυσμών της περιοχής αυτής, καθώς επίσης και ότι στη V6A υπάρχουν σωματαισθητικά κύτταρα με υποδεκτικά πεδία σε άπω και εγγύς τμήματα του αντίπλευρου άνω άκρου. Μελέτες εγκεφαλικών βλαβών σε πιθήκους και ανθρώπους, συνδέουν την ελατωματική συμπεριφορά κατά την εκτέλεση κινήσεων προσέγγισης και σύλληψης, όπως επίσης και την οπτική αταξία, με βλάβες εντοπισμένες στη V6A. Με βάση τα παραπάνω, φαίνεται ότι η περιοχή αυτή εμπλέκεται στον έλεγχο των κινήσεων σύλληψης με την άκρα χείρα, πιθανότατα ολοκληρώνοντας κινητικά και σωματαισθητικά ερεθίσματα για τη σύγχρονη (online) καθοδήγηση αυτής της κινητικής συμπεριφοράς.

Η περιοχή PGm/7m παρουσίασε αμφίπλευρα αυξημένη μεταβολική δραστηριότητα, τόσο κατά την εκτέλεση οπτικά καθοδηγούμενων κινήσεων σύλληψης, όσο και κατά την παρατήρηση αυτών. Τα αποτελέσματα αυτά σε συνδυασμό με βιβλιογραφικά δεδομένα δείχνουν ότι οι νευρώνες της PGm/7m συνδυάζουν οπτικά δεδομένα σχετικά με την κίνηση του χεριού (visuomanual) με οφθαλμοκινητικά δεδομένα, με

σκοπό τη σύνθεση εντολών (βασιζόμενων σε κιναισθητικά και οπτικά ερεθίσματα) για την πρόκληση της κίνησης.

Οι περιοχές 29 και 30, που αποτελούν το φλοιό του σπληνίου (RSC), βρέθηκαν αμφίπλευρα ενεργοποιημένες τόσο κατά την παρατήρηση, όσο και κατά την εκτέλεση οπτικά καθοδηγούμενων κινήσεων σύλληψης και πιθανά εμπλέκονται στην τοπογραφική χωρική πλοήγηση για την επίγνωση της θέσης ενός ατόμου (του παρατηρητή) στον περιβάλλοντα χώρο. Επίσης οι περιοχές αυτές θα μπορούσαν να κωδικοποιούν την τρέχουσα σημασία αντικειμένων ή γεγονότων στο άμεσο περιβάλλον και να συντελούν στην καθοδήγηση και τον προσανατολισμό προς αυτά.

Η περιοχή 31 εμφάνισε αυξημένη μεταβολική δραστηριότητα μόνο κατά τη διάρκεια της παρατήρησης κινήσεων σύλληψης που πραγματοποιούνταν από τον πειραματιστή. Η αύξηση στην κατανάλωση της δεοξυγλυκόζης ήταν αμφίπλευρη. Τα αποτελέσματα αυτά είναι συμβατά με προηγούμενες μελέτες που συνδέουν την περιοχή 31 με μνημονικές διαδικασίες και στην απόδοση μιας κινητικής συμπεριφοράς σε ένα τρίτο πρόσωπο, δηλαδή στην επίγνωση ότι κάποιος άλλος εκτελεί μια κίνηση σύλληψης. Στην παραπάνω υπόθεση συμβάλλει το γεγονός ότι η περιοχή αυτή παρουσίασε υψηλούς μεταβολικούς ρυθμούς (κατανάλωση δεοξυγλυκόζης) μόνο κατά τη διαδικασία της παρατήρησης (Ο) και όχι κατά την εκτέλεση της κίνησης. Αντίστοιχα και η περιοχή V6A η οποία έχει αυξημένη μεταβολική δραστηριότητα μόνο κατά την εκτέλεση κίνησης σύλληψης και όχι κατά την παρατήρησή της, θα μπορούσε να εμπλέκεται στην απόδοση της κινητικής αυτής συμπεριφοράς σε αυτόν που την πραγματοποιεί (εαυτό) και όχι σε κάποιο τρίτο πρόσωπο.

Η περιοχή 5IPp, η οποία καταλαμβάνει μέρος της οπίσθιας ενδοβρεγματικής περιοχής (PIP) και περιγράφεται για πρώτη φορά στην παρούσα μελέτη, παρουσίασε έντονη μεταβολική δραστηριότητα κατά την εκτέλεση κινήσεων σύλληψης τόσο παρουσία όσο και απουσία οπτικής πληροφορίας. Η δραστηριότητα αυτή ήταν έντονη και στα δύο ημισφαίρια των πιθήκων που εκτελούσαν τις προαναφερθείσες συμπεριφορές. Η δραστηριότητα της περιοχής αυτής κατά την εκτέλεση και όχι κατά την παρατήρηση της κίνησης σύλληψης, σε συνδυασμό με παλαιότερα βιβλιογραφικά δεδομένα που αναφέρουν ότι στην PIP γίνεται ολοκλήρωση της πληροφορίας για το σχήμα (με «ταίριασμα» οπτικών και απτικών δεδομένων), συγκλίνουν στην ιδέα ότι σε αυτή την περιοχή λαμβάνει χώρα η ολοκλήρωση (απαρτίωση) της πληροφορίας που αφορά το σχήμα, αλλά και ταυτόχρονα η απόδοση της κινητικής συμπεριφοράς σε αυτόν που την επιτελεί.

BIBLIOGRAPHY

Baker JT, Patel GH, Corbetta M, Snyder LH (2006) Distribution of activity across the monkey cerebral cortical surface, thalamus and midbrain during rapid, visually guided saccades. Cereb Cortex 16:447-459.

Bar M, Aminoff E (2003) Cortical analysis of visual context. Neuron 38:347-358.

Battaglini PP, Muzur A, Skrap M (2003) Visuomotor deficits and fast recovery after area V6A lesion in monkeys. Behav Brain Res 139:115-122.

Battaglini PP, Muzur A, Galletti C, Skrap M, Brovelli A, Fattori P (2002) Effects of lesions to area V6A in monkeys. Exp Brain Res 144:419-422.

Binkofski F, Buccino G, Dohle C, Seitz RJ, Freund HJ (1999) Mirror agnosia and mirror ataxia constitute different parietal lobe disorders. Ann Neurol 46:51-61.

Breveglieri R, Kutz DF, Fattori P, Gamberini M, Galletti C (2002) Somatosensory cells in the parieto-occipital area V6A of the macaque. Neuroreport 13:2113-2116.

Caminiti R, Genovesio A, Marconi B, Mayer AB, Onorati P, Ferraina S, Mitsuda T, Giannetti S, Squatrito S, Maioli MG, Molinari M (1999) Early coding of reaching: frontal and parietal association connections of parieto-occipital cortex. Eur J Neurosci 11:3339-3345.

Cavada C, Goldman-Rakic PS (1989a) Posterior parietal cortex in rhesus monkey: I. Parcellation of areas based on distinctive limbic and sensory corticocortical connections. J Comp Neurol 287:393-421.

Cavada C, Goldman-Rakic PS (1989b) Posterior parietal cortex in rhesus monkey: II. Evidence for segregated corticocortical networks linking sensory and limbic areas with the frontal lobe. J Comp Neurol 287:422-445.

Cavada C, Goldman-Rakic PS (1991) Topographic segregation of corticostriatal projections from posterior parietal subdivisions in the macaque monkey. Neuroscience 42:683-696.

Choo IH, Lee DY, Youn JC, Jhoo JH, Kim KW, Lee DS, Lee JS, Woo JI (2007). Topographic patterns of brain functional impairment progression according to clinical severity staging in 116 Alzheimer disease patients: FDG-PET study. Alzheimer Dis Assoc Disord 21(2):77-84

Colby CL, Duhamel JR (1991) Heterogeneity of extrastriate visual areas and multiple parietal areas in the macaque monkey. Neuropsychologia 29:517-537.

Colby CL, Gattass R, Olson CR, Gross CG (1988) Topographical organization of cortical afferents to extrastriate visual area PO in the macaque: a dual tracer study. J Comp Neurol 269:392-413.

Colby CL, Gattass R, Olson CR, Gross CG (1983) Cortical afferents to visual area PO in the macaque. Soc Neurosci Abstr 8:681

Covey ER, Gattass R, Gross CG (1982) A new visual area in the parieto-occipital sulcus of the macaque. Soc Neurosci Abstr 8:861

Dalezios Y, Raos VC, Savaki HE (1996) Metabolic activity pattern in the motor and somatosensory cortex of monkeys performing a visually guided reaching task with one forelimb. Neuroscience 72:325-333.

Dean HL, Crowley JC, Platt ML (2004) Visual and saccade-related activity in macaque posterior cingulate cortex. J Neurophysiol 92:3056-3068.

Duhamel JR, Bremmer F, BenHamed S, Graf W (1997) Spatial invariance of visual receptive fields in parietal cortex neurons. Nature 389:845-848.

Durand JB, Nelissen K, Joly O, Wardak C, Todd JT, Norman JF, Janssen P, Vanduffel W, Orban GA (2007) Anterior regions of monkey parietal cortex process visual 3D shape. Neuron 55:493-505.

Epstein RA, Parker WE, Feiler AM (2007) Where am I now? Distinct roles for parahippocampal and retrosplenial cortices in place recognition. J Neurosci 27:6141-6149.

Fattori P, Gamberini M, Mussio A, Breveglieri R, Kutz DF, Galletti C (1999) A visual-to-motor gradient within area V6A of the monkey parieto-occipital cortex. Neurosci Lett Supplement 52, S22

Fattori P, Gamberini M, Kutz DF, Galletti C (2001) 'Arm-reaching' neurons in the parietal area V6A of the macaque monkey. Eur J Neurosci 13:2309-2313.

Fattori P, Breveglieri R, Amoroso K, Galletti C (2004) Evidence for both reaching and grasping activity in the medial parieto-occipital cortex of the macaque. Eur J Neurosci 20:2457-2466.

Fattori P, Kutz DF, Breveglieri R, Marzocchi N, Galletti C (2005) Spatial tuning of reaching activity in the medial parieto-occipital cortex (area V6A) of macaque monkey. Eur J Neurosci 22:956-972.

Faugier-Grimaud S, Frenois C, Stein DG (1978) Effects of posterior parietal lesions on visually guided behavior in monkeys. Neuropsychologia 16:151-168.

Felleman DJ, Burkhalter A, Van Essen DC (1997) Cortical connections of areas V3 and VP of macaque monkey extrastriate visual cortex. J Comp Neurol 379:21-47.

Ferraina S, Garasto MR, Battaglia-Mayer A, Ferraresi P, Johnson PB, Lacquaniti F, Caminiti R (1997a) Visual control of hand-reaching movement: activity in parietal area 7m. Eur J Neurosci 9:1090-1095.

Ferraina S, Johnson PB, Garasto MR, Battaglia-Mayer A, Ercolani L, Bianchi L, Lacquaniti F, Caminiti R (1997b) Combination of hand and gaze signals during reaching: activity in parietal area 7 m of the monkey. J Neurophysiol 77:1034-1038.

Gattass R, Souza APB, Covey E (1985) Cortical visual areas of the macaque: possible substrates for pattern recognition mechanisms. Pontificiae Academiae Scientiarum Scripta Varia 54

Galletti C, Fattori P (2003) Neuronal mechanisms for detection of motion in the field of view. Neuropsychologia 41:1717-1727.

Galletti C, Battaglini PP, Fattori P (1991) Functional Properties of Neurons in the Anterior Bank of the Parieto-occipital Sulcus of the Macaque Monkey. Eur J Neurosci 3:452-461.

Galletti C, Battaglini PP, Fattori P (1993) Parietal neurons encoding spatial locations in craniotopic coordinates. Exp Brain Res 96:221-229.

Galletti C, Battaglini PP, Fattori P (1995) Eye position influence on the parieto-occipital area PO (V6) of the macaque monkey. Eur J Neurosci 7:2486-2501.

Galletti C, Fattori P, Kutz DF, Battaglini PP (1997) Arm movement-related neurons in the visual area V6A of the macaque superior parietal lobule. Eur J Neurosci 9:410-413.

Galletti C, Fattori P, Gamberini M, Kutz DF (1999a) The cortical visual area V6: brain location and visual topography. Eur J Neurosci 11:3922-3936.

Galletti C, Fattori P, Kutz DF, Gamberini M (1999b) Brain location and visual topography of cortical area V6A in the macaque monkey. Eur J Neurosci 11:575-582.

Galletti C, Fattori P, Battaglini PP, Shipp S, Zeki S (1996) Functional demarcation of a border between areas V6 and V6A in the superior parietal gyrus of the macaque monkey. Eur J Neurosci 8:30-52.

Galletti C, Gamberini M, Kutz DF, Fattori P, Luppino G, Matelli M (2001) The cortical connections of area V6: an occipito-parietal network processing visual information. Eur J Neurosci 13:1572-1588.

Goldman-Rakic PS, Selemon LD, Schwartz ML (1984) Dual pathways connecting the dorsolateral prefrontal cortex with the hippocampal formation and parahippocampal cortex in the rhesus monkey. Neuroscience 12:719-743.

Grezes J, Decety J (2001) Functional anatomy of execution, mental simulation, observation, and verb generation of actions: a meta-analysis. Hum Brain Mapp 12:1-19.

Hari R, Forss N, Avikainen S, Kirveskari E, Salenius S, Rizzolatti G (1998) Activation of human primary motor cortex during action observation: a neuromagnetic study. Proc Natl Acad Sci U S A 95:15061-15065.

Iaria G, Chen JK, Guariglia C, Ptito A, Petrides M (2007) Retrosplenial and hippocampal brain regions in human navigation: complementary functional contributions to the formation and use of cognitive maps. Eur J Neurosci 25:890-899.

Ino T, Doi T, Hirose S, Kimura T, Ito J, Fukuyama H (2007) Directional disorientation following left retrosplenial hemorrhage: a case report with fMRI studies. Cortex 43:248-254.

Johnson PB, Ferraina S, Caminiti R (1993) Cortical networks for visual reaching. Exp Brain Res 97:361-365.

Johnson PB, Ferraina S, Bianchi L, Caminiti R (1996) Cortical networks for visual reaching: physiological and anatomical organization of frontal and parietal lobe arm regions. Cereb Cortex 6:102-119.

Johnson SC, Baxter LC, Wilder LS, Pipe JG, Heiserman JE, Prigatano GP (2002) Neural correlates of self-reflection. Brain 125:1808-1814.

Karnath HO, Perenin MT (2005) Cortical control of visually guided reaching: evidence from patients with optic ataxia. Cereb Cortex 15:1561-1569.

Kennedy C, Sakurada O, Shinohara M, Jehle J, Sokoloff L (1978) Local cerebral glucose utilization in the normal conscious macaque monkey. Ann Neurol 4:293-301.

Kobayashi Y, Amaral DG (2003) Macaque monkey retrosplenial cortex: II. Cortical afferents. J Comp Neurol 466:48-79.

Kobayashi Y, Amaral DG (2007) Macaque monkey retrosplenial cortex: III. Cortical efferents. J Comp Neurol 502:810-833.

Kutz DF, Fattori P, Gamberini M, Breveglieri R, Galletti C (2003) Early- and late-responding cells to saccadic eye movements in the cortical area V6A of macaque monkey. Exp Brain Res 149:83-95.

Leichnetz GR (2001) Connections of the medial posterior parietal cortex (area 7m) in the monkey. Anat Rec 263:215-236.

Lewis JW, Van Essen DC (2000) Corticocortical connections of visual, sensorimotor, and multimodal processing areas in the parietal lobe of the macaque monkey. J Comp Neurol 428:112-137.

Luppino G, Hamed SB, Gamberini M, Matelli M, Galletti C (2005) Occipital (V6) and parietal (V6A) areas in the anterior wall of the parieto-occipital sulcus of the macaque: a cytoarchitectonic study. Eur J Neurosci 21:3056-3076.

Maddock RJ, Garrett AS, Buonocore MH (2001) Remembering familiar people: the posterior cingulate cortex and autobiographical memory retrieval. Neuroscience 104:667-676.

Marconi B, Genovesio A, Battaglia-Mayer A, Ferraina S, Squatrito S, Molinari M, Lacquaniti F, Caminiti R (2001) Eye-hand coordination during reaching. I. Anatomical relationships between parietal and frontal cortex. Cereb Cortex 11:513-527.

Matelli M, Luppino G (2001) Parietofrontal circuits for action and space perception in the macaque monkey. Neuroimage 14:S27-32.

Matelli M, Govoni P, Galletti C, Kutz DF, Luppino G (1998) Superior area 6 afferents from the superior parietal lobule in the macaque monkey. J Comp Neurol 402:327-352.

Matsunami K, Kawashima T, Satake H (1989) Mode of [14C] 2-deoxy-D-glucose uptake into retrosplenial cortex and other memory-related structures of the monkey during a delayed response. Brain Res Bull 22:829-838.

Mattar AA, Gribble PL (2005) Motor learning by observing. Neuron 46:153-160.

Minoshima S, Giordani B, Berent S, Frey KA, Foster NL, Kuhl DE (1997) Metabolic reduction in the posterior cingulate cortex in very early Alzheimer's disease. Ann Neurol 42:85-94.

Morecraft RJ, Cipolloni PB, Stilwell-Morecraft KS, Gedney MT, Pandya DN (2004) Cytoarchitecture and cortical connections of the posterior cingulate and adjacent somatosensory fields in the rhesus monkey. J Comp Neurol 469:37-69.

Morris R, Petrides M, Pandya DN (1999) Architecture and connections of retrosplenial area 30 in the rhesus monkey (Macaca mulatta). Eur J Neurosci 11:2506-2518.

Nakamura K, Chung HH, Graziano MS, Gross CG (1999) Dynamic representation of eye position in the parieto-occipital sulcus. J Neurophysiol 81:2374-2385.

Nelson CA, Greer WE, Morris MD (1984) The distribution of serum high density lipoprotein subfractions in non-human primates. Lipids 19:656-663.

Olson CR, Musil SY, Goldberg ME (1996) Single neurons in posterior cingulate cortex of behaving macaque: eye movement signals. J Neurophysiol 76:3285-3300.

Pandya DN, Seltzer B (1982) Intrinsic connections and architectonics of posterior parietal cortex in the rhesus monkey. J Comp Neurol 204:196-210.

Parvizi J, Van Hoesen GW, Buckwalter J, Damasio A (2006) Neural connections of the posteromedial cortex in the macaque. Proc Natl Acad Sci U S A 103:1563-1568.

Petrides M, Pandya DN (1984) Projections to the frontal cortex from the posterior parietal region in the rhesus monkey. J Comp Neurol 228:105-116.

Petrides M, Alivisatos B, Evans AC, Meyer E (1993) Dissociation of human mid-dorsolateral from posterior dorsolateral frontal cortex in memory processing. Proc Natl Acad Sci U S A 90:873-877.

Raffi M, Squatrito S, Maioli MG (2007) Gaze and smooth pursuit signals interact in parietal area 7m of the behaving monkey. Exp Brain Res 182:35-46.

Raos V, Evangeliou MN, Savaki HE (2004) Observation of action: grasping with the mind's hand. Neuroimage 23:193-201.

Raos V, Evangeliou MN, Savaki HE (2007) Mental simulation of action in the service of action perception. J Neurosci 27:12675-12683.

Raos V, Franchi G, Gallese V, Fogassi L (2003) Somatotopic organization of the lateral part of area F2 (dorsal premotor cortex) of the macaque monkey. J Neurophysiol 89:1503-1518.

Saito DN, Okada T, Morita Y, Yonekura Y, Sadato N (2003) Tactile-visual cross-modal shape matching: a functional MRI study. Brain Res Cogn Brain Res 17:14-25.

Savaki HE, Raos VC, Dalezios Y (1997) Spatial cortical patterns of metabolic activity in monkeys performing a visually guided reaching task with one forelimb. Neuroscience 76:1007-1034.

Savaki HE, Kennedy C, Sokoloff L, Mishkin M (1993) Visually guided reaching with the forelimb contralateral to a "blind" hemisphere: a metabolic mapping study in monkeys. J Neurosci 13:2772-2789.

Shipp S, Blanton M, Zeki S (1998) A visuo-somatomotor pathway through superior parietal cortex in the macaque monkey: cortical connections of areas V6 and V6A. Eur J Neurosci 10:3171-3193.

Sokoloff L, Reivich M, Kennedy C, Des Rosiers MH, Patlak CS, Pettigrew KD, Sakurada O, Shinohara M (1977) The [14C]deoxyglucose method for the measurement of local cerebral glucose utilization: theory, procedure, and normal values in the conscious and anesthetized albino rat. J Neurochem 28:897-916.

Strafella AP, Paus T (2000) Modulation of cortical excitability during action observation: a transcranial magnetic stimulation study. Neuroreport 11:2289-2292.

Takahashi N, Kawamura M, Shiota J, Kasahata N, Hirayama K (1997) Pure topographic disorientation due to right retrosplenial lesion. Neurology 49:464-469.

Tanne-Gariepy J, Rouiller EM, Boussaoud D (2002) Parietal inputs to dorsal versus ventral premotor areas in the macaque monkey: evidence for largely segregated visuomotor pathways. Exp Brain Res 145:91-103.

Tanne J, Boussaoud D, Boyer-Zeller N, Rouiller EM (1995) Direct visual pathways for reaching movements in the macaque monkey. Neuroreport 7:267-272.

Ungerleider LG, Galkin TW, Desimone R, Gattass R (2008) Cortical connections of area V4 in the macaque. Cereb Cortex 18:477-499.

Vanduffel W, Fize D, Mandeville JB, Nelissen K, Van Hecke P, Rosen BR, Tootell RB, Orban GA (2001) Visual motion processing investigated using contrast agent-enhanced fMRI in awake behaving monkeys. Neuron 32:565-577.

Vogt BA, Pandya DN (1987) Cingulate cortex of the rhesus monkey: II. Cortical afferents. J Comp Neurol 262:271-289.

Vogt BA, Pandya DN, Rosene DL (1987) Cingulate cortex of the rhesus monkey: I. Cytoarchitecture and thalamic afferents. J Comp Neurol 262:256-270.

Wise SP, Boussaoud D, Johnson PB, Caminiti R (1997) Premotor and parietal cortex: corticocortical connectivity and combinatorial computations. Annu Rev Neurosci 20:25-42.

Zeki S (1986) The anatomy and physiology of area V6 of macaque monkey visual cortex J Physiol 381, 62P

ELSEVIER

NeuroImage

www.elsevier.com/locate/ynimg
NeuroImage 23 (2004) 193–201

Observation of action: grasping with the mind's hand☆

Vassilis Raos, Mina N. Evangeliou, and Helen E. Savaki*

Department of Basic Sciences, Faculty of Medicine, School of Health Sciences, University of Crete, GR-71003, Iraklion, Crete, Greece
Institute of Applied and Computational Mathematics, Foundation for Research and Technology-Hellas, GR 71110, Iraklion, Crete, Greece

Received 24 January 2004; revised 22 March 2004; accepted 21 April 2004
Available online 7 July 2004

Engagement of the primary motor cortex (MI) during the observation of actions has been debated for a long time. In the present study, we used the quantitative ^{14}C-deoxyglucose method in monkeys that either grasped 3-D objects or observed the same movements executed by humans. We found that the forelimb regions of the MI and the primary somatosensory (SI) cortex were significantly activated in both cases. Our study resolves a debate in the literature, providing strong evidence for use of MI representations during the observation of actions. It demonstrates that the observation of an action is represented in the primary motor and somatosensory cortices as is its execution. It indicates that in terms of neural correlates, recognizing a motor behavior is like executing the same behavior, requiring the involvement of a distributed system encompassing not only the premotor but also the primary motor cortex. We suggest that movements and their proprioceptive components are stored as motor and somatosensory representations in motor and somatosensory cortices, respectively, and that these representations are recalled during observation of an action.

Keywords: Primary motor cortex; Primary somatosensory cortex; Action; Objects; 2-Deoxyglucose method

Introduction

Assigning meaning to the actions of other subjects is an essential aspect of social communication and efficient behavior. This underscores the importance of understanding where and how observed actions are represented in the primate cortex. A major contribution in this direction was the discovery of "mirror neurons" in area F5 of the ventral premotor cortex (di Pellegrino et al., 1992). These neurons fire both when a monkey grasps 3-D objects and when he observes humans executing the same movements, indicating the existence of an action observation-execution matching system, useful for understanding the actions performed by others (Gallese et al., 1996; Rizzolatti et al., 1996b). Conflicting results have been reported for the involvement of the primary motor cortex (MI) in observation of actions. The precentral motor cortex was not activated during observation of hand movements in previous PET and fMRI imaging studies (Decety et al., 1997; Grafton et al., 1996; Iacoboni et al., 1999; Rizzolatti et al., 1996b) whereas it was activated in a MEG study (Hari et al., 1998).

Here, the [^{14}C]-deoxyglucose (^{14}C-DG) quantitative autoradiographic method was employed to compare the activations in the MI cortex of primates induced by grasping-observation to those elicited by grasping-execution. Because the spatial resolution of our ^{14}C-DG study is much higher than that of any previous report, our data could resolve the long-standing debate regarding the involvement of MI in the observation of movements, a conflict largely due to the differential sensitivity of the techniques employed earlier. Furthermore, given the interplay between action and perception, and the intimate relation between a movement and its somatosensory perception, we also examined the effects of grasping-execution and grasping-observation in the primary somatosensory (SI) cortex. Our findings demonstrate that the forelimb regions of MI and SI are activated during the observation of hand movements. Moreover, they indicate that similar primary motor and somatosensory patterns of activity are deployed during the observation and the execution of the same hand movement.

Materials and methods

Subjects and tasks

Six adult female *Rhesus* monkeys weighing between 3.5 and 5 kg were used, with heads fixed during the ^{14}C-DG experiment. The behavioral apparatus was placed in front of the monkeys at shoulder height, 20 or 50 cm away, depending on whether the monkey or the experimenter had to execute the grasping movements. The behavioral apparatus contained a PC-controlled rotating turntable on which six 3-D geometrical solids of small size were accommodated. The following objects were used: plate (25 mm wide, 35 mm deep, and 3 mm thick), ring (diameter of 15 mm), sphere (diameter of 10 mm), cube (side of 10 mm), and cylinder (40 mm long with diameter of 5 mm). The objects were grasped as follows: the plate, with the primitive precision grip, performed by the use of the thumb and the radial surface of the second and third phalanxes of the index finger (the plate oriented horizontally or vertically was grasped with the hand half pronated or pronated, respectively); the ring, with the digging out grip with

☆ To the Memory of Massimo Mattelli.

* Corresponding author. Department of Basic Sciences, Faculty of Medicine, School of Health Sciences, University of Crete, PO Box 2208, GR-71003, Iraklion, Crete, Greece. Fax: +30-2810-394530.
E-mail address: savaki@med.uoc.gr (H.E. Savaki).
Available online on ScienceDirect (www.sciencedirect.com.)

1053-8119/$ - see front matter © 2004 Elsevier Inc. All rights reserved.
doi:10.1016/j.neuroimage.2004.04.024

the index finger inserted into a ring (horizontally oriented, grasped with the hand pronated); the cube and the sphere, with the side grip, performed by the thumb and the radial surface of the last phalanx of the index finger (grasped with the hand half pronated); and the cylinder, with the finger prehension, using the first three fingers (hand half pronated). A sliding window at the front side of the apparatus allowed access to only one object at a time. Opening of the window resulted in illumination of the compartment thus making the object visible. Eye movements were recorded with an infrared oculometer (Dr. Bouis). EMG was recorded (gain ×2000, band-pass filter 0.3–3000 kHz) using Ag-AgCl surface electrodes. Digitized electromyograms (1000 Hz) recorded from the biceps and wrist extensor muscles were aligned to the end of the movement, rectified, and averaged over 150 movements in each case. Monkeys performed their tasks during the whole experimental period of 45 min during the ^{14}C-DG experiment and received water as reward.

Two control monkeys were used in our study: the fixation control (Cf) and the arm-motion control (Cm).

The fixation control monkey, Cf, which had both hands restricted, was trained to maintain its gaze fixed on a central visual target (red spot of 1.5° diameter) throughout the period it was illuminated (4 s/trial). Intertrial intervals ranged between 200 and 300 ms.

The arm-motion control monkey, Cm, which had both hands restricted, was trained to maintain its gaze straight ahead during (i) the opening of a window of the behavioral apparatus, (ii) the presentation of illuminated 3-D objects behind the window, (iii) the closure of the window, and also (iv) while the experimenter was reaching with extended hand towards the closed window. Accordingly, the task of the Cm monkey contained all the components of the action–observation task with the exception of the object–hand interaction. Intertrial intervals ranged between 2 and 2.5 s.

Two monkeys (E, execution of grasping) were trained to reach and grasp 3-D objects (small sized geometrical solids) with their left forelimb while their right forelimbs were restricted. Each trial was initiated with the opening of the window and the illumination of the appearing 3-D object. The monkey had to fixate the object for 700–1000 ms until a dimming of the light would signal a reaching and grasping movement with the left forelimb within 1000 ms. The monkey was required to reach for, grasp, and pull the object while maintaining fixation to get the reward. Intertrial intervals ranged between 2 and 2.5 s.

Two monkeys (O, observation of grasping) were first trained to perform the task of the E monkeys and then trained to observe the same grasping movements executed by the experimenter. Although grasping training took place months before the ^{14}C-DG experiment to cancel any possible effect due to this earlier grasping training (and not to the observation behavior), one of these monkeys was trained to grasp with its left hand and the other one with its right hand. Thus, in the observing monkeys, any side-to-side effect due to the earlier grasping training would be canceled out by comparing the average quantitative map of the two left hemispheres with the average map of the two right hemispheres. During the ‘‘observation’’ training and experiments, both hands of the monkey were restricted. The experimenter always was standing on the right side of the monkey and was using her right arm to reach and grasp the objects. Both reaching and grasping components of the movement were visible to the monkey. All objects, reaching, and grasping parameters were similar to the ones described for the E task. To control for possible rate-related effects, the mean rate of movement was set to be similar for the execution and observation tasks.

Two dimensional reconstructions

The ^{14}C-DG experiment and the brain tissue processing for autoradiography were performed as previously described (Gregoriou and Savaki, 2001; Savaki et al., 1993). Two-dimensional (2-D) reconstruction (glucogram) of the spatiointensive pattern of metabolic activity in local cerebral glucose utilization (LCGU values in μmol/100 g/min) within the rostrocaudal and the dorsoventral extent of the unfolded central sulcus (CS) was generated in each hemisphere (Dalezios et al., 1996). According to this procedure, the distribution of activity in the rostrocaudal extent in each horizontal section was determined by measuring values of glucose consumption pixel by pixel (resolution up to 50 μm/pixel) along a line parallel to the surface of the cortex, covering all cortical layers. The data array from each horizontal section was aligned with the arrays obtained from adjacent horizontal sections, the total of 1000 serial sections of 20 μm thickness in each hemisphere. The fundus of the CS was used for the alignment of adjacent data arrays. Tickmarks in each horizontal section labeled the crowns and fundus of each CS. These tickmarks were used to match the 2-D maps obtained from different hemispheres and animals (geometrical normalization). The average of the LCGU values was calculated in sets of five adjacent sections (20 μm thick). In the illustrated average 2-D maps, the spatial resolution in both the rostrocaudal and dorsoventral dimensions is 100 μm. Normalization of LCGU values was based on the average unaffected gray matter value pooled across all monkeys (Gregoriou and Savaki, 2003).

Geometrical normalization

Geometrical normalization of the individual 2-D maps of activity (glucograms) in the MI and SI cortices of the CS was based on surface landmarks (its fundus and crowns) and was generated as follows. The average of all the individual CS landmark maps was used as reference. Then, the landmarks of each individual 2-D map were manipulated to fit all the surface landmarks of the reference map, with linear transformations of the plane (translation, stretching in one or more directions) using the Transform (Fortner Software LLC, Sterling, VA) and MATLAB software (Moschovakis et al., 2001). The geometrically normalized maps were used (i) to obtain average LCGU maps out of two control or two experimental hemispheres and (ii) to subtract control from experimental maps.

Statistical analysis

The average LCGU values were calculated in sets of five adjacent sections (20 μm thick) throughout the cortical area of the CS in each hemisphere. Experimental to control raw LCGU values were compared for statistical significances by the Student’s unpaired t test. Given that ipsi- to contralateral LCGU values in normal control monkeys range up to 7% (Kennedy et al., 1978), only the LCGU values of regions with differences higher than 7% were considered for statistical treatment. The percent LCGU differences between the motion control (Cm) and the fixation control (Cf) were calculated by the formula $(Cm - Cf)/Cf \times 100$. The percent LCGU differences between the

experimental (E) and the control (C) monkeys were generated using the formula (E − C)/C × 100. The effects induced by grasping-observation (O) were expressed as percent activation of the effects induced by grasping-execution (E) by the formula (100 × O)/E.

Results

The ^{14}C-DG quantitative autoradiographic method (Kennedy et al., 1978; Savaki et al., 1993; Sokoloff et al., 1977) was used to map the spatial distribution of metabolic activity in the trunk, forelimb, and mouth regions of the MI and SI cortical areas (Fig. 1C, Cf) within the central sulcus (CS) of 12 hemispheres in six (two control and four experimental) *Rhesus* monkeys during execution of an action and observation of the same action executed by another subject. Grasping movements were used as the motor act to be executed or observed by the monkeys because the knowledge pertaining to the hand shapes associated with specific motor interactions with objects could be stored in the form of motor representations.

To obtain the CS maps of metabolic activation pattern induced by repeated execution of grasping movements, two of the experimental monkeys were trained to grasp with the left hand 3-D objects positioned straight ahead (E, execution of grasping). These two monkeys performed an average of 98 grasping movements during the critical first 10 min of the ^{14}C-DG experiment. We generated a CS map (Fig. 1A, El) by averaging the two geometrically normalized quantitative CS maps of metabolic activity (glucograms) in the left hemispheres of the two grasping monkeys. When the average map of the right hemispheres (Fig. 1A, Er) is compared with the average map of the left hemispheres (Fig. 1A, El), increased metabolic activity is apparent in the (right) MI and SI forelimb regions contralateral to the grasping (left) hand. It should be noted that the sulcal MI forelimb region activated in our study, which involved grasping in the central space (in front of the chest), overlaps with the area demonstrated to emphasize manual dexterity (fine control of wrist, fingers, and forearm) in the central space (Graziano et al., 2002).

To obtain the CS maps of activity induced by observation of grasping movements executed by another subject, two additional experimental monkeys (which had been trained to grasp 3-D objects) were rewarded for observing the same grasping movements executed by the experimenter (O, observation of grasping). These monkeys observed an average of 109 grasping movements during the critical first 10 min of the ^{14}C-DG experiment. When the average map of the two right hemispheres (Fig. 1B, Or) is compared with the average map of the two left hemispheres (Fig. 1B, Ol), increased metabolic activity is apparent in the right MI and SI forelimb regions. This activation induced by observation of grasping (Fig. 1B, Or) is less pronounced than the activation induced by execution of grasping (Fig. 1A, Er).

To exclude potential effects induced by (i) unspecific arousal, (ii) intensive attention, and (iii) gaze fixation, we used the first control monkey, which was rewarded for maintaining its gaze fixed on a central illuminated spot (Cf, fixation control). During the critical first 10 min of the ^{14}C-DG experiment, the Cf monkey maintained fixation for 95% of the task period. The illustrated CS map (Fig. 1C, Cf) was generated by averaging the two geometrically normalized quantitative CS glucograms of the left and right hemispheres of the Cf monkey.

Finally, to exclude effects induced by (i) observation of the 3-D objects and eye movements due to scanning these objects and (ii) biological motion due to the reaching forelimb of the experimenter, we used the second control monkey. This monkey was rewarded for maintaining its gaze straight ahead during the presentation of 3-D objects and while the experimenter was reaching towards the position of the hidden objects (Cm, arm-motion control). During the critical ten first minutes of the ^{14}C-DG experiment, the Cm monkey maintained fixation for 85% of the task period. Given that the side-to-side difference in glucose consumption in the Cm monkey was not significant, an average image of the two quantitative CS glucograms of the left and the right hemispheres was generated (Fig. 1C, Cm). Although perception of biological motion would be expected to represent a capacity of the visual rather than the motor system, the MI and SI forelimb regions in the average map of the Cm monkey (Fig. 1C, Cm) were found to be slightly more active than the corresponding regions in the average map of the Cf monkey (Fig. 1C, Cf). Although these differences are not significant (Table 1), the map of the Cm monkey has been used for comparisons with the maps of the experimental monkeys in following figures.

To graphically demonstrate the spatial distribution of metabolic activity within the affected regions, we plotted the local cerebral glucose utilization values (LCGU, μmol/100 g/min) in the MI and SI forelimb regions (Fig. 1D). Each plot represents the average LCGU values and 95% confidence intervals (per 100 μm) along the anteroposterior extent of the CS (from the anterior crown, through the fundus, then to the posterior crown) of two hemispheres. When compared with the LCGU plot of the fixation control (Cf plot), the corresponding plots of the other monkeys demonstrate that the forelimb regions in MI and SI are (i) strongly activated, on the right, when the monkeys execute grasping movements with their left hand (Er plot), (ii) considerably activated, on the right, when the monkeys observe the same grasping movements performed by the experimenter (Or plot), and (iii) weakly activated when the monkey observes the 3-D objects and the moving arm of the experimenter (Cm plot).

Of interest is that although MI and SI forelimb regions were activated in the grasping-execution and the grasping-observation animals, only the monkeys executing (and not the ones observing) grasping movements displayed an increase of sustained muscle activity in the biceps and wrist extensor of their performing forelimb (Fig. 2). Sustained activity in these two muscles was equally unaffected in both forelimbs of the monkeys observing grasping movements and in the nonperforming (right) forelimb of the monkeys executing grasping movements (with their left forelimb).

To reveal the regions that were significantly affected in the motion-control, we statistically compared the LCGU values in the trunk, forelimb, and mouth regions of MI and SI in the two hemispheres of the Cm monkey with the corresponding values in the fixation control (Table 1). Neither the weak activations in MI and SI forelimb regions nor any other differences in the trunk and mouth regions were found to be significant.

Images illustrating the percent LCGU differences between the grasping-execution monkeys and the motion control demonstrate that execution of grasping induces profound activation of the forelimb representations in MI and SI cortices, as compared with the Cm, while the SI trunk region is less affected and the mouth regions remain unaffected (Fig. 3A, Er/Cm). Statistical analysis demonstrated that the activations in the MI and SI forelimb regions

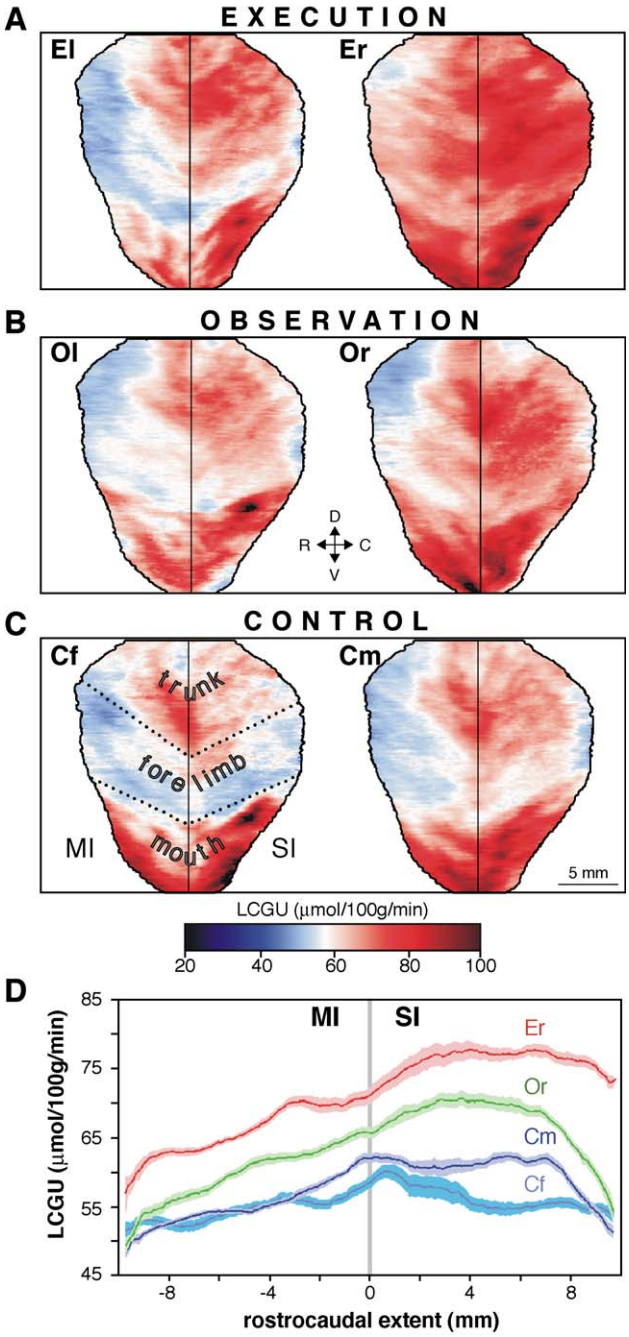

Fig. 1. Metabolic effects induced by execution and observation of grasping movements in the MI and SI cortices of the CS. Each color-coded map represents the average of the geometrically normalized, quantitative maps (glucograms) in two hemispheres. The central sulcus (CS) is unfolded to reveal the reconstructed cortex in its banks. In each map, the black solid line represents the fundus of the CS whereas the two dotted lines represent its two crowns. The anterior bank containing area 4 (MI) and the posterior bank containing areas 3a, 3b, and part of 1 (SI) are on the left and right side of the fundus, respectively. Color bar represents the LCGU values in μmol/100 g/min. C, caudal; D, dorsal; R, rostral; V, ventral. (A) Average CS maps in the left (El, ipsilateral) and right (Er, contralateral) hemispheres of the two monkeys executing grasping movements with their left forelimb. A pronounced activation of the MI and SI forelimb region is apparent in the Er, contralateral to the grasping forelimb, as compared with the ipsilateral side (El). (B) Average CS maps in the left (Ol) and the right (Or) hemispheres of the two monkeys observing right hand grasping movements executed by the experimenter. A significant activation of the MI and SI forelimb region in the Or, as compared with the Ol, is apparent. (C) Average CS maps of the two hemispheres of the fixation control monkey (Cf) and the two hemispheres of the arm-motion control monkey (Cm). Representations of body parts (trunk, forelimb, and mouth) within MI and SI are indicated in the Cf map. (D) Plot of the LCGU values in the MI and SI forelimb regions in the control monkeys (average of the two hemispheres of the Cf and of the two hemispheres of the Cm) and in the experimental monkeys (average of the two right hemispheres of the executing Er monkeys and of the two right hemispheres of the observing Or subjects). Each plot represents average LCGU values and 95% confidence intervals per 100 μm along the anteroposterior extent of the CS of two hemispheres. The illustrated length of the CS extends from its anterior crown (−10 mm), through the fundus (0 mm), to its posterior crown (+10 mm). MI and SI forelimb regions are strongly activated in the monkeys executing grasping movements (Er) and considerably activated in the monkeys observing the same grasping movements performed by the experimenter (Or), as compared with both controls (Cf and Cm).

Table 1
Metabolic effects in the trunk, forelimb, and mouth regions of the primary motor (MI) and primary somatosensory (SI) cortices

Cortical area	Cf	Cm	Cm/Cf (%)	El	Er	Er/Cm (%)	Ol	Or	Or/Cm (%)
Trunk motor (103)	62 ± 7	62 ± 6	−0.1	62 ± 6	66 ± 6	6.0	60 ± 6	62 ± 8	0.0
Trunk sensory (103)	63 ± 4	66 ± 4	5.0	71 ± 5	75 ± 5	**13.9**	66 ± 4	69 ± 7	4.4
Forelimb motor (123)	55 ± 3	56 ± 3	1.4	55 ± 4	67 ± 5	**20.4**	57 ± 3	60 ± 5	**8.5**
Forelimb sensory (123)	57 ± 4	61 ± 4	7.0	63 ± 5	77 ± 5	**27.4**	62 ± 4	68 ± 5	**12.4**
Mouth motor (103)	70 ± 10	72 ± 11	2.8	62 ± 6	74 ± 8	3.7	66 ± 6	75 ± 9	4.3
Mouth sensory (103)	76 ± 13	77 ± 8	1.3	72 ± 9	80 ± 8	4.8	72 ± 9	76 ± 9	−1.4

Note. Values represent the mean glucose utilization (LCGU) expressed in μmol/100 g/min ± SD. Cf, average of left and right hemispheres of the control fixating monkey. Cm, average of left and right hemispheres of the motion control monkey. El, average of the two left hemispheres of the monkeys executing grasping movements with the left forelimb. Er, average of the two right hemispheres of the grasping-execution monkeys. Ol, average of the two left hemispheres of the monkeys observing grasping movements executed by another subject. Or, average of the two right hemispheres of the grasping-observation monkeys. Er/Cm (%) and Or/Cm (%), experimental-to-control percent differences. The number of sets of five adjacent horizontal sections, used for statistics in each region of each hemisphere, is indicated within parenthesis next to the cortical areas. Values in bold indicate statistically significant differences by the Student's unpaired *t* test at the level of $P < 0.001$ (see Materials and methods).

(by 20% and 27%, respectively, as compared with Cm, and by 22% and 36% as compared with Cf), in the hemisphere contralateral to the grasping hand, are significant (Table 1). The smaller though significant activation induced in the trunk region, contralateral to the moving forelimb, is due to postural adjustment of the monkeys during reaching to grasp (Savaki and Dalezios, 1999). Also, observation of grasping activated considerably the MI and SI forelimb regions but not the trunk and mouth ones when compared with Cm (Fig. 3A, Or/Cm). Statistical analysis demonstrated that only the activations in the MI and SI forelimb regions (by 9% and 12% as compared with Cm and by 10% and 20% as compared with Cf) are significant (Table 1).

To graphically represent these effects in reference to the Cm values, the percent LCGU differences have been plotted in the MI and SI forelimb regions across the entire anteroposterior extent of the CS (Fig. 3B). The activations (relative to Cm) induced by grasping-observation (Fig. 3B, Or/Cm) are lower in intensity than those induced by grasping-execution (Fig. 3B, Er/Cm) across the whole extent of the sulcal cortex. However, the pattern of neural activation, in the forelimb regions of MI and SI, induced by the observation of grasping is very similar to that elicited by the execution of the same action.

To demonstrate the observation-to-execution (Or/Er) percent activation, we used the formula (100 × O)/E. Both the so-generated 2-D map (Fig. 4A) and LCGU plot (Fig. 4B) indicate that grasping-observation induces an average activation of the MI and SI forelimb regions, which is about 50% smaller than that elicited by grasping-execution. Moreover, this plot illustrates two peaks (of 60% differences) in the forelimb regions within the CS (Dalezios et al., 1996). The first peak is located in area 4 of the anterior bank (4.5 mm distal to the fundus), and the second one in area 3b of the posterior bank (3 mm distal to the fundus).

Discussion

Our study demonstrates significant activations of the MI and SI forelimb regions within the CS during execution of grasping movements and during observation of the same movements executed by another subject. It indicates overlapping neural correlates of motor program execution and motor percept creation. It also demonstrates that the activations induced by grasping-execution and grasping-observation in the MI and SI forelimb regions have a very similar pattern, although differ in intensity. The activation induced by observation of grasping is about 50% weaker in intensity than that induced by execution of grasping.

Comparison of the LCGU values in the grasping-observation monkeys with those in the fixation control subject indicates that the MI and SI forelimb activations during observation of grasping can be due neither to unspecific arousal nor to intensive attention. Comparison of the grasping-observation monkeys with the arm-motion control indicates that the MI and SI forelimb activations

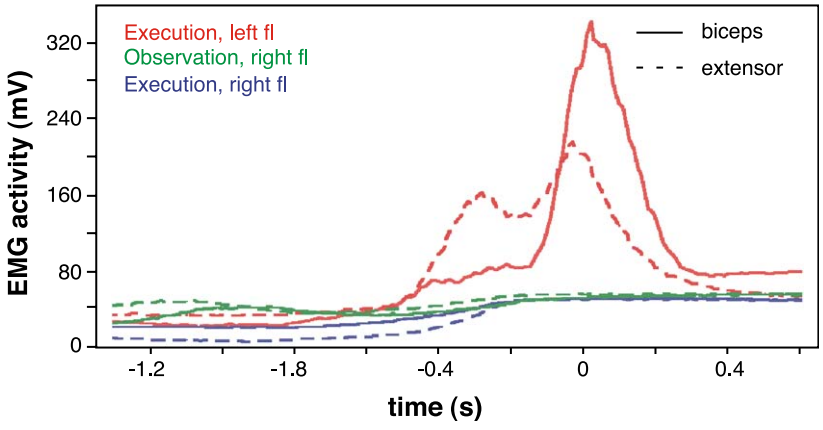

Fig. 2. Effects induced by execution and observation of grasping on muscle activity. Averaged rectified electromyographic records demonstrate that only the grasping (left) forelimb of the monkeys executing hand movements displays an increase of sustained muscle activity in the biceps and wrist extensor.

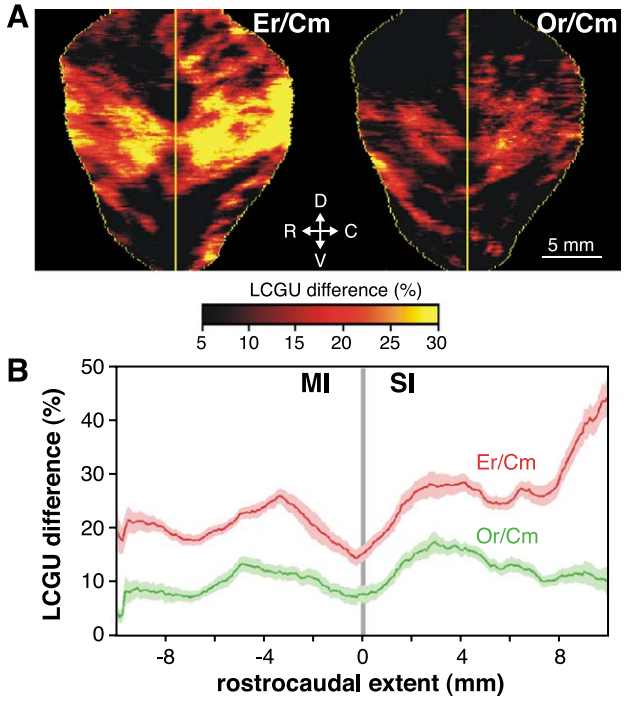

Fig. 3. Percent differences in activations induced by execution and observation of grasping as compared with the motion control. (A) CS maps of relative activations. The Er/Cm image demonstrates that execution of grasping (Er) induces profound activation of the MI and SI forelimb regions contralateral to the moving forelimb as compared with the motion control (Cm). The Or/Cm image demonstrates that observation of grasping (Or) also activates the MI and SI forelimb regions as compared with the motion control. Color bar indicates the percent differences in metabolic activations. Only statistically significant activations (greater than 10%) are illustrated. (B) CS plots, demonstrating the percent activations within the entire anteroposterior extent of the MI and the SI cortices, in the grasping-execution (Er/Cm) and in the grasping-observation (Or/Cm) monkeys as compared with the motion control. Zero represents the fundus, whereas −10 and +10 represent the anterior and posterior crowns of the CS, respectively.

during observation of grasping can be due neither to the viewing of the 3-D objects nor to the biological motion of the reaching arm. Moreover, the absence of increased muscle activity in the observing monkeys indicates that the MI and SI forelimb activations during observation of grasping cannot be due to movements of the immobilized forelimbs.

We suggest that the activation of the MI forelimb region during action observation is related to the "mirror" phenomenon described in the monkey premotor cortex (Gallese et al., 1996; Rizzolatti et al., 1996a). Our data complement previous findings suggesting that action plans may be used in action observation (Randall-Flanagan and Johansson, 2003) and are in agreement with the suggestion that the action observation-execution matching system involves the primary motor cortex in humans (Hari et al., 1998; Nishitani and Hari, 2000, 2002). They are also in accord with studies demonstrating that the functioning of the motor pathway is modified during observation of hand movements (Fadiga et al., 1995; Maeda et al., 2002; Strafella and Paus, 2000), an effect that takes place in the MI cortex (Strafella and Paus, 2000). On the other hand, PET and fMRI studies failed to demonstrate activation of the precentral cortex during observation of hand movements (Decety et al., 1997; Grafton et al., 1996; Iacoboni et al., 1999; Rizzolatti et al., 1996b).

Possible sources of discrepancy are the nature of observed actions, the observer's intention, and the differential sensitivity of the used techniques. We have reasons to believe that the actual source of discrepancy is the lower sensitivity of the techniques used in these previous studies. Our findings are based on (i) cerebral glucose utilization values, which directly reflect brain functional activity, (ii) images of a much higher spatial resolution (20 μm sampling, 100 μm plotting) than those used in previous imaging studies, and (iii) quantitative (and not semiquantitative as in previous studies) values. Evidently, the 10% activation of only the forelimb region within the sulcal MI, measured in our study, could easily have been missed in lower resolution studies.

Thus, our study resolves a debate in the literature, providing strong evidence for the use of MI representations during the observation of actions. In effect, understanding an action may

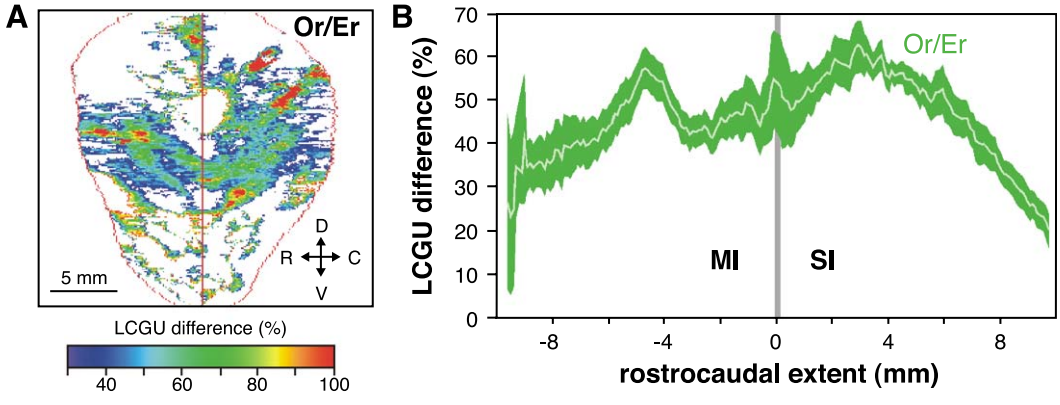

Fig. 4. Comparison of activations induced by grasping-observation with those elicited by grasping-execution. (A) CS map of the grasping-observation effects expressed as percentage of the activations induced by grasping-execution (Or/Er). This image demonstrates that the observation of grasping induces activations of lower intensity than those induced by the execution of grasping. Color bar indicates the percent differences in metabolic activations. (B) CS plots of the comparative observation-to-execution effects, demonstrating the percent activations within the entire anteroposterior extent of the MI and the SI cortices in the grasping-observation as compared with the grasping-execution (Or/Er) monkeys. Zero indicates the fundus, whereas −10 and +10 represent the anterior and posterior crowns of the CS, respectively.

result from the utilization of stored action representations in MI and in associated premotor cortices. The ventral premotor cortex, which is predominantly linked to the mirror neuron system (Rizzolatti et al., 1996a) and which displays strong connections to M1 (Matelli et al., 1986), may exert an influence on MI activity during the observation of actions (Rizzolatti et al., 2001). Accordingly, stored motor representations in MI may fundamentally bias motor perception, and recognition of actions may be constrained by the subject's motor system. This is not the first time that a cognitive role has been assigned to the primate primary cortex. It has been reported that MI plays a crucial role in the processing of cognitive information related to motor function, such as mental rotation (Georgopoulos et al., 1989), visuomotor adaptation (Wise et al., 1998), and context recall (Carpenter et al., 1999). This is not also the first time that a cognitive role has been associated with the primate motor system. It has been reported that the human ability to explain and predict other people's behavior by attributing to them independent mental states (the theory of mind) has evolved from a system representing actions (Frith and Frith, 1999).

During observation of grasping, the MI activation in the absence of EMG activation has at least two explanations. The first one is that the observed MI cortical activation, mainly due to incoming synaptic activity (Mata et al., 1980; Schwartz et al., 1979), did not reach the overall action potential firing threshold to generate an excitatory output. The second and more possible explanation is that an excitatory MI output was generated, which was blocked somewhere downstream of MI, most probably at a spinal level, to prevent motoneurons from triggering an action. Indeed, it has been suggested that during action observation, a motor corticospinal excitation may be suppressed by a superimposed cortico-brainstem-spinal inhibition at the spinal level, which after all may prevent the overt action (Baldissera et al., 2001). Although EMG was not activated during observation of grasping movements in our study, the SI forelimb region was significantly activated, an effect induced by the subject's observation of grasping in the absence of overt movement and in the absence of apparent sensory input. The SI forelimb activation measured in our study is in agreement with a previous report demonstrating that the SI activity was enhanced not only during manipulative hand actions but also during the observation of the same actions performed by another subject (Avikainen et al., 2002). These findings indicate that during the observation of an action, the representation of movement is retrieved together with its kinesthetic component. Accordingly, movement representations and their kinesthetic components maybe stored as motor and somatosensory representations in MI and SI, respectively, and action observation may involve access to these representations.

The MI and SI forelimb activations during observation of actions may also imply that subjects mentally rehearse the movements executed by others. In this case, the activation of SI would imply that the motor mental rehearsal contains a somatosensory component analogous to the feedback, which normally accompanies overt actions. The MI and SI neural activations during observation of a movement would reflect the effects of (i) mental rehearsal of this movement by the observer (in the absence of overt action) and (ii) recall of previous knowledge about the sensory effects of this movement (in the absence of sensory input).

The involvement of MI in motor imagery, that is, the mental rehearsal of a motor act that is not accompanied by overt movement, is also a matter of considerable debate. Early cerebral blood flow studies provided no evidence for perirolandic activations (Ingvar and Philipson, 1977; Roland et al., 1980), whereas conflicting results have been reported recently by EEG, MEG, PET, and fMRI studies. Involvement of MI during imagery of hand movements (Beisteiner et al., 1995; Schnitzler et al., 1997), internal simulation of action (Lang et al., 1996), and mental representation of upper extremities movements (Stefan et al., 1995) has been shown in some studies, and lack of MI involvement in imagery of grasp movements (Decety et al., 1994) and hand rotations (Parsons et al., 1995) has been shown in others. Moreover, involvement of the primary motor and somatosensory cortices in motor imagery was found by some groups (Gerardin et al., 2000; Leonardo et al., 1995; Lotze et al., 1999; Naito et al., 2002; Porro et al., 1996; Roth et al., 1996; Sabbah et al., 1995) and not by others (Deiber et al., 1998; Hanakawa et al., 2003; Rao et al., 1993; Sanes et al., 1995). Finally, the reports that mental simulation of a movement results in a large increase in excitability of the spinal reflex pathway (Bonnet et al., 1997), and that mental motor images are constrained by the same psychophysical and physiological limitations that apply to movement execution (Cooper and Shepard, 1975; Parsons, 1994; Sekiyama, 1982; Sirigu et al., 1995, 1996), constitute indications of overlapping neuronal substrates subserving motor imagery and motor execution.

The MI activation during action observation and motor mental imagery is equivalent to the reported activation of the primary visual cortex (V1) during visual recall and visual mental imagery (Kosslyn et al., 1995; Le Biham et al., 1993; see also opposite findings Howard et al., 1998). Accordingly, recognition of observed actions may rely on similar mechanisms to those used in the top-down hypothesis testing during visual perception. Same way as knowledge (visual recall) can fundamentally bias what one sees (visual perception), motor recall may fundamentally bias action recognition. Independently of any possible explanation (memory retrieval or mental rehearsal), our findings extend the cortical system matching observation-execution of goal-related motor actions from the premotor cortex (Rizzolatti et al., 1996a) to the primary motor and somatosensory cortices.

The lateralization of MI and SI activations contralateral to the moving forelimb during execution of grasping is compatible with classical knowledge and our previous reports (Savaki and Dalezios, 1999). The fact that the MI and SI activations during observation of grasping were found always in the right hemisphere, that is, ipsilateral to the experimenter's arm position, and independent of the forelimb used in previous grasping experience of these monkeys (see Materials and methods) is intriguing. This finding is consistent with the right hemisphere dominance for visuospatial processes relative to movements (Chua et al., 1992; Decety, 1996; Perani et al., 2001). Moreover, this finding complements previous reports (Farrer and Frith, 2002; Farrer et al., 2003; Gallagher et al., 2000; Meltzoff and Decety, 2003; Ruby and Decety, 2001; Siegal et al., 1996), suggesting that the right hemisphere is responsible for attribution of the cause or the control of an action (the grasping movement in this case) to another agent (the experimenter) distinguished from the self (the monkey). Finally, this preferred lateralization is also reported in a recent fMRI study, which demonstrated that predicting the actions of other people (or forming a mental image of third-person actions) activates the right (although ipsilateral to the moving arm) primary motor cortex (Ramnani and Miall, 2004).

In conclusion, our study provides strong evidence for the involvement of the MI and SI cortices in observation of actions performed by other subjects. It demonstrates that action observa-

tion involves access, not only to ventral premotor representations (Gallese and Goldman, 1998; Rizzolatti et al., 2000), but also to primary motor and somatosensory representations constructed by action execution. It indicates that in terms of neural correlates, recognition of an action involves matching of its mental percept with its stored mental construct. The parallel anatomofunctional substrate of action observation and action execution in the ventral premotor cortex (Rizzolatti et al., 2001) and in the primary motor and somatosensory cortices could indicate that we recognize the act while we execute it, and we mentally rehearse the act while we observe it. The recruitment of primary motor or kinesthetic programs during action observation is important not only for understanding actions of other subjects, and acquiring motor skills by observation, but also for the formulation of cognitive theories such as motor theories of perception. ‘‘High level’’ cognitive theories may be supported by ‘‘low-level’’ motor and somatosensory cortical function.

Acknowledgments

We thank A.K. Moschovakis for constructive comments, S. Erimaki and N. Papadimitriou for assistance in EMG recording, G.G. Gregoriou for the development of matlab scripts, and M. Kefaloyianni, L. Papadaki, and M. Giatroudaki for technical assistance. This work was supported by the EU (FP5 grant QLRT-2001-00746). V. Raos was supported by the Greek General Secretariat of Research and Technology (97EL-35).

References

Avikainen, S., Forss, N., Hari, R., 2002. Modulated activation of the human SI and SII cortices during observation of hand actions. NeuroImage 15, 640–646.

Baldissera, F., Canallari, P., Craighero, L., Fadiga, L., 2001. Modulation of spinal excitability during observation of hand actions in humans. Eur. J. Neurosci. 13, 190–194.

Beisteiner, R., Hollinger, P., Lindinger, G., Lang, W., Berthoz, A., 1995. Mental representations of movements. Brain potentials associated with imagination of hand movements. Electroencephalogr. Clin. Neurophysiol. 96, 183–193.

Bonnet, M., Decety, J., Jeannerod, M., Requin, J., 1997. Mental simulation of an action modulates the excitability of spinal reflex pathways in man. Cogn. Brain Res. 5, 221–228.

Carpenter, A., Georgopoulos, A., Pellizzer, G., 1999. Motor cortical encoding of serial order in a context-recall task. Science 283, 1752–1757.

Chua, R., Carson, R.G., Goodman, D., Elliot, D., 1992. Asymmetries in the spatial localization of transformed targets. Brain Cogn. 20, 227–235.

Cooper, L.A., Shepard, R.N., 1975. Mental transformations in the identification of left and right hands. J. Exp. Psychol. 104 (1), 48–56.

Dalezios, Y., Raos, V.C., Savaki, H.E., 1996. Metabolic activity pattern in the motor and somatosensory cortex of monkeys performing a visually guided reaching task with one forelimb. Neuroscience 72 (2), 325–333.

Decety, J., 1996. Do imagined and executed actions share the same neural substrate? Cogn. Brain Res. 3, 87–93.

Decety, J., Perani, D., Jeannerod, M., Bettinardi, V., Tadary, B., Woods, R., Mazziota, J.C., Fazio, F., 1994. Mapping motor representations with positron emission tomography. Nature 371, 600–602.

Decety, J., Grezes, J., Costes, N., Perani, D., Jeannerod, M., Procyk, E., Grassi, F., Fazio, F., 1997. Brain activity during observation of actions. Influence of action content and subject’s strategy. Brain 120, 1763–1777.

Deiber, M.P., Ibanez, V., Honda, M., Sadato, N., Raman, R., Hallett, M., 1998. Cerebral processes related to visuomotor imagery and generation of simple finger movements studied with positron emission tomography. NeuroImage 7, 73–85.

di Pellegrino, G., Fadiga, L., Fogassi, L., Gallese, V., Rizzolatti, G., 1992. Understanding motor events: a neurophysiological study. Exp. Brain Res. 91, 176–180.

Fadiga, L., Fogassi, L., Pavesi, G., Rizzolatti, G., 1995. Motor facilitation during action observation: a magnetic stimulation study. J. Neurophysiol. 73 (6), 2608–2611.

Farrer, C., Frith, C.D., 2002. Experiencing oneself vs another person as being the cause of an action: the neural correlates of the experience of agency. NeuroImage 15 (3), 596–603.

Farrer, C., Franck, N., Georgieff, N., Frith, C.D., Decety, J., Jeannerod, M., 2003. Modulating the experience of agency: a positron emission tomography study. NeuroImage 18, 324–333.

Frith, C.D., Frith, U., 1999. Interacting minds—A biological basis. Cogn. Psychol. 286, 1692–1695.

Gallagher, H.L., Happe, F., Brunswick, N., Fletcher, P.C., Frith, U., Frith, C.D., 2000. Reading the mind in cartoons and stories: an fMRI study of ‘‘theory of mind’’ in verbal and nonverbal tasks. Neuropsychologia 38, 11–21.

Gallese, V., Goldman, A., 1998. Mirror neurons and the simulation theory of mind-reading. Trends Cogn. Sci. 2, 493–501.

Gallese, V., Fadiga, L., Fogassi, L., Rizzolatti, G., 1996. Action recognition in the premotor cortex. Brain 119, 593–609.

Georgopoulos, A.P., Lurito, J.T., Petrides, M., Schwartz, A.B., Massey, J.T., 1989. Mental rotation of the neuronal population vector. Science 243, 234–236.

Gerardin, E., Sirigu, A., Lehericy, S., Poline, J.B., Gaymard, B., Marsault, C., Agid, Y., Bihan, D., 2000. Partially overlapping neural networks for real and imagined hand movements. Cereb. Cortex 10, 1093–1104.

Grafton, S.T., Arbib, M.A., Fadiga, L., Rizzolatti, G., 1996. Localization of grasp representations in humans by positron emission tomography. 2. Observation compared with imagination. Exp. Brain Res. 112, 103–111.

Graziano, M.S.A., Taylor, C.S.R., Moore, T., 2002. Complex movements evoked by microstimulation of precentral cortex. Neuron 34, 841–851.

Gregoriou, G.G., Savaki, H.E., 2001. The intraparietal cortex: subregions involved in fixation, saccades, and in the visual and somatosensory guidance of reaching. J. Cereb. Blood Flow Metab. 21, 671–682.

Gregoriou, G.G., Savaki, H.E., 2003. When vision guides movement: a functional imaging study of the monkey brain. NeuroImage 19, 959–967.

Hanakawa, T., Immisch, I., Keiichiro, T., Dimyan, M.A., Gelderen, P., Hallett, M., 2003. Functional properties of brain areas associated with motor execution and imagery. J. Neurophysiol. 89, 989–1002.

Hari, R., Forss, N., Avikainen, S., Kirveskari, E., Salenius, S., Rizzolatti, G., 1998. Activation of human primary motor cortex during action observation: a neuromagnetic study. Proc. Natl. Acad. Sci. 95, 15061–15065.

Howard, R.J., Ffytche, D.H., McKeefry, D., Ha, Y., Woodruff, P.W., Bullmore, E.T., Simmons, A., Williams, S.C.R., David, A.S., Brammer, M., 1998. The functional anatomy of imagining and perceiving colour. NeuroReport 9, 1019–1023.

Iacoboni, M., Woods, R.P., Brass, M., Bekkering, H., Mazziotta, J.C., Rizzolatti, G., 1999. Cortical mechanisms of human imitation. Science 286, 2526–2528.

Ingvar, D.H., Philipson, L., 1977. Distribution of cerebral blood flow in the dominant hemisphere during motor ideation and motor performance. Ann. Neurol. 2, 230–237.

Kennedy, C., Sakurada, O., Shinohara, M., Jehle, J., Sokoloff, L., 1978. Local cerebral glucose utilization in the normal conscious macaque monkey. Ann. Neurol. 4, 293–301.

Kosslyn, S.M., Thompson, W.L., Kim, I.J., Alpert, N.M., 1995. Topographical representations of mental images in primary visual cortex. Nature 378, 496–498.

Lang, W., Cheyne, D., Hollinger, P., Gerschlager, W., Lindinger, G., 1996.

Electric and magnetic fields of the brain accompanying internal simulation of movement. Cogn. Brain Res. 3, 125–129.
Le Biham, D., Turner, R., Zeffiro, T.A., Cuenod, C.A., Jezzard, P., Bonnerot, V., 1993. Activation of human primary visual cortex during visual recall: a magnetic resonance imaging study. Proc. Natl. Acad. Sci. 90, 11802–11805.
Leonardo, M., Fieldman, J., Sadato, N., Campbell, G., Ibanez, V., Cohen, L., Deiber, M.-P., Jezzard, P., Pons, T., Turner, L., Le Biham, D., Hallet, M., 1995. A functional magnetic resonance imaging study of cortical regions associated with motor task execution and motor ideation in humans. Hum. Brain Mapp. 3, 83–92.
Lotze, M., Montoya, P., Erb, M., Hulsmann, E., Flor, H., Klose, U., Birbaumer, N., Grodd, W., 1999. Activation of cortical and cerebellar motor areas during executed and imagined hand movements: an fMRI study. J. Cogn. Neurosci. 11, 491–501.
Maeda, F., Kleiner-Fisman, G., Pascual-Leone, A., 2002. Motor facilitation while observing hand actions: specificity of the effect and role of observer' s orientation. J. Neurophysiol. 87, 1329–1335.
Mata, M., Fink, D., Gainer, H., Smith, C., Davidsen, L., Savaki, H., Schwartz, W., Sokoloff, L., 1980. Activity-dependent energy metabolism in rat posterior pituitary primarily reflects sodium pump activity. J. Neurochem. 34 (1), 213–215.
Matelli, M., Camarda, R., Glickstein, M., Rizzolatti, G., 1986. Afferent and efferent projections of the inferior area 6 in the macaque monkey. J. Comp. Neurol. 251, 281–298.
Meltzoff, A.N., Decety, J., 2003. What imitation tells us about social cognition: a rapprochement between developmental psychology and cognitive neuroscience. Philos. Trans. R. Soc. Lond. 358, 491–500.
Moschovakis, A.K., Gregoriou, G., Savaki, H.E., 2001. Functional imaging of the primate superior colliculus during saccades to visual targets. Nat. Neurosci. 4, 1026–1031.
Naito, E., Kochiyama, T., Kitada, R., Nakamura, S., Matsumura, M., Yonekura, Y., Sadato, N., 2002. Internally simulated movement sensations during motor imagery activate cortical motor areas and the cerebellum. J. Neurosci. 22 (9), 3683–3691.
Nishitani, N., Hari, R., 2000. Temporal dynamics of cortical representation for action. Proc. Natl. Acad. Sci. U. S. A. 97 (2), 913–918.
Nishitani, N., Hari, R., 2002. Viewing lip forms: cortical dynamics. Neuron 36, 1211–1220.
Parsons, L.M., 1994. Temporal and kinematic properties of motor behavior reflected in mentally simulated action. J. Exp. Psychol. 20 (4), 709–730.
Parsons, L.M., Fox, R.T., Downs, J.H., Glass, T., Hirsch, T.B., Martin, C.C., Jerabek, P.A., Lancaster, J.L., 1995. Use of implicit motor imagery for visual shape discrimination as revealed by PET. Nature 375, 54–58.
Perani, D., Fazio, F., Borghese, N.A., Tettamanti, M., Ferrari, S., Decety, J., Gilardi, M.C., 2001. Different brain correlates for watching real and virtual hand actions. NeuroImage 14, 749–758.
Porro, C.A., Francescato, M.P., Cettolo, V., Diamond, M.E., Baraldi, P., Zuiani, C., Bazzocchi, M., Prampero, P.E., 1996. Primary motor and sensory cortex activation during motor performance and motor imagery: a functional magnetic resonance imaging study. J. Neurosci. 16 (23), 7688–7698.
Ramnani, N., Miall, R.C., 2004. A system in the human brain for predicting the actions of others. Nat. Neurosci. 7, 85–90.
Randall-Flanagan, J., Johansson, R.S., 2003. Action plans used in action observation. Nature 424, 769–771.
Rao, S.M., Binder, J.R., Bandettini, P.A., Hammeke, T.A., Yetkin, F.Z., Jesmanowicz, A., Lisk, L.M., Morris, G.L., Mueller, W.M., Estkowski, L.D., Wong, E.C., Haughton, V.M., Hyde, J.S., 1993. Functional magnetic resonance imaging of complex human movements. Neurology 43, 2311–2318.
Rizzolatti, G., Fadiga, L., Gallese, V., Fogassi, L., 1996a. Premotor cortex and the recognition of motor actions. Cogn. Brain Res. 3, 131–141.
Rizzolatti, G., Fadiga, L., Matelli, M., Bettinardi, V., Paulesu, E., Perani, D., Fazio, F., 1996b. Localization of grasp representations in humans by PET: 1. Observation versus execution. Exp. Brain Res. 111, 246–252.
Rizzolatti, G., Fogassi, L., Gallese, V., 2000. Cortical mechanisms subserving object grasping and action recognition: a new view on the cortical motor functions. In: Gazzaniga, M.S. (Ed.), The New Cognitive Neurosciences, second ed. A Bradford Book, MIT Press, Cambridge, MA, pp. 539–552.
Rizzolatti, G., Fogassi, L., Gallese, V., 2001. Neurophysiological mechanisms underlying the understanding and imitation of action. Nat. Rev. Neurosci. 2, 661–670.
Roland, P.E., Larsen, N.A., Skinhoj, E., 1980. Supplementary motor area and other cortical areas in organization of voluntary movements in man. J. Neurophysiol. 43, 118–136.
Roth, M., Decety, J., Raybaudi, M., Massarelli, R., Delon-Martin, C., Segebarth, C., Morand, S., Gemignani, A., Décorps, M., Jeannerod, M., 1996. Possible involvement of primary motor cortex in mentally simulated movement: a functional magnetic resonance imaging study. NeuroReport 7, 1280–1284.
Ruby, P., Decety, J., 2001. Effect of subjective perspective taking during simulation of action: a PET investigation of agency. Nat. Neurosci. 4 (5), 546–550.
Sabbah, P., Simond, G., Levrier, O., Habib, M., Trabaud, V., Murayama, N., Mazoyer, B.M., Briant, J.F., Raybaud, C., Salamon, G., 1995. Functional magnetic resonance imaging at 1.5 T during sensory motor and cognitive tasks. Eur. Neurol. 35, 131–136.
Sanes, J.N., Donoghue, J.P., Thangaraj, V., Edelman, R.R., Warach, S., 1995. Shared neural substrates controlling hand movements in human motor cortex. Science 268, 1775–1777.
Savaki, H.E., Dalezios, Y., 1999. ^{14}C-Deoxyglucose mapping of the monkey brain during reaching to visual targets. Prog. Neurobiol. 58, 479–540.
Savaki, H.E., Kennedy, C., Sokoloff, L., Mishkin, M., 1993. Visually guided reaching with the forelimb contralateral to a "blind" hemisphere: a metabolic mapping study in monkeys. J. Neurosci. 13 (7), 2772–2789.
Schnitzler, A., Salenius, S., Salmelin, R., Jousmaki, V., Hari, R., 1997. Involvement of primary motor cortex in motor imagery: a neuromagnetic study. NeuroImage 6, 201–208.
Schwartz, W.J., Smith, C.B., Davidsen, L., Savaki, H., Sokoloff, L., Mata, M., Fink, D.J., Gainer, H., 1979. Metabolic mapping of functional activity in the hypothalamo-neurohypophysial system of the rat. Science 205, 723–725.
Sekiyama, K., 1982. Kinesthetic aspects of mental representations in the identification of left and right hands. Percept. Psychophys. 32 (2), 89–95.
Siegal, M., Carrington, J., Radel, M., 1996. Theory of mind and pragmatic understanding following right hemisphere damage. Brain Lang. 53, 40–50.
Sirigu, A., Cohen, L., Duhamel, J.R., Pillon, B., Dubois, B., Agid, Y., Pierrot-Deseilligny, C., 1995. Congruent unilateral impairments for real and imagined hand movements. NeuroReport 6, 997–1001.
Sirigu, A., Duhamel, J.R., Cohen, L., Pillon, B., Dubois, B., Agid, Y., 1996. The mental representation of hand movements after parietal cortex damage. Science 273, 1564–1568.
Sokoloff, L., Reivich, M., Kennedy, C., Des Rosiers, M.H., Patlak, C.S., Pettigrew, K.S., Sakurada, O., Shinohara, M., 1977. The [^{14}C]-deoxyglucose method for the measurement of local cerebral glugose utilization: theory, procedure, and normal values in the conscious and anesthetized albino rat. J. Neurochem. 28, 879–916.
Stefan, K.M., Fink, G.R., Passingham, R.E., Silbersweig, D., Ceballos-Baumann, A.O., Frith, C.D., Frackowiak, R.S.J., 1995. Functional anatomy of the mental representation of upper extremity movements in healthy subjects. J. Neurophysiol. 73, 373–386.
Strafella, A.P., Paus, T., 2000. Modulation of cortical excitability during action observation: a transcranial magnetic stimulation study. NeuroReport 11 (10), 2289–2292.
Wise, S., Moody, S., Blomstrom, K., Mitz, A., 1998. Changes in motor cortical activity during visuomotor adaptation. Exp. Brain Res. 121, 285–299.

Behavioral/Systems/Cognitive

Mental Simulation of Action in the Service of Action Perception

Vassilis Raos, Mina N. Evangeliou, and Helen E. Savaki

Department of Basic Sciences, Faculty of Medicine, School of Health Sciences, University of Crete, Iraklion, 71003 Crete, Greece, and Institute of Applied and Computational Mathematics, Foundation for Research and Technology-Hellas, 71110 Iraklion, Crete, Greece

We used the quantitative ^{14}C-deoxyglucose method to map the activity pattern throughout the frontal cortex of rhesus monkeys, which either grasped a three-dimensional object or observed the same grasping movements executed by a human. We found that virtually the same frontal cortical networks were recruited for the generation and the perception of action, including the primary motor cortex (MI/F1), premotor cortical areas (F2, F5, and F6), the primary (SI) and supplementary (SSA) somatosensory cortex, medial cortical areas (8m and 9m), and the anterior cingulate. The overlapping networks for action execution and action observation support the notion that mental simulation of action could underlie the perception of others' actions. We suggest that the premotor and the somatotopic MI/F1 activations induced by action observation reflect motor grasp of the observed action, whereas the somatotopic SI and the SSA activations reflect recruitment of learned sensory–motor associations enabling perceptual understanding of the anticipated somatosensory feedback. We also found that the premotor activations were stronger for action observation, in contrast to the primary somatosensory–motor ones, which were stronger for action execution, and that activations induced by observation were bilateral, whereas those induced by execution were contralateral to the moving forelimb. We suggest that these differences in intensity and lateralization of activations between the executive and the perceptual networks help attribute the action to the correct agent, i.e., to the "self" during action execution and to the "other" during action observation. Accordingly, the "sense of agency" could be articulated within the core components of the circuitry supporting action execution/observation.

Key words: **action observation; action recognition; mental simulation; motor cortex; premotor cortex; somatosensory cortex**

Introduction

The premotor cortical area F5 contains "mirror neurons," which discharge both when a monkey performs an object-related hand action and when the monkey observes another individual performing the same action, and could thus be responsible for the capacity of individuals to recognize actions made by others (Gallese et al., 1996; Rizzolatti et al., 1996). However, the resonant system that helps match action perception to action generation encompasses much more of the cortex than the mirror neuron concept would lead one to believe. We recently found that the forelimb regions of the primary motor (MI/F1) and somatosensory (SI) cortices within the central sulcus (Cs) are activated when subjects observe object-related hand actions, and they are activated somatotopically as they are for execution of the same actions (Raos et al., 2004).

The aim of the present study was to explore whether frontal areas other than MI/F1 and F5 are also involved in action observation. We used the [^{14}C]-deoxyglucose (^{14}C-DG) quantitative autoradiographic method (Sokoloff et al., 1977) to obtain high-resolution functional images of the monkey frontal and cingulate cortical areas activated for grasping execution and grasping observation. The ^{14}C-DG method is the only imaging approach to offer the following advantages: (1) assessment of brain activity directly and not indirectly via blood flow changes, (2) quantitative measurement of glucose consumption instead of semiquantitative relative differences, (3) resolution of 20 μm, and (4) cytoarchitectonic identification of cortical areas in sections adjacent to the autoradiographic ones.

We examined the lateral premotor cortex, including the dorsal areas F2 and F7 and the ventral areas F4 and F5 (Matelli et al., 1991; Geyer et al., 2000), as well as the medial premotor cortex, including the supplementary motor areas F3 or SMA-proper and F6 or pre-SMA, as well as the rostral (CMAr), dorsal (CMAd), and ventral (CMAv) cingulate motor areas (Matelli et al., 1991; He et al., 1995). We also examined additional medial cortical areas such as the 8-medial (8m), 9-medial (9m), 24, 23, and the supplementary somatosensory area (SSA) (Murray and Coulter, 1981; Morecraft et al., 2004). Histological examination of the brain sections enabled us to assign most of the activated regions of the reconstructed metabolic maps to cytoarchitectonically defined areas of the frontal lobe.

We found that, far from being restricted to frontal areas F5, MI/F1, and SI, the so-called "action observation/execution

Received July 1, 2007; revised Aug. 16, 2007; accepted Oct. 1, 2007.

This work was supported by the European Union (FP6 Grant IST-027574) and the General Secretariat of Research and Technology, Hellas (Grant 01ED111). We thank A. K. Moschovakis for constructive comments, G. G. Gregoriou for advice and help regarding histology, and M. Kefaloyianni for technical assistance.

Correspondence should be addressed to Helen E. Savaki, Department of Basic Sciences, Faculty of Medicine, School of Health Sciences, University of Crete, P.O. Box 2208, Iraklion, GR-71003 Crete, Greece. E-mail: savaki@med.uoc.gr.

DOI:10.1523/JNEUROSCI.2988-07.2007

 0270-6474/07/2712675-09$15.00/0

matching system" also involves extensive regions of both the lateral- and medial-frontal cortex. Because, as shown here, nearly the same widespread frontal and cingulate cortical circuits are recruited for both action perception and action generation, and because the mental simulation theory assigns the role of perceiving others' actions to the neural substrate that is also responsible for action execution, our data suggest that "mental simulation" of actions rather than "mirroring" (Goldman and Sebanz, 2005) better accounts for the recognition of actions performed by others.

Materials and Methods

Subjects and behavioral tasks. Six head-fixed adult female monkeys (*Macaca mulatta*) weighing between 3 and 5 kg were used. Experiments were approved by the institutional animal use committee in accordance with the European Council Directive 86/609/EEC. A detailed description of surgical procedures, behavioral apparatus, EMG, and eye position recording was reported previously (Raos et al., 2004). In brief, a sliding window at the front side of the behavioral apparatus allowed the subject (monkey or experimenter) to grasp a horizontally oriented ring with the index finger inserted into it (with the hand pronated) while eye movements were recorded (see Fig. 1) with an infrared oculometer (Dr. Bouis, Karlsruhe, Germany). All monkeys were trained for several months before the ^{14}C-DG experiment to perform their tasks continuously for at least 1 h per day. On the day of the ^{14}C-DG experiment, monkeys performed their tasks for the entire ^{14}C-DG experimental period (45 min) without any breaks, and successful completion of each trial was rewarded with water.

The arm-motion control (Cm) monkey had to maintain its gaze straight ahead for 2.7–3 s, during the opening of the window of the behavioral apparatus, the presentation of the illuminated object behind the window, and the closure of the window, and while the experimenter was reaching with extended hand toward the closed window. Thus, this control monkey was used to exclude not only the potential effects of the biological motion of the reaching forelimb, but also the possible effects of unspecific arousal and attention, gaze fixation, visual stimulation by the three-dimensional (3D) object, and eye movements used to scan the object. The intertrial intervals ranged between 2 and 2.5 s. During the training and the ^{14}C-DG experiment both forelimbs of this monkey were restricted.

Two grasping-execution (E) monkeys were trained to reach and grasp with their left forelimbs while the right ones were restricted. These monkeys had to fixate the object for 0.7–1 s, until a dimming of the light would signal reaching, grasping, and pulling the ring with the left forelimb (within 1 s) while maintaining fixation (intertrial intervals: 2–2.5 s).

Three grasping-observation (O) monkeys were first trained to perform the task of the E monkeys and then trained to observe the same grasping movements executed by the experimenter. Both forelimbs of the O monkeys were restricted during the observation training and during the ^{14}C-DG experiment. Although grasping training took place months before the ^{14}C-DG experiment, to cancel any possible side-to-side effects caused by this earlier grasping training, the first monkey was trained to grasp with its left hand, the second one with its right hand, and the third one with both hands consecutively. The experimenter was always standing on the right side of the monkey and was using the right arm/hand for reaching/grasping. Both reaching and grasping components of the movement were visible to the monkey. Object and movement parameters were similar to the ones described for the E task. To control for possible rate-related effects, the mean rate of movements was set to be similar for the arm-motion control, the execution, and the observation tasks.

Reconstruction of two-dimensional maps of activity. We used the ^{14}C-DG quantitative autoradiographic method (Sokoloff et al., 1977) to obtain high-resolution functional images of the monkey frontal and cingulate cortical areas activated for grasping execution and grasping observation. The ^{14}C-DG experiment and the brain tissue processing for autoradiography were performed as described previously (Savaki et al., 1993; Raos et al., 2004). In brief, the tracer was injected intravenously 5 min after initiation of task performance, and arterial blood samples were drawn for the next 45 min as per the original description of the method (Sokoloff et al., 1977). Plasma glucose levels, blood pressure, hematocrit, and blood gases ranged within normal values in all monkeys and remained constant throughout the ^{14}C-DG experiment. Glucose utilization values (in micromoles per 100 g per minute) were calculated from the original operational equation of the method (Sokoloff et al., 1977).

To cover the full extent of the lateral-frontal cortex of interest, ~1000 serial horizontal sections of 20 μm thickness were used from each hemisphere of each monkey, and 800 sections were used for the reconstruction of the medial-frontal cortex. For each horizontal section, a data array was obtained by sampling the local cerebral glucose utilization (LCGU) values along a rostrocaudal line parallel to the surface of the cortex and covering all cortical layers (anteroposterior sampling spatial resolution, 50 μm/pixel). Every five adjacent sections of 20 μm, data arrays were averaged and plotted to produce one line in the 2D maps of activity (spatial resolution of plots, 100 μm). The anterior crown of the Cs was used for the alignment of adjacent data arrays in the lateral cortex, and the anterior tip of the brain was used for alignment of the medial cortex. One section every 500 μm was stained with thionine for identification of the cytoarchitectonic borders of sensory–motor and premotor cortical areas (Matelli et al., 1991; Geyer et al., 2000; Gregoriou et al., 2005). Tick marks in each horizontal section labeling (1) surface landmarks of the brain (such as crown, fundus, and tip) and (2) cytoarchitectonically identified borders of cortical areas of interest were used to match the 2D maps obtained from different hemispheres and animals (see geometrical normalization of maps, below). Normalization of LCGU values was based on the averaged unaffected gray matter value pooled across all monkeys (Savaki et al., 1993).

Geometrical normalization of the two-dimensional maps of activity. The geometrical normalization of the individual 2D maps of LCGU values (glucograms) in the lateral and medial cortices was based on combined cytoarchitectonic and surface landmarks and was generated as follows.

In the dorsal portion of all lateral-frontal cortical maps, the section-by-section distances between (1) the anterior cytoarchitectonic border of F7 and the anterior border of F2, (2) the latter and the anterior border of MI/F1, (3) the latter and the anterior crown of the Cs (point of alignment), (4) the latter and the fundus of Cs, and (5) the fundus and the posterior crown of the Cs were measured. The average of these measures was computed to produce a reference map of landmarks (see Fig. 2*b*, dorsal segment). The areal surface in mm^2 ± SE was 166.7 ± 6.4 for F1/MI bank, 97.6 ± 11.1 for F1/MI convexity, 164.7 ± 8.1 for SI bank, 75.2 ± 6.7 for F2, and 32.4 ± 2.9 for F7. The reference map of landmarks in the ventral portion of the lateral-frontal cortex was generated similarly. The distances used here were those between (1) the fundus of the arcuate sulcus (As) and its crown, (2) the latter and the posterior border of F5, (3) the latter and the anterior crown of the Cs, (4) the latter and the fundus of Cs, and (5) the fundus and the posterior crown of Cs (see Fig. 2*b*, ventral segment). The areal surface in mm^2 ± SE was 21.3 ± 2.8 for F5 convexity, 81.1 ± 4.7 for F5 bank, and 37.7 ± 2.3 for F4. Each individual lateral-frontal cortical map with its own dorsal and ventral segments' landmarks was linearly transformed in Matlab (MathWorks, Natick, MA) to match the reference map. This allowed us to overlay functional and cytoarchitectonic maps from all hemispheres of all monkeys to obtain averaged maps per case and to subtract control from experimental maps.

In the dorsal portion of the medial-frontal convexity, the distances used to produce the reference map of landmarks were those between (1) the anterior tip of the brain (point of alignment) and the anterior border of F3, (2) the latter and the anterior border of MI/F1, (3) the latter and the anterior border of SI, (4) the latter and the dorsal crown of the cingulate sulcus (Cgs) (see Fig. 3*b*, above the dorsal crown of the Cgs). The areal surface was 45.3 ± 4.3 for SI, 46.1 ± 1.9 for F1, 46.4 ± 1.9 for F3, and 46.7 ± 3.2 for F6. The distance used to generate the reference map of landmarks in the dorsal bank of the Cgs was that between the dorsal crown of the Cgs and its fundus, separately for its anterior, middle, and posterior segments (see Fig. 3*b*). The corresponding areal surfaces were 69.5 ± 3.9, 79.2 ± 5, and 36.5 ± 3.9. The distance used to produce the reference map of landmarks in the ventral bank of the Cgs was that

between the fundus and the ventral crown of the Cgs, separately for its anterior, middle, and posterior segments (see Fig. 3*b*). The corresponding areal surfaces were 48.5 ± 2, 74.2 ± 3.8, and 29.4 ± 3. The distance used to produce the reference map of landmarks in the ventral convexity was that between the ventral crown of the Cgs and (1) the extension of the posterior tip of Cgs for the dorsalmost sections or (2) the corpus callosum for the ventralmost sections. The corresponding areal surfaces were 191.3 ± 6 and 86.2 ± 4.5, respectively. Although its total surface changed considerably when an area was geometrically normalized, the intensity and the spatial distribution of LCGU effects were preserved within each single area because these effects were proportionally shrunk or expanded within its borders.

Statistical analysis. The average LCGU values were calculated in sets of five adjacent sections (20 μm thick) throughout each cortical area of interest in each hemisphere. Experimental to control LCGU values were compared for statistical significances by the Student's unpaired *t* test. Given that ipsilateral to contralateral LCGU values in normal control monkeys range up to 7% (Kennedy et al., 1978), only differences >7% were considered for statistical treatment. The percentage LCGU differences between the experimental (E and O) and the Cm monkeys were generated using the formulas (E − Cm)/Cm × 100 and (O − Cm)/Cm × 100.

Results

During the critical first 10 min of the ^{14}C-DG experiment, the Cm monkey observed nine movements of the experimenter's arm per minute. The dwell time of the line of sight of the Cm monkey in different eye positions during the critical first 10 min of the experiment is illustrated in Figure 1*a*. Because we found no significant side-to-side difference of glucose consumption in the Cm monkey (see LCGU values for left and right hemispheres separately in Table 1), the quantitative glucograms (quantitative maps of LCGU) of the lateral (Fig. 2*c*) and the medial-frontal and cingulate (Fig. 3*c*) cortices of one side were averaged with the corresponding ones of the other side.

The E monkeys performed an average of 10 grasping movements per minute during the critical first 10 min of the ^{14}C-DG experiment. The dwell time of the line of sight in different eye positions during the critical first 10 min of the ^{14}C-DG experiment averaged over the two E monkeys is shown in Figure 1*b*. We generated LCGU maps of the lateral (Fig. 2*d*) and the medial (Fig. 3*d*) cortices by averaging the two corresponding, geometrically normalized glucograms in the right hemispheres (contralateral to the moving forelimb) of the two E monkeys. The latter glucograms as well as the equivalent ones in the left hemispheres (ipsilateral to the moving forelimb) were used for measurement of the LCGU values in cortical areas of interest, their statistical comparisons, and the estimation of the percentage differences from the Cm control values (Table 1).

To illustrate the percentage LCGU differences between the E monkeys and the Cm, we generated images using the formula (E − Cm)/Cm × 100 for each one of the lateral and the medial cortical maps. When the averaged maps (lateral or medial) of the right hemispheres of the E monkeys are compared with the averaged maps of the Cm monkey, increased metabolic activity (net activation) is apparent in several frontal and cingulate cortical regions. Areas activated for execution of grasping movements include the proximal forelimb representation of F1-convexity, F2-forelimb region, F5-bank, and F5-convexity, in addition to the forelimb representations in the SI and the MI/F1 of the Cs (Fig. 4*a*, Table 1). They also include several medial areas such as the F3/SMA-proper, F6/pre-SMA, CMAd, CMAv, CMAr, 8m, 9m, 24, 23, and SSA (Fig. 5*a*, Table 1). Most of the activated regions were found in the hemisphere contralateral to the grasping hand (Table 1).

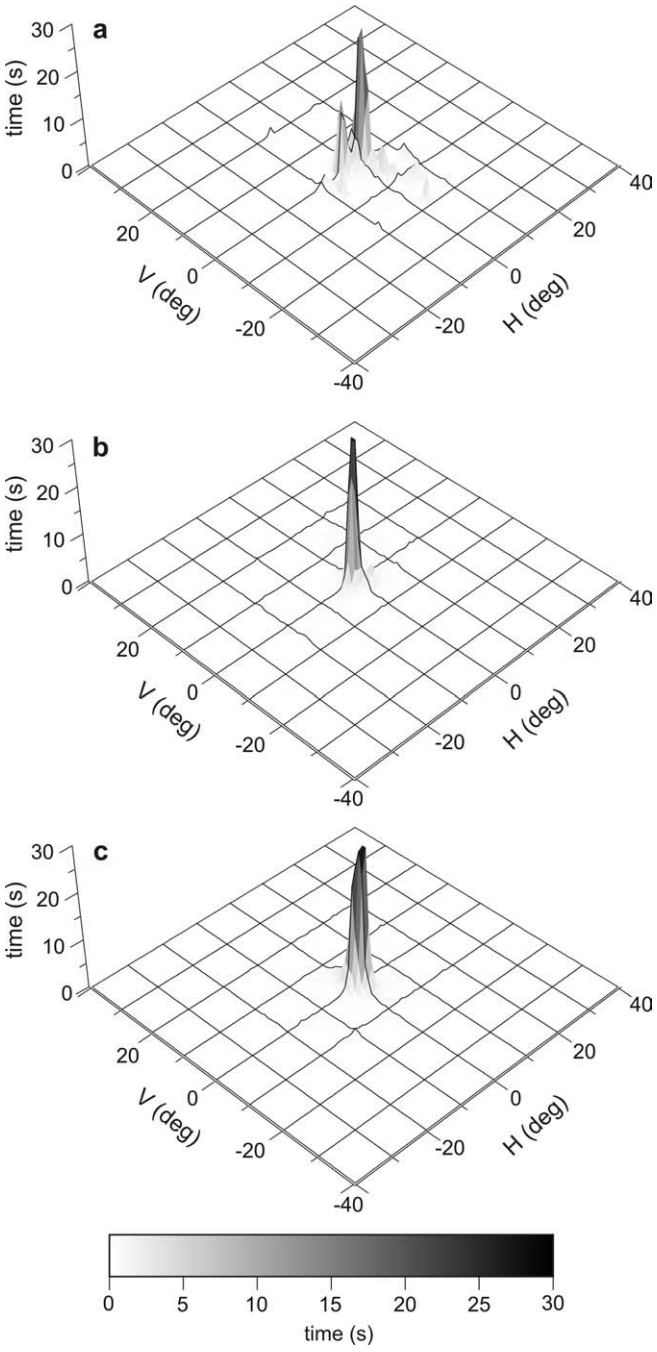

Figure 1. Three-dimensional histograms of the dwell time of the line of sight as a function of eye position during the critical first 10 min of the ^{14}C-DG experiment. ***a***, Motion-control monkey. ***b***, Averaged oculomotor behavior from the two grasping-execution monkeys. ***c***, Averaged behavior from the three grasping-observation monkeys. Horizontal axis (H; *x*) and vertical axis (V; *y*) in degrees, *z*-axis in seconds. Grayscale bar indicates time in seconds.

The O monkeys observed an average of 12 grasping movements per minute during the critical first 10 min of the ^{14}C-DG experiment. The dwell time of the line of sight in different eye positions during the critical first 10 min of the experiment averaged over the three O monkeys is shown in Figure 1*c*. When the averaged maps of the lateral (Fig. 2*e*) and the medial and cingulate (Fig. 3*e*) cortex of the right hemispheres of the three O monkeys are compared with the averaged Cm maps (Figs. 2*c*, 3*c*), regions of increased metabolic activity included lateral-frontal areas, such as the F7, F2-forelimb, F5-bank, and F5-convexity, in

Table 1. Metabolic effects in frontal cortical areas of the monkey brain

Cortical area	*n*	Cml LCGU ± SD	Cmr LCGU ± SD	Cm LCGU ± SD	El LCGU ± SD	Er LCGU ± SD	Ol LCGU ± SD	Or LCGU ± SD	El/Cm (%)	Er/Cm (%)	Ol/Cm (%)	Or/Cm (%)
Primary somatosensory and motor areas												
SI-forelimb (central sulcus)	98	62 ± 2	61 ± 2	61 ± 2	62 ± 3	76 ± 5	64 ± 3	68 ± 3	2	25	5	11
SI-forelimb (max, central sulcus)	24	63 ± 3	58 ± 1	60 ± 2	61 ± 2	77 ± 3	69 ± 1	72 ± 2	2	28	15	20
SI-trunk (central sulcus)	80	66 ± 4	67 ± 3	66 ± 3	69 ± 4	75 ± 4	70 ± 5	70 ± 6	5	14	6	6
SI-hindlimb (medial cortex)	65	59 ± 3	57 ± 2	58 ± 2	58 ± 3	59 ± 2	57 ± 2	58 ± 2	0	2	−2	0
F1-forelimb (central sulcus)	103	58 ± 3	55 ± 3	56 ± 3	55 ± 4	66 ± 3	58 ± 4	61 ± 5	−2	18	4	9
F1-forelimb (max, central sulcus)	28	59 ± 2	54 ± 1	57 ± 1	58 ± 1	71 ± 2	61 ± 1	63 ± 1	2	25	7	11
F1-forelimb convexity	65	51 ± 1	51 ± 2	51 ± 1	50 ± 2	58 ± 2	50 ± 1	54 ± 2	−2	14	−2	6
F1-trunk (central sulcus)	80	63 ± 6	63 ± 4	63 ± 4	61 ± 2	65 ± 3	67 ± 7	65 ± 5	−3	3	6	3
F1-trunk convexity	42	51 ± 2	51 ± 3	51 ± 2	53 ± 2	54 ± 1	52 ± 1	52 ± 1	4	6	2	2
F1-hindlimb (medial cortex)	65	52 ± 4	52 ± 4	52 ± 3	54 ± 3	54 ± 4	52 ± 2	52 ± 2	4	4	0	0
Lateral premotor areas (dorsal)												
F7	60	44 ± 2	45 ± 2	45 ± 1	44 ± 5	47 ± 4	49 ± 2	50 ± 1	−2	4	9	11
F2-forelimb	48	45 ± 3	46 ± 3	45 ± 3	46 ± 2	51 ± 2	49 ± 2	52 ± 2	2	13	9	16
F2-forelimb convexity	47	45 ± 2	46 ± 3	46 ± 3	46 ± 2	51 ± 1	48 ± 1	52 ± 3	0	11	4	13
F2-forelimb bank	32	45 ± 4	45 ± 3	45 ± 3	44 ± 3	51 ± 3	50 ± 2	54 ± 1	−2	13	11	20
F2-hindlimb convexity	42	53 ± 6	51 ± 4	52 ± 4	53 ± 6	55 ± 4	52 ± 2	50 ± 2	2	6	0	−4
Lateral premotor areas (ventral)												
F5 bank	98	55 ± 4	53 ± 3	54 ± 2	56 ± 3	59 ± 3	62 ± 3	62 ± 2	4	9	15	15
F5 bank dorsal	40	54 ± 5	52 ± 3	53 ± 3	53 ± 1	56 ± 2	59 ± 1	61 ± 2	0	6	11	15
F5 bank ventral	58	55 ± 3	52 ± 3	54 ± 2	58 ± 2	61 ± 1	64 ± 2	62 ± 2	7	13	19	15
F5 convexity	65	56 ± 5	55 ± 5	55 ± 4	61 ± 5	62 ± 2	59 ± 2	59 ± 2	11	13	7	7
F5 convexity (max)	33	55 ± 2	50 ± 4	53 ± 2	64 ± 4	64 ± 1	59 ± 1	59 ± 2	21	21	11	11
F4	76	68 ± 4	64 ± 3	66 ± 3	65 ± 5	65 ± 5	65 ± 3	67 ± 4	−2	−2	−2	2
Medial cortical areas (dorsal convexity)												
9m convexity anterior	49	41 ± 1	40 ± 3	41 ± 2	48 ± 1	50 ± 1	43 ± 1	45 ± 2	17	22	5	10
9m convexity posterior	22	46 ± 2	47 ± 2	47 ± 1	49 ± 1	50 ± 1	47 ± 1	46 ± 1	4	6	0	−2
8m (max)	24	47 ± 2	49 ± 2	48 ± 1	53 ± 2	57 ± 4	55 ± 1	52 ± 1	10	19	15	8
F6/pre-SMA (max)	24	56 ± 5	54 ± 1	55 ± 2	58 ± 1	62 ± 3	60 ± 1	58 ± 3	5	13	9	5
F3/SMA-proper (max)	31	51 ± 1	49 ± 3	50 ± 2	51 ± 2	54 ± 1	52 ± 1	53 ± 1	2	8	4	6
Cingulate sulcus (dorsal bank)												
24d anterior	43	41 ± 3	41 ± 3	41 ± 2	47 ± 2	50 ± 2	49 ± 2	48 ± 2	15	22	20	17
24d middle	41	57 ± 3	55 ± 3	56 ± 2	56 ± 3	50 ± 4	55 ± 2	51 ± 1	0	−11	−2	−9
24d posterior (dCMAr)	28	54 ± 3	55 ± 2	55 ± 2	59 ± 1	62 ± 2	57 ± 1	56 ± 2	7	13	4	2
23d	33	49 ± 3	49 ± 3	49 ± 2	49 ± 4	53 ± 3	50 ± 2	52 ± 3	0	8	2	6
23d anterior (CMAd)	33	52 ± 3	49 ± 2	51 ± 2	50 ± 6	57 ± 3	52 ± 3	54 ± 2	2	12	2	6
SSA dorsal bank	53	46 ± 3	47 ± 4	46 ± 3	55 ± 4	56 ± 2	52 ± 2	54 ± 4	20	22	13	17
Cingulate sulcus (ventral bank)												
24c anterior	33	45 ± 3	46 ± 5	45 ± 3	50 ± 2	50 ± 3	50 ± 3	50 ± 3	11	11	11	11
24c middle	37	50 ± 5	50 ± 2	49 ± 3	53 ± 2	59 ± 2	54 ± 3	53 ± 5	8	20	10	8
24c posterior (vCMAr)	28	49 ± 4	51 ± 5	50 ± 3	52 ± 6	54 ± 6	52 ± 3	50 ± 5	4	8	4	0
23c (CMAv)	30	42 ± 2	42 ± 2	42 ± 2	46 ± 2	50 ± 3	45 ± 1	45 ± 1	10	19	7	7
SSA ventral bank	77	42 ± 3	45 ± 3	44 ± 4	46 ± 3	48 ± 1	46 ± 1	46 ± 2	5	9	5	5
Medial areas (ventral convexity)												
24ab anterior	51	34 ± 2	34 ± 2	34 ± 2	36 ± 3	38 ± 2	40 ± 1	40 ± 2	6	12	18	18
24ab posterior	51	39 ± 4	40 ± 2	40 ± 2	40 ± 2	45 ± 3	44 ± 1	43 ± 2	0	13	10	8
23ab	69	41 ± 3	43 ± 3	42 ± 3	43 ± 4	47 ± 2	43 ± 3	45 ± 2	2	12	2	7
31	103	42 ± 2	44 ± 4	43 ± 2	42 ± 2	45 ± 2	44 ± 2	46 ± 2	−2	5	2	7

n, Number of sets of five adjacent horizontal sections used to obtain the mean LCGU values (in micromoles per 100 g per min) for each region. Cm values represent the average LCGU values from the two hemispheres of the motion-control monkey. El and Er values represent the average LCGU values from the two left and the two right hemispheres of the grasping-execution monkeys, respectively. Ol and Or values represent the average LCGU values from the three left and the three right hemispheres of the grasping-observation monkeys, respectively. El/Cm, Er/Cm, Ol/Cm, and Or/Cm represent percentage differences between El, Er, Ol, and Or and Cm, respectively, calculated as (experimental − control)/control × 100. Values in bold indicate statistically significant differences by the Student's unpaired *t* test at the level of $p < 0.001$.

addition to the SI-forelimb region and to the distal (but not proximal) forelimb representation in MI/F1 (Fig. 4*b*, Table 1). Activations were also found in medial cortical areas, such as the F6/pre-SMA, 9m, 8m, 24, and SSA (Fig. 5*b*, Table 1). Most of the activations were found to be bilateral (Table 1). The only significant depression that we measured was in the middle portion of 24d (dorsal bank of Cgs) in the right hemispheres of both E and O cases (Table 1). The absence of increased activity in EMG records of the O monkeys convinced us that the herein documented cortical effects are not attributable to and do not generate muscular contractions.

When spatially analyzed, the activations induced by observation of grasping movements were found to largely overlap those induced by execution of the same movements within both the lateral (Fig. 4*c*) and the medial (Fig. 5*c*) cortical maps of activity. In the latter figures, red, green, and yellow correspond to

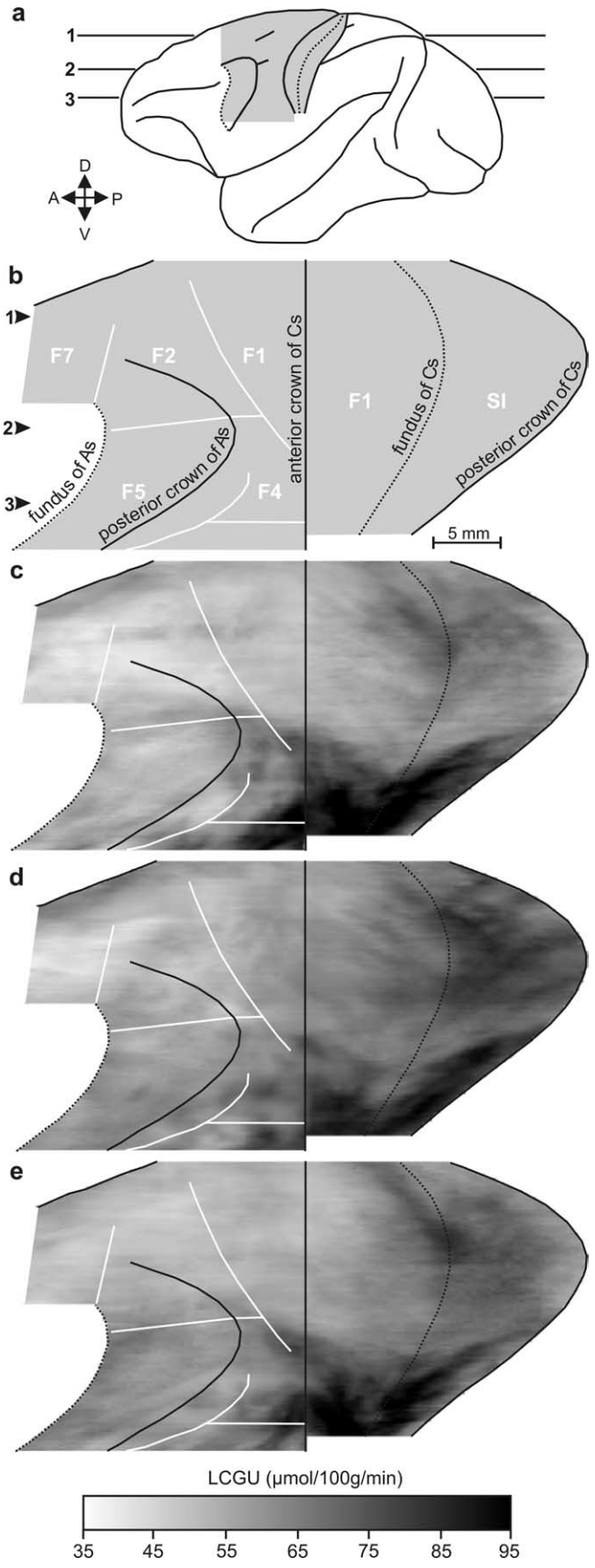

Figure 2. Quantitative 2D maps of metabolic activity in the lateral-frontal cortex. ***a***, Lateral view of a monkey brain with the Cs and the posterior bank of the As unfolded. Dotted lines depict the fundus of the As and that of the Cs. Shaded area indicates the reconstructed cortex. Horizontal lines 1–3 correspond to three different dorsoventral levels of brain sectioning. A, Anterior; D, dorsal; P, posterior; V, ventral. ***b***, Schematic illustration of the geometrically normalized reconstructed cortical field. Black lines correspond to surface landmarks and white lines to cytoarchitectonically identified borders of the labeled cortical areas. Arrows 1–3 indicate the dorsoventral levels of the corresponding lines in ***a***. ***c***, Averaged map from the two hemispheres of the motion-control monkey. ***d***, Averaged map from the right hemispheres (contralateral to the moving forelimb) of the two grasping-execution monkeys. ***e***, Averaged map from the right hemispheres of the three grasping-observation monkeys. Grayscale bar indicates LCGU values in micromoles per 100 g per minute.

execution-induced, observation-elicited, and common activations, respectively. However, when the intensity of activation was also taken into account, the effects of action execution differed from those of action observation. To graphically illustrate the spatio-intensive distribution of metabolic activity within the affected regions, we plotted the differences between the experimental monkeys and the Cm (as percentage LCGU values and 95% confidence intervals per 100 μm) across the rostrocaudal extent in the reconstructed maps (Fig. 6). The plots in this figure represent the percentage differences between the E and the Cm monkeys (red lines) as well as between the O and the Cm monkeys (green lines). Baseline indicates 0% difference from the Cm. The plots in Figure 6*a* represent differences in the forelimb representations of the dorsal premotor and the primary sensory-motor cortices along the ribbon highlighted in the brain sketch above the graphs. In the left hemispheres of the two E monkeys ipsilateral to the grasping hand, activity of all cortical areas is similar to that of the corresponding areas in the Cm (Fig. 6*a*, dotted red line fluctuates around 0%). In contrast, significantly larger activations were found within the premotor and primary sensory-motor cortices of the hemispheres contralateral to the grasping hand (Fig. 6*a*, solid red line) resulting in a pronounced side-to-side difference in the E monkeys. Interestingly, the corresponding side-to-side difference in the O monkeys is much smaller (Fig. 6*a*, distance between the solid and the dotted green lines). Consequently, the sensory-motor activations induced by action execution are mostly contralateral to the moving forelimb, in contrast to those elicited by action observation, which are mainly bilateral (see also Table 1). Moreover, in the O monkeys the primary sensory-motor cortex is less activated, whereas the dorsal premotor is more activated, than the corresponding areas of the affected hemisphere (contralateral to the moving forelimb) of the E monkeys (Fig. 6*a*, Table 1). The plots in Figure 6*b* represent percentage LCGU differences between the experimental and the Cm monkeys across the rostrocaudal extent of the dorsal bank of the cingulate sulcus. Smaller side-to-side differences and higher anterior (than posterior) activations in the O relative to the E monkeys were also found in this case (Fig. 6*b*) as well as in other medial cortical areas (Table 1).

Discussion

Effects induced by grasping execution and grasping observation

Our quantitative high-resolution neuroimaging study combined with cytoarchitectonic identification of cortical areas demonstrates conclusively for the first time the extensive overlap of the action execution and action observation systems within the lateral and medial frontal and cingulate sensory-motor cortical network of primates. Of course, the overlapping activations for action execution and action observation do not necessarily indicate involvement of the same cell populations in the two conditions.

Of the lateral-frontal cortical areas we examined, the distal forelimb representations in MI/F1 and SI of the Cs were activated

for both execution and observation, in contrast to the proximal forelimb representation in the MI/F1 of the convexity (rostral to the Cs), which was activated only for grasping execution. The F2-forelimb representation, the F5-bank, and F5-convexity were involved in both execution and observation of grasping. Our findings confirm previous reports demonstrating that mere observation of goal-directed hand actions modulates activity in the MI/F1 and SI (Hari et al., 1998; Avikainen et al., 2002), the dorsal (Grafton et al., 1996; Decety et al., 1997; Buccino et al., 2001; Cisek and Kalaska, 2004; Filimon et al., 2007), and the ventral premotor (Grafton et al., 1996; Rizzolatti et al., 1996; Decety et al., 1997; Nelissen et al., 2005) cortical areas, which are normally activated by execution of the same hand movements, and facilitates the excitability of the observer's spinal circuitry, which is normally involved in hand movement execution (Fadiga et al., 1995; Maeda et al., 2002; Romani et al., 2005). Our findings also confirm previous studies reporting that the motor circuitry is activated mainly contralaterally to the moving forelimb for action execution (Gregoriou et al., 2005) and bilaterally for action observation (Nishitani and Hari, 2000; Costantini et al., 2005; Filimon et al., 2007). Our finding that F7 is involved in observation, F2 in both observation and execution, and MI/F1-convexity in execution is compatible with reports that the rostral part of the human premotor cortex is more active during motor imagery and the caudal part during motor execution of hand movements (Gerardin et al., 2000; Lacourse et al., 2005).

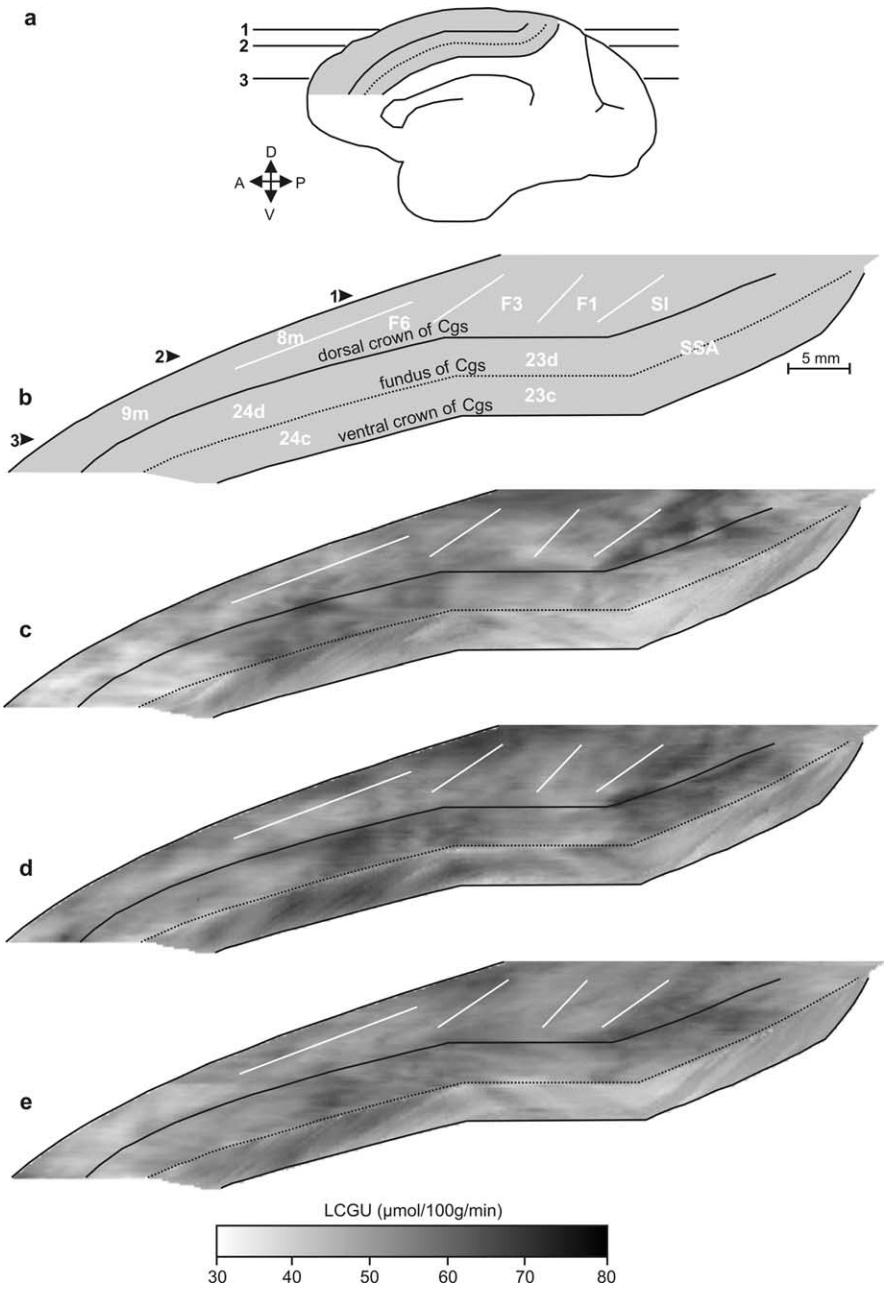

Figure 3. Quantitative 2D maps of metabolic activity in the medial convexity and the Cgs. ***a***, Medial view of a monkey brain with the Cgs unfolded. Dotted line depicts the fundus of the sulcus. Shaded area represents the reconstructed cortex. ***b***, Schematic illustration of the geometrically normalized reconstructed cortical field. Black lines correspond to surface landmarks and white lines to cytoarchitectonically identified borders of the labeled cortical areas. ***c***, Averaged map from the two hemispheres of the motion-control monkey. ***d***, Averaged map from the right hemispheres (contralateral to the moving forelimb) of the two grasping-execution monkeys. ***e***, Averaged map from the right hemispheres of the three grasping-observation monkeys. Other conventions are as in Figure 2.

Of the medial-frontal and cingulate cortical areas that we examined, F6/pre-SMA, 8m, 9m, anterior 24d, 24c, 24ab, and SSA were involved in both execution and observation, whereas F3/SMA-proper, CMAs, and area 23 were involved mainly in execution. Our findings confirm previous reports demonstrating that observation and execution of goal-directed hand actions activate in common medial-frontal areas 9 and 6-rostral (Grafton et al., 1996; Decety et al., 1997). Interestingly, area F6/pre-SMA herein documented to be involved in both action execution and action observation has been associated with effector-independent aspects of motor behavior (Fujii et al., 2002), whereas area F3/SMA-proper herein found to be involved only in action execution is known to project directly to MI/F1 and the spinal cord (He et al., 1995) and to be more closely associated with actual execution (Fujii et al., 2002). Our finding that only the F6/pre-SMA is involved in action observation, whereas both F6/pre-SMA and F3/SMA-proper are involved in action execution, is consistent with reports of a covert-to-overt rostrocaudal segregation reported in the medial-frontal cortex (Stephan et al., 1995; Decety, 1996; Grafton et al., 1996; Gerardin et al., 2000; Nishitani and Hari, 2000; Costantini et al., 2005; Filimon et al., 2007). Also, our finding that the medial cortical area 9 and the anterior part of area 24 are involved in both execution and observation is compatible with the suggestion that these areas control a goal-based action selection (Matsumoto et al., 2003). Finally, the region in the caudalmost portion of the Cgs, which was activated for both execution and observation of action in our study, corresponds to an area that has been designated as the transitional and supple-

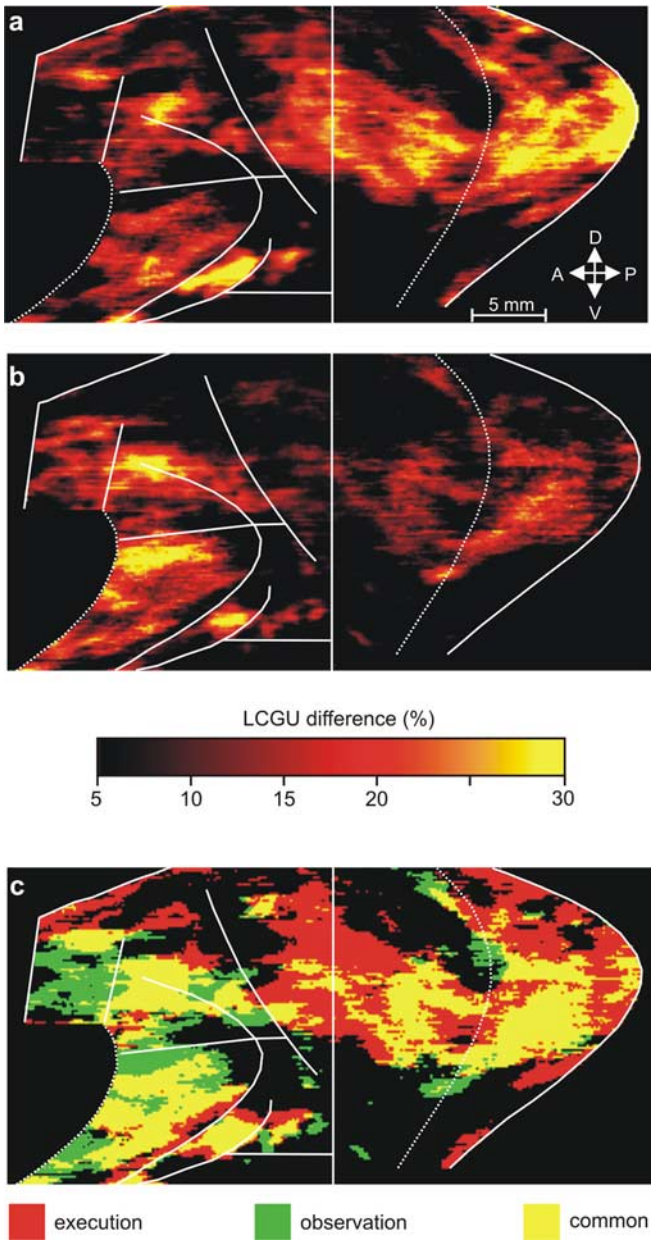

Figure 4. Lateral-frontal cortical maps of percentage LCGU differences from the Cm. Percentage differences were calculated using the formula (E − Cm)/Cm × 100 for execution and (O − Cm)/Cm × 100 for observation. ***a***, Map of net execution-induced activations averaged from the right hemispheres (contralateral to the moving forelimb) of the two grasping-execution monkeys. ***b***, Map of net observation-induced activations averaged from the right hemispheres of the three grasping-observation monkeys. Color bar indicates percentage LCGU differences from the Cm. ***c***, Superimposition of ***a*** and ***b***. Red and green represent activations >10% induced by grasping execution and grasping observation, respectively. Yellow stands for activations induced by both execution and observation of the same action. White lines correspond to the surface landmarks and the cytoarchitectonic borders illustrated in Figure 2.

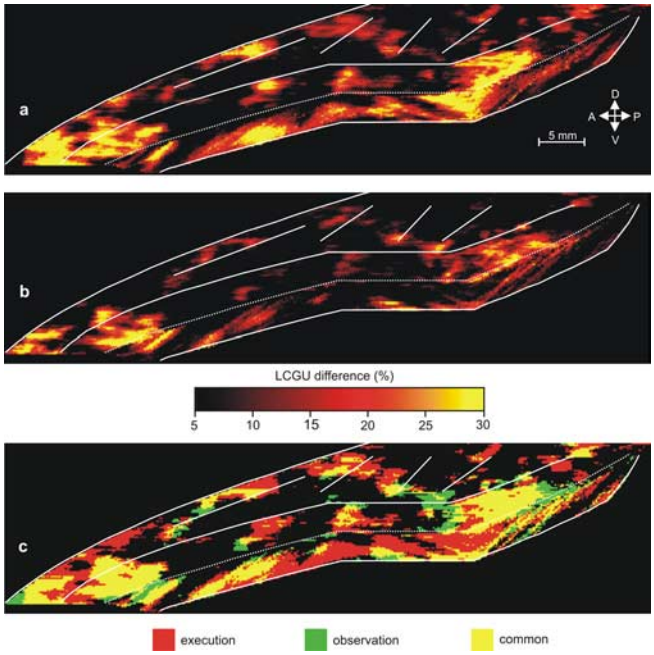

Figure 5. Maps of the medial convexity and the cingulate sulcus: percentage LCGU differences from the Cm. ***a***, Map of net execution-induced activations averaged from the right hemispheres (contralateral to the moving forelimb) of the two grasping-execution monkeys. ***b***, Map of net observation-induced activations averaged from the right hemispheres of the three grasping-observation monkeys. Color bar indicates percentage LCGU differences from the Cm. ***c***, Superimposition of ***a*** and ***b***. Red and green represent activations >10% induced by grasping execution and grasping observation, respectively. Yellow stands for activations matched for execution and observation. White lines correspond to the surface landmarks and the cytoarchitectonic borders illustrated in Figure 3.

mentary somatosensory area (SSA) and that is strongly connected to the sensory-motor specific cortices (Murray and Coulter, 1981; Morecraft et al., 2004).

Mental simulation of actions in the service of action recognition

The fact that the execution and the observation of the same action rely on a largely common distributed neural system indicates that they are functionally intertwined and substantiates the often-considered parity between perception and action. Our finding that observing an action excites the motor programs used to execute that same action implies that observation of an action corresponds to simulation of its overt counterpart. Therefore, to recognize the actions of another person and to understand his behavior, the observer may be putting himself in the actor's shoes. This mechanism resembles the internal recital or the mental rehearsal of the observed action. In other words, we could be decoding the actions of others by activating our own action system. We could understand observed actions by executing them "mentally."

It is reasonable to ask why the activation of the motor system during observation of an action does not result in overt movements. As previously proposed, a dual mechanism may operate at the spinal level, involving a subthreshold excitatory corticospinal input (preparation to move) and a parallel inhibitory influence (suppression of overt movement) via the brainstem or the cerebellum (Blakemore et al., 2001; Jeannerod, 2001). The herein documented smaller (by 50%) activation of the MI/F1-forelimb in the Cs for action observation than for action execution supports the hypothesis that the actions of others are decoded by activating one's own corticospinal system at a subthreshold level. Similarly, our finding that the rostrodorsal and rostroventral lateral premotor cortical activations are higher (by 40%) for action observation than for action execution supports the hypothesis that a parallel inhibitory influence may block the overt action. For example, area F7, which is activated for observation but not for execution, may inhibit the α-motoneurons via the brainstem (Keizer and Kuypers, 1989). A more detailed picture of the possible underlying inhibitory network(s) will be obtained when the

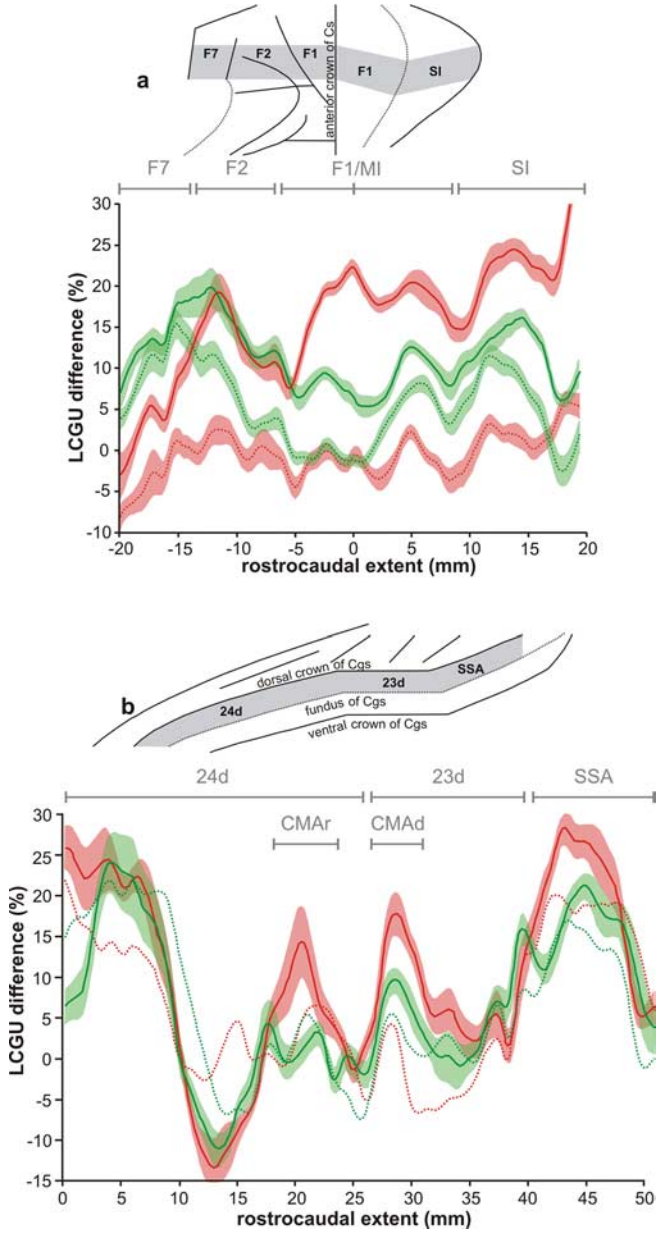

Figure 6. Plots of percentage LCGU differences along the rostrocaudal extent of the reconstructed cortical fields. Red plots illustrate the differences between the two execution monkeys and the Cm. Green plots illustrate the differences between the three observation monkeys and the Cm. Plots with solid and dotted lines correspond to the right and the left hemispheres, respectively. Red and green shaded areas indicate 95% confidence intervals. Baseline corresponds to 0% LCGU difference from the Cm. ***a***, Plot along the rostrocaudal extent of the forelimb representations in the dorsal premotor (F7, F2) and the primary sensory-motor (F1/MI, SI) cortices (along the ribbon highlighted in the drawing above the plots). Zero rostrocaudal extent represents the point of alignment of the horizontal brain sections in the lateral-frontal reconstructed maps, i.e., the anterior crown of the Cs. Areas rostral and caudal to the anterior crown of the Cs are represented by negative and positive values, respectively. ***b***, Plot along the rostrocaudal extent of the dorsal bank of the Cgs, highlighted in the drawing above the plots.

cerebellar and brainstem motor components of our monkeys are analyzed.

It is also reasonable to expect that the simulation of actual movements, which as we suggest underlies action observation, would cause facilitation of their subsequent execution. As a consequence, motor skills could be learned by observation (Mattar and Gribble, 2005). Indeed, the role of observation and imagery (or mental practice) in the teaching of motor skills has already been stated (Hall et al., 1992). Accordingly, we may build our motor repertory by incorporating not only our motor experiences, but also those of other individuals.

All in all, our results undermine the "mirror neuron system" concept. The herein documented fact that the neural correlates of the observation-driven system in the frontal cortex extend well beyond the F5-convexity, where the "mirror neurons" reside (Gallese et al., 1996; Rizzolatti et al., 1996), supports the suggestion that a broader process such as "mental simulation of action" rather than "mirroring" is responsible for action recognition (Goldman and Sebanz, 2005). The concept of mirroring reflects the function of a certain class of cells in premotor area F5 and parietal area PF, which discharge both when a monkey executes an action and when the same monkey observes another subject executing the same action. It thus provides a possible neural substrate for understanding the actions of others. In contrast, the mental simulation theory assigns the role of understanding others' actions to the entire distributed neural network, which is responsible for the execution of actions. In this scenario, action simulation serves the perception of action. Once in place, the neural circuitry that supports action execution can be also used to support the recognition of actions (Goldman and Sebanz, 2005). Neural networks that originally evolved to generate actions ran off-line (decoupled from actual movement) to help understand the actions of others. Accordingly, motor cognition is embodied in action, a notion that supports perceptual (rather than amodal) theories of knowledge claiming that sensory–motor simulators implement fully functional conceptual systems (Barsalou, 1999).

Attribution of action to the correct agent

The activations induced by observation of grasping movements in anterior premotor areas of the lateral-frontal cortices were stronger than those induced by execution of grasping. In contrast, the activation induced by observation of grasping in the MI/SI-forelimb area was weaker than that induced by execution of grasping. Also, the effects induced by action observation were mainly bilateral, whereas those induced by action execution were mostly contralateral to the moving forelimb. These differential activations of premotor and primary sensory–motor cortices could play a role in attributing the action to the correct agent, i.e., to the other agent during action observation and to the self during action execution. For example, the higher level of MI/FI-forelimb cortical activity for action execution may reflect the intended movement (input from the activated premotor cortex) and the actual motor command (MI/F1 cellular activity), whereas the 50% lower activity for action observation may reflect the intended movement only. Also, the higher level of SI-forelimb cortical activity for action execution may reflect the anticipated sensory consequence of the movement (based on efference copy from MI/F1) and the actual afferent feedback (signal from the muscles), whereas the 50% lower activity for action observation may reflect the anticipated consequence of the movement only. Furthermore, although there is no direct evidence from our data, we suggest that the bilateral and more intense (dorsal and ventral) lateral premotor cortical activations for action observation could reflect the discrepancy between the programmed (represented) movement and the lack of the corresponding sensory feedback. In other words, they could reflect the incongruence between the predicted consequence of the triggered movement representation and the lack of its actual afferent feedback during mere observation. Interestingly, the experience of ourselves or others as the cause of an action may derive from the ability to compare motor commands with reafference from the body

movements and external events caused by the commands (Johnson and Haggard, 2005). There are several reports assigning to the anterior section of the frontal cortex a role in sense of agency (feeling in control over a sensory event linked to one's own action), action attribution (deciding which action belongs to which agent), and mental-state ascription [for review, see Decety and Sommerville (2003) and Gallagher and Frith (2003)]. However, our findings suggest that the anterior frontal cortical areas associated with attribution of action in the abovementioned studies may constitute central components of the execution/perception distributed sensory–motor circuit rather than extra machinery functioning on a side path of this circuitry.

References

Avikainen S, Forss N, Hari R (2002) Modulated activation of the human SI and SII cortices during observation of hand actions. NeuroImage 15:640–646.

Barsalou LW (1999) Perceptual symbol systems. Behav Brain Sci 22:577–609.

Blakemore SJ, Frith CD, Wolpert DW (2001) The cerebellum is involved in predicting the sensory consequences of action. NeuroReport 12:1879–1885.

Buccino G, Binkofski F, Fink GR, Fadiga L, Fogassi L, Gallese V, Seitz RJ, Zilles K, Rizzolatti G, Freund HJ (2001) Action observation activates premotor and parietal areas in a somatotopic manner: an fMRI study. Eur J Neurosci 13:400–404.

Cisek P, Kalaska JF (2004) Neural correlates of mental rehearsal in dorsal premotor cortex. Nature 431:993–996.

Costantini M, Galati G, Ferretti A, Caulo M, Tartaro A, Romani GL, Aglioti SM (2005) Neural systems underlying observation of humanly impossible movements: an FMRI study. Cereb Cortex 15:1761–1767.

Decety J (1996) Do imagined and executed actions share the same neural substrate? Cogn Brain Res 3:87–93.

Decety J, Sommerville JA (2003) Shared representations between self and other: a social cognitive neuroscience view. Trends Cogn Sci 7:527–533.

Decety J, Grezes J, Costes N, Perani D, Jeannerod M, Procyk E, Grassi F, Fazio F (1997) Brain activity during observation of actions. Influence of action content and subject's strategy. Brain 120:1763–1777.

Fadiga L, Fogassi L, Pavesi G, Rizzolatti G (1995) Motor facilitation during action observation: a magnetic stimulation study. J Neurophysiol 73:2608–2611.

Filimon F, Nelson JD, Hagler DJ, Sereno MI (2007) Human cortical representations for reaching: mirror neurons for execution, observation, and imagery. NeuroImage 37:1315–1328.

Fujii N, Mushiake H, Tanji J (2002) Distribution of eye- and arm-movement-related neuronal activity in the SEF and in the SMA and pre-SMA of monkeys. J Neurophysiol 87:2158–2166.

Gallagher HL, Frith CD (2003) Functional imaging of "theory mind." Trends Cogn Sci 7:77–83.

Gallese V, Fadiga L, Fogassi L, Rizzolatti G (1996) Action recognition in the premotor cortex. Brain 119:593–609.

Gerardin E, Sirigu A, Lehericy S, Poline JB, Gaymard B, Marsault C, Agid Y, Bihan D (2000) Partially overlapping neural networks for real and imagined hand movements. Cereb Cortex 10:1093–1104.

Geyer S, Matelli M, Luppino G, Zilles K (2000) Functional neuroanatomy of the primate isocortical motor system. Anat Embryol 202:443–474.

Goldman AI, Sebanz N (2005) Simulation, mirroring, and a different argument from error. Trends Cogn Sci 9:320.

Grafton ST, Arbib MA, Fadiga L, Rizzolatti G (1996) Localization of grasp representations in humans by positron emission tomography. 2. Observation compared with imagination. Exp Brain Res 112:103–111.

Gregoriou GG, Luppino G, Matelli M, Savaki HE (2005) Frontal cortical areas of the monkey brain engaged in reaching behavior: a (14)C-deoxyglucose imaging study. NeuroImage 27:442–464.

Hall C, Buckolz E, Fishburne GJ (1992) Imagery and the acquisition of motor skills. J Can Sport Sci 17:19–27.

Hari R, Forss N, Avikainen S, Kirveskari E, Salenius S, Rizzolatti G (1998) Activation of human primary motor cortex during action observation: a neuromagnetic study. Proc Natl Acad Sci USA 95:15061–15065.

He S-Q, Dum RP, Strick PL (1995) Topographic organization of corticospinal projections from the frontal lobe: motor areas on the medial surface of the hemisphere. J Neurosci 15:3284–3306.

Jeannerod M (2001) Neural simulation of action: a unifying mechanism for motor cognition. NeuroImage 14:S103–S109.

Johnson H, Haggard P (2005) Motor awareness without perceptual awareness. Neuropsychologia 43:227–237.

Keizer K, Kuypers HGJM (1989) Distribution of corticospinal neurons with collaterals to the lower brain stem reticular formation in monkey. Exp Brain Res 74:311–318.

Kennedy C, Sakurada O, Shinohara M, Jehle J, Sokoloff L (1978) Local cerebral glucose utilization in the normal conscious macaque monkey. Ann Neurol 4:293–301.

Lacourse MG, Orr EL, Cramer SC, Cohen MJ (2005) Brain activation during execution and motor imagery of novel and skilled sequential hand movements. NeuroImage 27:505–519.

Maeda F, Kleiner-Fisman G, Pascual-Leone A (2002) Motor facilitation while observing hand actions: specificity of the effect and role of observer's orientation. J Neurophysiol 87:1329–1335.

Matelli M, Luppino G, Rizzolatti G (1991) Architecture of superior and mesial area 6 and the adjacent cingulate cortex in the macaque monkey. J Comp Neurol 311:445–462.

Matsumoto K, Suzuki W, Tanaka K (2003) Neuronal correlates of goal-based motor selection in the prefrontal cortex. Science 301:229–232.

Mattar AA, Gribble PL (2005) Motor learning by observing. Neuron 46:153–160.

Morecraft RJ, Cipolloni PB, Stilwell-Morecraft KS, Gedney MT, Pandya DN (2004) Cytoarchitecture and cortical connections of the posterior cingulate and adjacent somatosensory fields in the rhesus monkey. J Comp Neurol 469:37–69.

Murray EA, Coulter JD (1981) Supplementary sensory area. The medial parietal cortex in monkey. Clifton, NJ: Humana.

Nelissen K, Luppino G, Vanduffel W, Rizzolatti G, Orban GA (2005) Observing others: multiple action representation in the frontal lobe. Science 310:332–336.

Nishitani N, Hari R (2000) Temporal dynamics of cortical representation for action. Proc Natl Acad Sci USA 97:913–918.

Raos V, Evangeliou MN, Savaki HE (2004) Observation of action: grasping with the mind's hand. NeuroImage 23:193–201.

Rizzolatti G, Fadiga L, Gallese V, Fogassi L (1996) Premotor cortex and the recognition of motor actions. Cogn Brain Res 3:131–141.

Romani M, Cesari P, Urgesi C, Facchini S, Aglioti SM (2005) Motor facilitation of the human cortico-spinal system during observation of biomechanically impossible movements. NeuroImage 26:755–763.

Savaki HE, Kennedy C, Sokoloff L, Mishkin M (1993) Visually guided reaching with the forelimb contralateral to a "blind" hemisphere: a metabolic mapping study in monkeys. J Neurosci 13:2772–2789.

Sokoloff L, Reivich M, Kennedy C, Des Rosiers MH, Patlak CS, Pettigrew KS, Sakurada O, Shinohara M (1977) The [^{14}C]-deoxyglucose method for the measurement of local cerebral glucose utilization: theory, procedure, and normal values in the conscious and anesthetized albino rat. J Neurochem 28:879–916.

Stephan KM, Fink GR, Passingham RE, Silbersweig D, Ceballos-Baumann AO, Frith CD, Frackowiak RS (1995) Functional anatomy of the mental representation of upper extremity movements in healthy subjects. J Neurophysiol 73:373–386.

Cerebral Cortex
doi:10.1093/cercor/bhn116

Functional Imaging of the Parietal Cortex during Action Execution and Observation

Mina N. Evangeliou[1], Vassilis Raos[1], Claudio Galletti[2] and Helen E. Savaki[1]

[1]Department of Basic Sciences, Faculty of Medicine, School of Health Sciences, University of Crete and Institute of Applied and Computational Mathematics, Foundation for Research and Technology Hellas, Greece and [2]Dipartimento di Fisiologia Umana e Generale, Università di Bologna, Bologna, Italy

We used the ^{14}C-deoxyglucose method to map the functional activity in the cortex of the lateral and medial parietal convexity, the intraparietal and the parietoccipital sulci of monkeys which either reached and grasped a 3D-object or observed the same reaching-to-grasp movements executed by a human. Execution of reaching-to-grasp induced activations in the superior parietal areas SI-forelimb/convexity, PE, PEc; in the intraparietal areas PEip, MIP, 5IPp, VIP, AIP, LIP dorsal; in the inferior parietal areas PF, PFG, PG; in the parietoccipital areas V6, V6A-dorsal; in the medial cortical areas PGm/7m and retrosplenial cortex. Observation of reaching-to-grasp activated areas SI-forelimb/convexity, PE lateral, PEc, PEip, MIP, VIP, AIP, PF, V6, PGm/7m, 31, and retrosplenial cortex. The common activations were stronger for execution than for observation and the interhemispheric differences were smaller for observation than for execution, contributing to the attribution of action to the correct agent. The extensive overlap of parietal networks activated for action execution and observation supports the "mental simulation theory" which assigns the role of understanding others' actions to the entire distributed neural network responsible for the execution of actions, and not the concept of "mirroring" which reflects the function of a certain class of cells in a couple of cortical areas.

Keywords: action observation, grasping, intraparietal cortex, mental simulation, parietal lobule, parietoccipital cortex

Introduction

Attributing actions to the correct agent and assigning meaning to the actions of other subjects is an essential aspect of efficient behavior. This underlines the importance of examining whether the production and perception of actions rely on different or common distributed neural systems. It was recently shown that the neural system that helps match action perception to action generation encompasses widespread frontal and cingulate cortical circuits. We demonstrated that extensive regions of both the lateral- and medial-frontal cortex, including several premotor and cingulate areas as well as the primary motor and somatosensory cortices are activated when subjects observe object-related hand actions, and they are activated somatotopically as they are for execution of the same actions (Raos et al. 2004, 2007).

Because the parietal cortex is considered a bridge between perception and action, with neurons in the superior (SPL, mainly Brodmann's area 5) and inferior parietal lobule (IPL, area 7) involved in higher order sensorimotor integration during hand manipulation tasks (Mountcastle et al. 1975), receiving convergent input from different sensory modalities as well as efference copy signals from motor areas to guide eye and forelimb movements (Andersen 1989; Kalaska et al. 1990; Savaki et al. 1993; Colby and Goldberg 1999), we decided to explore whether parietal areas are also involved in the so called "action observation/action execution matching system." We used the [^{14}C]-deoxyglucose (^{14}C-DG) quantitative autoradiographic method (Sokoloff et al. 1977) to obtain high-resolution functional images of the monkey parietal cortical areas activated for execution and observation of reaching-to-grasp. The ^{14}C-DG method is the only imaging approach to offer the following advantages: 1) direct assessment of brain activity, 2) quantitative measurement of glucose consumption, 3) resolution of 20 μm, and 4) cytoarchitectonic identification of cortical areas in sections adjacent to the autoradiographic ones.

We examined 1) the parietal convexity including the superior parietal areas SI, PE, PEc and the inferior parietal areas PF, PFG, PG, and Opt (Pandya and Seltzer 1982; Gregoriou et al. 2006), 2) the intraparietal cortex including areas, PEip, MIP, 5VIP (Colby et al. 1988; Matelli et al. 1998; Gregoriou and Savaki 2001) and the caudalmost intraparietal region of the medial bank (5IPp) as well as areas AIP, LIP, LOP/CIP, 7VIP of the lateral bank (Colby et al. 1993; Lewis and Van Essen 2000a, 2000b; Gregoriou and Savaki 2001; Tsutsui et al. 2003; Borra et al. 2008), and 3) the medial parietoccipital cortical areas V6A, V6 (Galletti, Fattori, Gamberini, et al. 1999; Galletti, Fattori, Kutz, et al. 1999). Finally, we examined additional medial cortical regions such as the PGm/7m (Pandya and Seltzer 1982; Cavada and Goldman-Rakic 1989a, 1989b) and the retrosplenial cortical areas 29 and 30 (Morris et al. 1999) as well as area 31 located at the medial surface between the posterior cingulate area 23c and the medial parietal area PGm/7m (Morecraft et al. 2004). Histological examination of the brain sections enabled us to assign most of the activated regions of the reconstructed metabolic maps to cytoarchitectonically defined areas of the parietal lobe.

As we demonstrated earlier for the frontal lobe (Raos et al. 2004, 2007), here we show also for the parietal lobe that largely overlapping widespread cortical circuits are recruited for both action perception and action generation. Thus, far from being restricted to the medial and lateral frontal cortical areas, the action observation/execution matching system also involves extensive regions of the lateral, medial and intraparietal cortex of the primate brain. The present findings provide further support to our earlier suggestion that we understand the actions of others by recruiting the same cortical circuits which are responsible for execution of the same actions, in other words that we understand others' actions by mentally simulating them (Raos et al. 2007).

Methods

Subjects

Six adult female monkeys (*Macaca mulatta*) weighing between 4 and 5 kg were used. Experiments were approved by the institutional animal use committee in accordance with European Council Directive 86/609/EEC. A detailed description of the surgical procedures, the [AQ9] behavioral apparatus and the tasks, the EMG recording and the eye-position recording was previously reported (Raos et al. 2004). In brief, monkeys had their heads fixed and a water delivery tube attached close to their mouth. For immobilization of the head, a metal bolt was surgically implanted on the head of each monkey with the use of mandibular plates that were secured on the bone by titanium screws [AQ10] (Synthes). All surgical procedures were performed under general anesthesia using aseptic techniques. Digitized electromyograms, recorded from the biceps and wrist extensor muscles with surface electrodes, were previously reported (Raos et al. 2004). Eye movements were recorded with an infrared oculometer (Fig. 1). All monkeys were trained to perform their tasks continuously for at least 1 h/day for several months before the ^{14}C-DG experiment, receiving water as reward. On the day of the ^{14}C-DG experiment, monkeys performed their tasks during the entire experimental period of 45 min.

Behavioral Tasks

The behavioral apparatus was placed in front of the monkeys at shoulder height, 20 or 50 cm away depending on whether the monkey or the experimenter had to reach and grasp. A sliding window (circular window of 8° diameter) at the front side of the apparatus allowed the subject (monkey or experimenter) to grasp a horizontally oriented ring using a digging out grip with the index finger inserted into it (with pronated hand). In order to control for possible rate-related effects, the mean rate of movements was set to be similar for the execution and the observation tasks, as well as for the arm-motion control.

Two grasping-execution (E) monkeys were trained to reach and grasp with their left forelimbs, whereas the right ones were restricted. These monkeys were required to fixate the illuminated object behind the opened window for 0.7–1 s, until a dimming of the light would signal reaching, grasping and pulling the ring with the left forelimb while maintaining fixation. The maximum latency to grasp the object was set to 1 s, although the movement was usually completed within 500–600 ms. The E monkeys were allowed to move their eyes outside the window only during the intertrial intervals, which ranged between 2 and 2.5 s.

Three grasping-observation (O) monkeys were first trained to perform the task of the E monkeys, and then trained to observe the same reaching-to-grasp movements executed by the experimenter. Although execution-training took place months before the ^{14}C-DG experiment, in order to cancel any possible interhemispheric effects due to this earlier training, the first monkey was trained to reach and grasp with its left hand, the second one with its right hand and the third one with both hands consecutively. Thus in the observing monkeys, any interhemispheric effect due to the earlier grasping-training would be canceled out by comparing the average quantitative map of the 3 left hemispheres with the average map of the 3 right hemispheres. Both forelimbs of the O monkeys were restricted during the observation-training and during the ^{14}C-DG experiment. The experimenter was always standing on the right side of the monkey and was using the right arm/hand for reaching/grasping. Both reaching and grasping components of the movement were visible to the monkey. Object and movement parameters as well as eye movements and intertrial intervals were similar to the ones described for the E monkeys.

The arm-motion control (Cm) monkey had both hands restricted and was trained to maintain its gaze straight ahead (within the 8° diameter circular window) during the opening of the window of the apparatus, the presentation of the illuminated object behind the opened window, the closure of the window, and while the experimenter was reaching with extended hand toward the closed window (for a total period of 2.7–3 s per trial). The direction of motion and velocity of the experimenter's arm were the same as in the observation task, but the Cm monkey was not exposed to the view of hand preshaping and object-hand interaction. Accordingly, this control monkey was used to take into account the effects of 1) the biological motion of the purposeless (non-goal–directed) reaching arm and 2) the visual stimulation by the 3D object. Therefore, subtraction of the Cm activity from that of the reaching and grasping monkeys revealed the effects of the goal-directed reaching-to-grasp behavioral component. The Cm monkey was allowed to move its eyes outside the circular window only during the intertrial intervals, which ranged between 2 and 2.5 s.

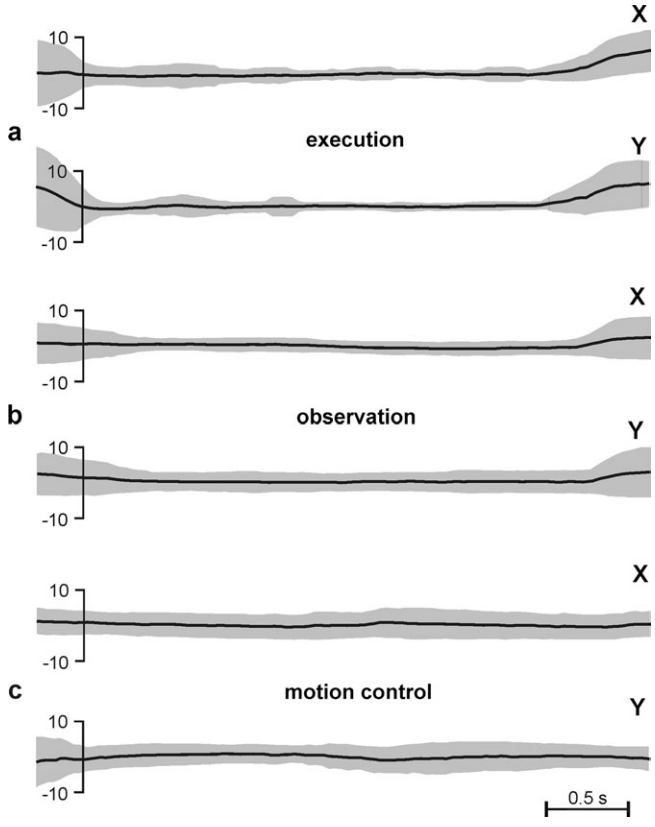

Figure 1. Instantaneous eye-position as a function of time. Solid lines of plots correspond to the instantaneous eye-position averaged over all trials during the critical 10 first min of the ^{14}C-DG experiment. Shaded area around solid lines represents the standard deviation. Eye-position calibration bars (ranging between −10 and +10°) are aligned on the onset of trials. (*a*) Action execution: average of 2 monkeys. (*b*) Action observation: average of 3 monkeys, and (*c*), biological motion control.

^{14}C-DG Experiments

During the day of the ^{14}C-DG experiment, monkeys were subjected to femoral vein and artery catheterization under general anesthesia, and were allowed 4–5 h to recover. Plasma glucose levels, blood pressure, hematocrit, and blood gases ranged within normal values in all monkeys and remained constant throughout the ^{14}C-DG experiment. A pulse of 100 μCi/kg of 2-deoxy-D-[1-^{14}C] glucose (specific activity 55 mCi/mmol, ARC) dissolved in saline was delivered (by intravenous injection) 5 min after each monkey started its behavioral task. Arterial samples were collected from the catheterized femoral artery during the succeeding 45 min, and the plasma ^{14}C-DG and glucose concentrations were measured. At 45 min, the monkey was sacrificed by intravenous injections of 50 mg sodium thiopental in 5 ml of saline, and then a saturated potassium chloride solution. The cerebral hemispheres, the cerebellum and the spinal cord were removed, frozen in isopentane at −50 °C and stored at −80 °C. Serial 20-μm-thick horizontal sections were cut in a cryostat at −20 °C. Autoradiographs were prepared by exposing these sections, together with precalibrated ^{14}C-standards, with medical X-ray film (Kodak Biomax MR) in X-ray cassettes. [AQ11]

One section every 500 μm was stained with thionine for identification of the cytoarchitectonic borders of cortical areas of the parietal

convexity (Pandya and Seltzer 1982; Gregoriou et al. 2006), the IPs [AQ12] (Medalla and Barbas 2006), and the POs (Luppino et al. 2005). Labeling of cortical areas of interest was based on their position relative to surface brain landmarks and their cytoarchitectonically identified borders. Quantitative densitometric analysis of autoradiographs was performed with a computerized image processing system (Imaging Research, Ontario, Canada), which allowed integration of the local cerebral glucose utilization (LCGU) values within each area of interest. LCGU values (in μmol/100 g/min) were calculated as in the authors' previous experiments (Savaki et al. 1993; Raos et al. 2004), from the appropriate kinetic constants for the monkey (Kennedy et al. 1978), by the original operational equation of the ^{14}C-DG method (Sokoloff et al. 1977). Normalization of LCGU values was based on the averaged unaffected gray matter value pooled across all monkeys (Savaki et al. 1993; Gregoriou and Savaki 2003).

Reconstruction of Two-Dimensional Maps of Activity

Two-dimensional (2D) reconstructions of the spatial distribution of metabolic activity within the rostrocaudal and the dorsoventral extent of the cortical areas of the parietal lobe in each hemisphere were generated as previously described (Dalezios et al. 1996; Savaki et al. 1997). To cover the full extent of the cortex of the parietal convexity about 1000 serial horizontal sections, 20 μm thick, were used from each hemisphere of each monkey, whereas 500 sections were used for the reconstruction of the intraparietal cortex, and 650 for the reconstruction of the parietoccipital and the medial parietal cortex. For each horizontal section, a data array was obtained by sampling the LCGU values along a rostrocaudal line parallel to the surface of the cortex and covering all cortical layers (anteroposterior sampling spatial resolution 50 μm/pixel). Every 5 adjacent horizontal sections of 20 μm, data arrays were averaged and plotted to produce one line in the 2D-maps of activity (spatial resolution of plots 100 μm). The posterior crown of the central sulcus (Cs) was used for the alignment of adjacent data arrays in the reconstruction of the parietal convexity. The caudalmost part of the IPs, that is, the intersection of the IPs with the POs and the lunate sulcus (Ls) was used for the alignment of adjacent data arrays in the reconstruction of the IPs. Finally, the intersection of the anterior bank of the POs with the medial surface of the cortical hemisphere (i.e., the medial crown of POs) was used for the alignment of adjacent data arrays in the reconstruction of the POs. Tick marks in each horizontal section labeling surface landmarks of the brain, such as crown, fundus and intersections of sulci, as well as cytoarchitectonically identified borders of cortical areas of interest were used to match the 2D-maps obtained from different hemispheres and animals (see geometrical normalization of maps, below).

Geometrical Normalization of the 2D Maps of Activity

In order to allow for the direct comparison of the sites of activation despite the inter- and intrahemispheric variability, the individual functional (^{14}C-DG) and anatomical (cytoarchitectonic) 2D-maps were further processed to match a reference map. The general procedure of the geometrical normalization of these maps was previously described (Bakola et al. 2006; Raos et al. 2007). In specific, for the parietal-convexity maps (Fig. 2*a*,*b*), the section by section rostrocaudal distances between 1) the posterior crown of the Cs (point of alignment) and the surface landmarks (anterior crown, fundus, posterior crown) of the postcentral dimple (pcd) (for dorsal sections) or the IPs (for middle sections) or the lateral fissure (for ventral sections), 2) the latter and the posterior tip of the brain (for dorsal sections) or the anterior crown of either the superior temporal sulcus or the lateral fissure (for middle sections) were measured. Moreover, the section by section dorsoventral distances between 1) the dorsalmost tip of the brain and the IPs, 2) the latter and the cytoarchitectonically identified Opt/PG border, 3) the latter and the cytoarchitectonic border between PG and PFG, 4) the latter and the PFG/PF border, 5) the latter and the ventral PF border, 6) the latter and the ventralmost section of the reconstruction were also measured. The average of each one of these measures was computed to produce a reference map of landmarks (Fig. 2*b*). The reference map of landmarks in the intraparietal cortex was generated similarly (Fig. 3*a*,*b*). The distances used here were those between the anterior crown of the IPs, its fundus and its posterior crown for the dorsoventral dimension. For the anteroposterior dimension, the distances used were

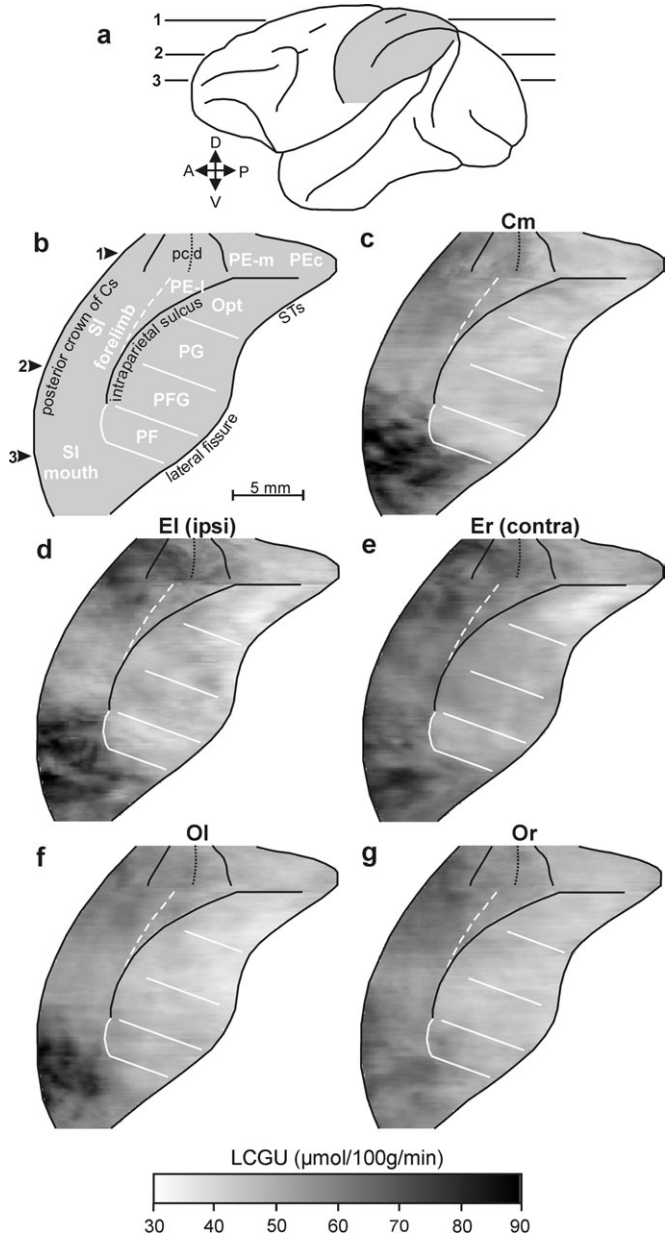

Figure 2. Quantitative 2D-maps of metabolic activity in the lateral parietal cortex. (*a*) Lateral view of the left hemisphere of a monkey brain. Shaded area indicates the reconstructed cortex around the intraparietal sulcus (IPs), surrounded by the central (Cs) and superior temporal (STs) sulci and the lateral fissure. Horizontal lines 1–3 correspond to 3 different dorsoventral levels of brain sectioning. A, anterior; D, dorsal; P, posterior; V, ventral. (*b*) Schematic representation of the geometrically normalized reconstructed cortical field. Black lines correspond to surface landmarks, solid white lines to cytoarchitectonically identified borders of the labeled cortical areas, and the interrupted white line to the SI/PE border based on reported maps. Arrows 1–3 indicate the dorsoventral levels of the corresponding lines in panel a. pcd, postcentral dimple unfolded, with the dotted line representing its fundus and the solid lines its crowns. PE-l, PE-m, lateral and medial portions of area PE. The rest of abbreviated cortical areas are described in the text. (*c*) Averaged map from the 2 hemispheres of the motion-control monkey, Cm. (*d*) Averaged map from the left hemispheres of the 2 action execution monkeys, EI (ipsi). (*e*) Averaged map from the right hemispheres (contralateral to the moving forelimb) of the 2 action execution monkeys, Er (contra). (*f*) Averaged map from the left hemispheres of the 3 action observation monkeys, OI. (*g*) Averaged map from the right hemispheres of the 3 action observation monkeys, Or. Gray-scale bar indicates LCGU values in μmol/100 g/min.

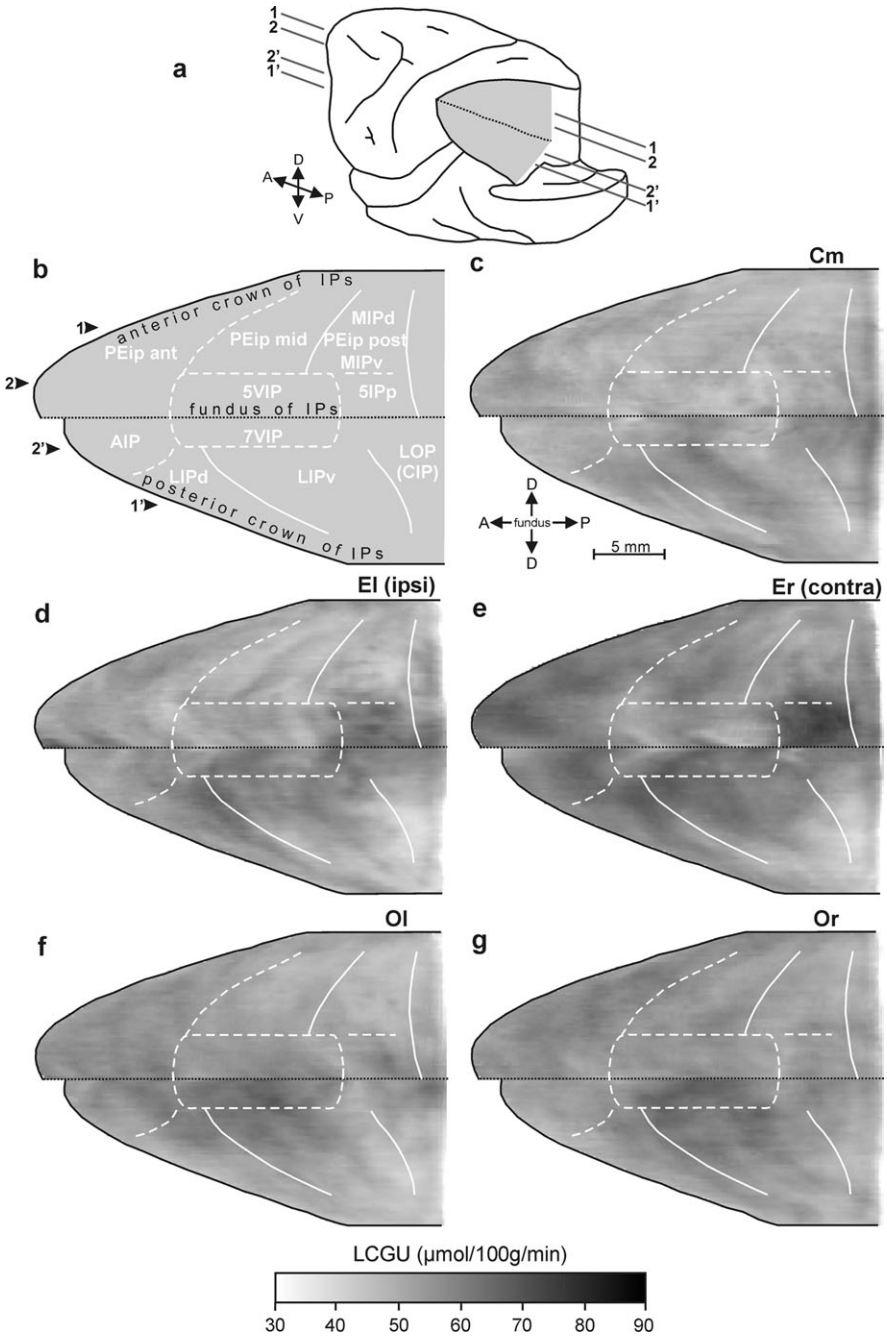

Figure 3. Quantitative 2D-maps of metabolic activity in the intraparietal sulcus (IPs). (*a*) Postero-lateral view of the partially dissected left hemisphere of a monkey brain. The IPL was cut away at the level of the posterior crown of the IPs, the occipital lobe was also cut away at the level of the fundus of POs and Ls, and the IPs was unfolded. Dotted black line depicts the fundus of the sulcus. Shaded area represents the reconstructed medial (upper) and lateral (lower) banks of the cortex. (*b*) Schematic illustration of the geometrically normalized reconstructed cortical field. Black lines correspond to surface landmarks, solid and interrupted white lines correspond to cytoarchitectonically and functionally identified borders, respectively, of the labeled cortical areas. (*c*) Averaged map from the 2 hemispheres of the Cm monkey, Cm. (*d*) Averaged map from the left hemispheres of the 2 execution monkeys, El (ipsi). (*e*) Averaged map from the right hemispheres (contralateral to the moving forelimb) of the same monkeys, Er (contra). (*f*) Averaged map from the left hemispheres of the 3 observation monkeys, Ol. (*g*) Averaged map from the right hemispheres of the 3 observation monkeys, Or. Other conventions as in Figure 2.

those between the cytoarchitectonically identified borders of LIP dorsal and LIP ventral for the lateral bank, and those between the functionally identified border of PEip and the cytoarchitectonic borders of area MIP for the medial bank (Fig. 3*b*). Finally, the reference map of landmarks in the parietoccipital cortex was generated similarly (Fig. 4*a*,*b*). The distances used here were those between the surface landmarks of the medial parietoccipital sulcus (POm) and the medial and lateral crowns of POs as well as those between the cytoarchitectonic borders of V6 and V6A (Fig. 4*b*, white lines). Each individual cortical map with its own segments' landmarks was linearly transformed in Matlab (MathWorks, Inc.) to match the reference map. With this procedure, although the total surface of an area may change when it is geometrically normalized, the intensity and the spatial distribution of LCGU effects are preserved within it because these effects are proportionally shrunk or expanded within its borders. The geometrically normalized maps were used 1) to obtain average-LCGU maps out of control or experimental hemispheres and 2) to subtract control from experimental averaged maps.

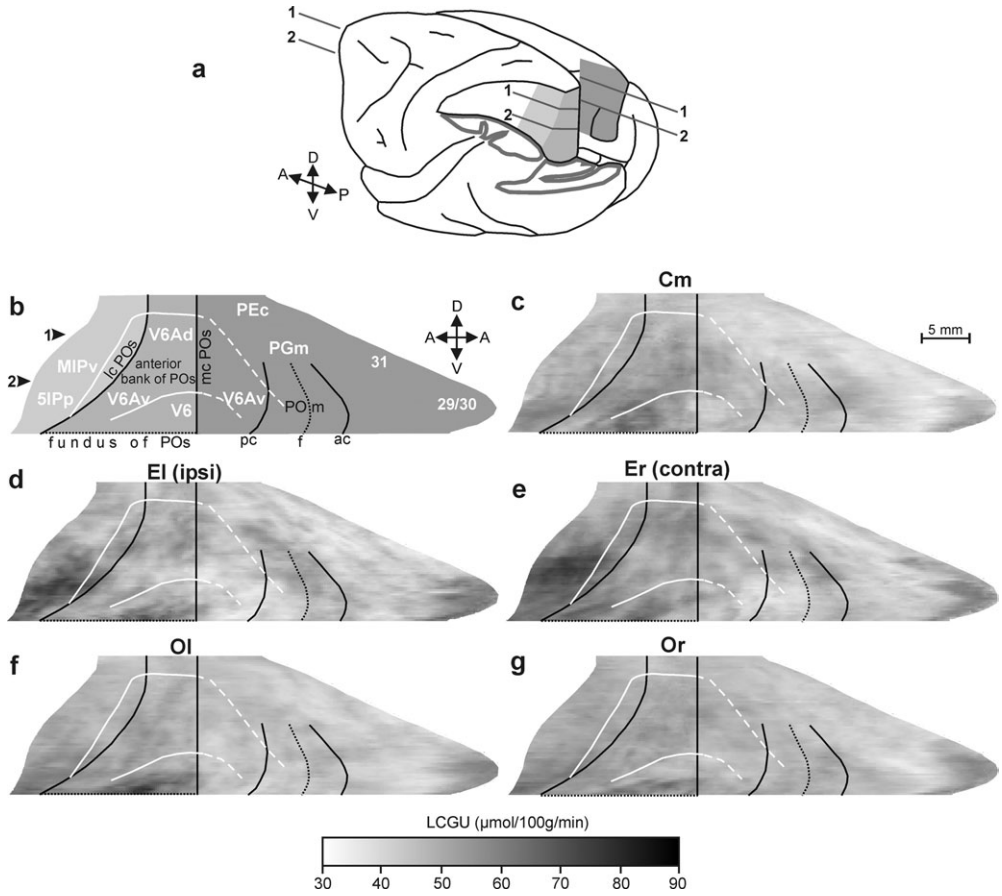

Figure 4. Quantitative 2D-maps of metabolic activity in the medial parietal and parietoccipital cortex. (*a*) Postero-lateral view of the partly dissected left hemisphere of a monkey brain with partial view of its mesial surface. The IPL was cut away at the level of the fundus of the IPs to show the cortex of the medial bank of this sulcus. The occipital lobe of the same hemisphere was also cut away at the level of the fundus of the POs and the Ls to show the cortex of the anterior bank of POs. Shaded area represents the reconstructed cortex including part of the medial bank of IPs, the anterior bank of POs and the adjacent part of the medial parietal cortex. (*b*) Schematic illustration of the geometrically normalized reconstructed cortical field. Different shades of gray correspond to those in panel a. Black lines represent surface landmarks, solid and interrupted white lines represent cytoarchitectonically and functionally identified borders, respectively, of the labeled cortical areas. The vertical black line in the middle of the reconstructed field depicts the medial crown of the anterior bank of POs (mc POs), point of alignment of the serial horizontal sections. The black line on its left demarcates the lateral crown of POs (lc POs) which partially corresponds to the intersection of the 3 sulci: IPs, POs and Ls. POm, medial parietoccipital sulcus, which is unfolded, with labeled its anterior crown (ac), fundus (f), and posterior crown (pc). (*c*) Averaged map from the 2 hemispheres of the motion-control monkey, Cm. (*d*) Averaged map from the left hemispheres of the 2 execution monkeys, El (ipsi). (*e*) Averaged map from the right hemispheres (contralateral to the moving forelimb) of the same monkeys, Er (contra). (*f*) Averaged map from the left hemispheres of the 3 observation monkeys, Ol. (*g*) Averaged map from the right hemispheres of the same monkeys, Or. POm, medial parietoccipital sulcus. Other conventions as in Figure 2.

Statistical Analysis

The average-LCGU values were calculated in sets of 5 adjacent sections (20 µm thick) throughout each cortical area of interest in each hemisphere. Experimental (E and O) to control (Cm) LCGU values were compared for statistical significances by the Student's unpaired *t*-test. Given that ipsilateral to contralateral LCGU values in normal control monkeys range up to 7% (Kennedy et al. 1978), only differences from the Cm higher than 7% were considered for statistical treatment (Bakola et al. 2006). The percent LCGU differences between the experimental (E and O) and the control (Cm) monkeys were generated using the formulae (E – Cm)/Cm × 100 and (O – Cm)/Cm × 100.

Results

All monkeys were trained for several months before the ^{14}C-DG experiment to perform their tasks continuously for at least 1 h/day. On the day of the ^{14}C-DG experiment, monkeys performed their tasks for the entire experimental period (45 min) without any breaks, and successful completion of each trial was rewarded with water. Success rate remained roughly constant (>90%) throughout the experiment. The mean rate of movements was similar for the execution and the observation tasks, as well as for the arm-motion control. To examine whether the differences in the performance of animals could influence our results, we compared the glucose consumption of the affected cortical areas between the 2 E monkeys which displayed a 33% difference in performance (executing 8 and 12 movements per min, respectively). This comparison showed that the differences in glucose consumption ranged between 4% and 9%, despite the fact that the performance differed by 33%. Apparently, the activation of the task-related areas in 2 different monkeys is similar provided that their task-performance exceeds a certain threshold. The amount of time that the monkeys spent fixating within the window of the behavioral apparatus during the critical 10 first minutes of the ^{14}C-DG experiment ranged between 6 and 7 min. For the rest of the time, the animals did not display any systematic oculomotor behavior that could account for false-positive effects in oculomotor related areas. In other words the line of sight of all the experimental monkeys was at random positions throughout the entire oculomotor space, same way as that of the biological motion control.

During the critical 10 first minutes of the ^{14}C-DG experiment, the Cm monkey observed 9 movements of the experimenter's arm per min and fixated within the window of the behavioral apparatus for 6 min. Because we found no significant interhemispheric difference of glucose consumption in any parietal area of the Cm monkey, the quantitative glucograms (maps of LCGU) of the cortex of the parietal convexity (Fig. 2*c*), the intraparietal cortex (Fig. 3*c*) and the parietoccipital/medial parietal cortices (Fig. 4*c*) of one side were averaged with the corresponding ones of the other side. The averaged glucogram of this monkey was used for measurement of control LCGU values in cortical areas of interest and comparisons with the experimental monkeys (Table 1).

The E monkeys executed an average of 10 movements per min during the critical 10 first minutes of the ^{14}C-DG experiment and fixated within the window of the behavioral apparatus for 7 min. We generated glucograms of the parietal convexity (Fig. 2*d*), the intraparietal (Fig. 3*d*) and the parietoccipital (Fig. 4*d*) cortices by averaging the 2 corresponding geometrically normalized glucograms in the left hemispheres (ipsilateral to the moving forelimb) of the 2 E monkeys. The latter glucograms as well as the equivalent ones in the right hemispheres (Figs 2*e*, 3*e*, and 4*e*, contralateral to the moving forelimb) were used for measurement of the LCGU values in cortical areas of interest, their statistical comparisons, and the estimation of the percent differences from the corresponding values of the Cm monkey (Table 1).

The O monkeys observed an average of 12 movements per min during the critical 10 first minutes of the ^{14}C-DG experiment and fixated within the window of the apparatus for 7 min. We generated glucograms of the parietal convexity (Fig. 2*f*), the intraparietal (Fig. 3*f*) and the parietoccipital (Fig. 4*f*) cortices by averaging the 3 corresponding, geometrically normalized glucograms in the left hemispheres of the 3 O monkeys. The latter glucograms as well as the equivalent ones in the right hemispheres (Figs 2*g*, 3*g*, and 4*g*) were used for measurement of the LCGU values in cortical areas of interest, their statistical comparisons, and the estimation of the percent differences from the Cm respective values (Table 1).

To illustrate the percent LCGU differences between the E monkeys and the Cm, we generated images of the spatio-intensive pattern of distribution of the metabolic activations, using the formula (E – Cm)/Cm × 100 for each one of the parietal-convexity, intraparietal and parietoccipital cortical glucograms. When the averaged maps of the parietal-convexity cortex in the left or in the right hemispheres of the E monkeys are compared with the corresponding averaged map of the Cm monkey (Fig. 5*a*,*b*, respectively), increased metabolic activity (net activation) is apparent in several cortical regions (see also Table 1). Superior parietal areas activated for execution of grasping movements include the widespread forelimb representation of S1-convexity (Pons et al. 1985) and area PEc contralaterally to the grasping forelimb, as well as area PE lateral (corresponding to the forelimb representation in area 5

Table 1
Metabolic effects in parietal cortical areas of the monkey brain

Cortical area	*n*	Cm (LCGU ± SD)	El (LCGU ± SD)	Er (LCGU ± SD)	Ol (LCGU ± SD)	Or (LCGU ± SD)	El/Cm (%)	Er/Cm (%)	Ol/Cm (%)	Or/Cm (%)
SPL										
SI convexity—pcd	32	52 ± 1	62 ± 3	61 ± 2	54 ± 1	55 ± 1	**19**	**17**	4	6
SI convexity—forelimb	48	56 ± 3	55 ± 5	65 ± 4	56 ± 4	61 ± 3	−2	**16**	0	**9**
SI convexity—forelimb (max)	20	53 ± 2	53 ± 2	65 ± 2	57 ± 2	63 ± 2	0	**23**	**8**	**19**
PE lateral (5-forelimb)	17	49 ± 1	53 ± 1	57 ± 1	53 ± 2	53 ± 1	**8**	**16**	**8**	**8**
PE medial	31	44 ± 1	48 ± 1	51 ± 2	47 ± 1	46 ± 1	**9**	**16**	7	5
PEc	28	43 ± 1	44 ± 2	50 ± 1	45 ± 1	47 ± 1	2	**16**	5	**9**
Medial intraparietal bank										
PEip anterior	102	49 ± 2	52 ± 2	60 ± 2	54 ± 2	57 ± 1	6	**22**	**10**	**16**
PEip middle	73	48 ± 1	48 ± 2	56 ± 2	50 ± 2	54 ± 1	0	**17**	4	**13**
PEip posterior dorsal (MIPd)	37	46 ± 1	48 ± 1	52 ± 2	47 ± 2	52 ± 1	4	**13**	2	**13**
PEip posterior ventral (MIPv)	35	48 ± 1	49 ± 3	57 ± 2	49 ± 1	52 ± 1	2	**19**	2	**8**
5IPp	53	53 ± 4	65 ± 4	67 ± 4	56 ± 4	56 ± 4	**23**	**26**	6	6
5VIP	28	47 ± 1	52 ± 1	54 ± 1	54 ± 1	54 ± 1	**11**	**15**	**15**	**15**
Lateral intraparietal bank										
AIP	45	49 ± 1	53 ± 1	60 ± 2	54 ± 3	51 ± 2	**8**	**22**	**10**	4
LIP dorsal	82	51 ± 2	55 ± 4	58 ± 5	52 ± 5	54 ± 3	**8**	**14**	2	6
LIP ventral	82	52 ± 2	50 ± 6	53 ± 7	51 ± 5	54 ± 5	−4	2	−2	4
LOP/CIP	102	51 ± 4	46 ± 7	47 ± 7	47 ± 4	51 ± 3	−10	−8	−8	0
7VIP	19	52 ± 1	59 ± 1	62 ± 1	61 ± 1	61 ± 1	**13**	**19**	**17**	**17**
Inferior parietal lobe										
PF	44	45 ± 2	45 ± 2	50 ± 2	50 ± 2	50 ± 1	0	**11**	**11**	**11**
PFG	57	44 ± 1	46 ± 2	51 ± 3	45 ± 1	45 ± 1	5	**16**	2	2
PG	59	43 ± 1	46 ± 3	50 ± 1	41 ± 3	45 ± 3	7	**16**	−5	5
Opt	44	43 ± 2	41 ± 2	44 ± 1	40 ± 2	44 ± 1	−5	2	−7	2
Anterior parieto-occipital bank										
V6Ad	34	48 ± 2	49 ± 1	54 ± 2	47 ± 1	49 ± 1	2	**13**	−2	2
V6Av	80	51 ± 1	47 ± 2	52 ± 2	49 ± 2	51 ± 1	−8	2	−4	0
V6 (max)	18	47 ± 2	51 ± 4	51 ± 2	55 ± 3	52 ± 3	**9**	**9**	**17**	**11**
Medial parietal areas										
PGm/7m (max)	66	42 ± 3	48 ± 3	50 ± 3	46 ± 2	46 ± 2	**14**	**19**	**10**	**10**
31 (max)	72	39 ± 1	40 ± 2	41 ± 1	42 ± 1	42 ± 1	3	5	**8**	**8**
Retrosplenial cortex (29/30)	69	41 ± 3	48 ± 8	48 ± 3	45 ± 4	46 ± 4	**17**	**17**	**10**	**12**

Note: *n*, number of sets of 5 adjacent horizontal sections used to obtain the mean LCGU values (in μmol/100 g/min) for each region. Cm values represent the average LCGU values from the 2 hemispheres of the motion-control monkey. El and Er values represent the average LCGU values from the 2 left and the 2 right hemispheres of the grasping-execution monkeys, respectively. Ol and Or values represent the average LCGU values from the 3 left and the 3 right hemispheres of the grasping-observation monkeys, respectively. SD, standard deviation of the mean. El/Cm, Er/Cm, Ol/Cm, Or/Cm, percent differences between El, Er, Ol, Or, and Cm, respectively, calculated as (experimental-control)/control × 100. pcd, pcd; (max), LCGU value in the region of maximal effect. Values in bold indicate statistically significant differences by the Student's unpaired *t*-test at the level of $P < 0.001$.

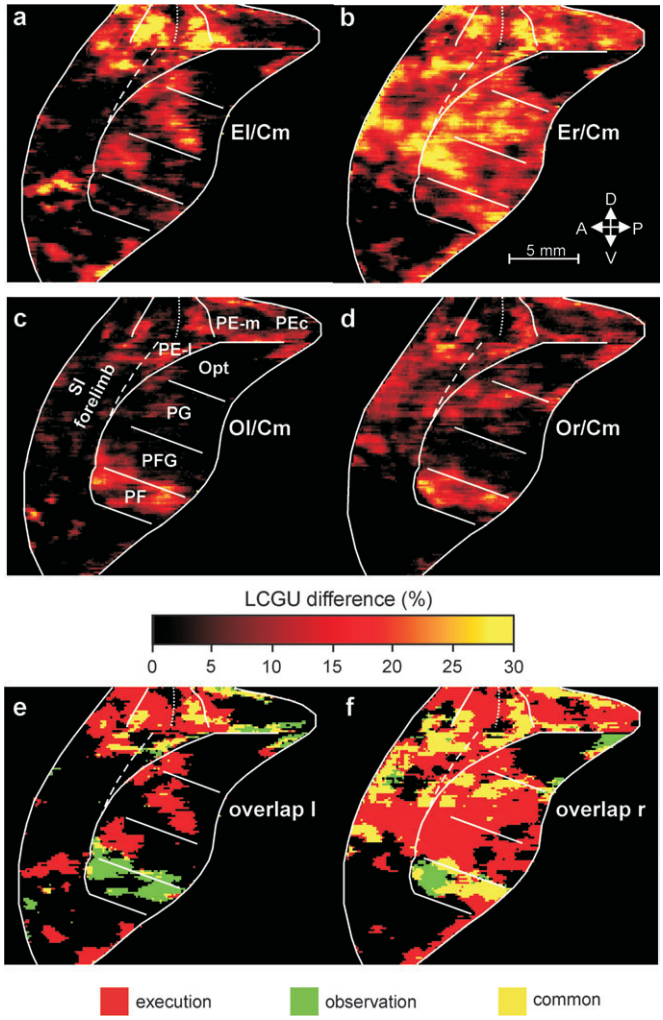

Figure 5. Lateral parietal cortical maps of percent LCGU differences from the motion control. Percent differences were calculated using the formula (E − Cm)/Cm × 100 for execution and (O − Cm)/Cm × 100 for observation. (*a*) Map of net execution-induced activations averaged from the left hemispheres of the 2 execution monkeys, El/Cm. (*b*) Map of net execution-induced activations averaged from the right hemispheres (contralateral to the moving forelimb) of the same monkeys, Er/Cm. (*c*) Map of net observation-induced activations averaged from the left hemispheres of the 3 observation monkeys, Ol/Cm. White lines correspond to the surface landmarks and the cytoarchitectonic borders of labeled areas, as in Figure 2. (*d*) Map of net observation-induced activations averaged from the right hemispheres of the observation monkeys, Or/Cm. Color bar indicates % LCGU differences from the Cm. (*e*) Superimposition of (*a*) and (*c*) panels. (*f*) Superimposition of (*b*) and (*d*) panels. In (*e*) and (*f*) panels, red and green represent activations higher than 10% induced by action execution and action observation, respectively. Yellow stands for activations induced by both execution and observation of the same action.

(Pons et al. 1985) and PE medial (corresponding to the trunk representation of area 5 (Pons et al. 1985) bilaterally (with more marked the contra- than the ipsilateral activations). Also bilaterally activated was found the trunk representation of area 2 around the pcd of only the E monkeys (Fig. 5, Table 1), presumably due to postural adjustments during reaching and grasping (Raos et al. 2004), whereas unaffected remained the mouth representation of the SI convexity at the ventralmost part of the reconstructions (Fig. 5). Inferior parietal areas activated for execution of reaching-to-grasp include the contralateral PF, PFG, and PG. When the averaged maps of the parietal-convexity cortex in the left and in the right hemispheres of the O monkeys are compared with the corresponding Cm map (Fig. 5*c*,*d*, respectively), observation-induced (net) activations are apparent in SI convexity-forelimb representation and area PEc of the right hemispheres, as well as in area PE lateral (or 5-forelimb) and PF bilaterally (see also Table 1). It should be noted that the latter 2 activations and the maximally activated region (max) within the SI convexity-forelimb representation displayed smaller interhemispheric differences in the O than in the E monkeys (Table 1).

When the averaged maps of the IPs cortex in the left or in the right hemispheres of the E monkeys are compared with the corresponding averaged map of the Cm monkey (Fig 6a and 6b, respectively), increased activity is apparent in several cortical regions (see also Table 1). Areas activated for execution of reaching-to-grasp in the medial intraparietal bank include the anterior and middle PEip and the dorsal and ventral MIP contralaterally to the grasping forelimb, as well as the 5VIP and the 5IPp bilaterally. Area 5IPp is an area we report for the first time, which does not correspond to any region previously described in the literature. It occupies the caudalmost and ventralmost region of the medial bank of the IPs. It is located rostral to area PIP, which has been described in the most anterior and lateral part of POs (Colby et al. 1988). Area 5IPp is ventrally demarcated by the fundus of IPs and borders areas MIP dorsally, 5VIP rostrally and V6A caudally. Interestingly, 5IPp displayed the highest parietal activation for grasping execution in the present study, but no effect during action observation. Of interest is also that the activations in the anterior and middle PEip of the medial bank of the IPs are distributed in anteroposterior (parallel to the crown) bands, which are very similar to those described in the past as projection bands from the SI-forelimb representation (Pearson and Powell 1985). In the lateral intraparietal bank, areas activated for execution of grasping include the AIP, the dorsal LIP and the 7VIP bilaterally, with the contralateral activations more marked than the ipsilateral ones. When the averaged maps of the IPs cortex in the left and in the right hemispheres of the O monkeys are compared with the corresponding Cm map (Fig. 6*c*,*d*, respectively), observation-induced activation is apparent in medial intraparietal areas such as the middle PEip and the dorsal and ventral MIP of the right hemispheres, as well as in the anterior PEip and the 5VIP bilaterally. Observation-induced activations also include the lateral intraparietal areas AIP of the left hemispheres and the 7VIP bilaterally. It should be noted that activations in areas 5VIP and 7VIP display no interhemispheric differences in the O monkeys (Table 1). A consistently significant depression was measured in an area corresponding to LOP or CIP in both hemispheres of the E monkeys and in the left hemispheres of the O monkeys (Table 1).

Finally, when the Cm map of the POs cortex is compared with the corresponding averaged maps in the left and the right hemispheres of the E monkeys (Fig. 7*a*,*b*, respectively), execution-induced activations are apparent in a portion of area V6 around the medial crown of the POs bilaterally, in the dorsal V6A contralaterally to the grasping hand, as well as in the PGm/7m and the retrosplenial cortical areas 29 and 30 bilaterally. When the Cm map of the POs cortex is compared with the corresponding averaged maps in the left and the right hemispheres of the O monkeys (Fig. 7*c*,*d*, respectively), observation-induced activations are apparent bilaterally in the same part of area V6 which was affected by execution, and in areas PGm/7m, 31, and 29/30 of the retrosplenial cortex, (see also Table 1).

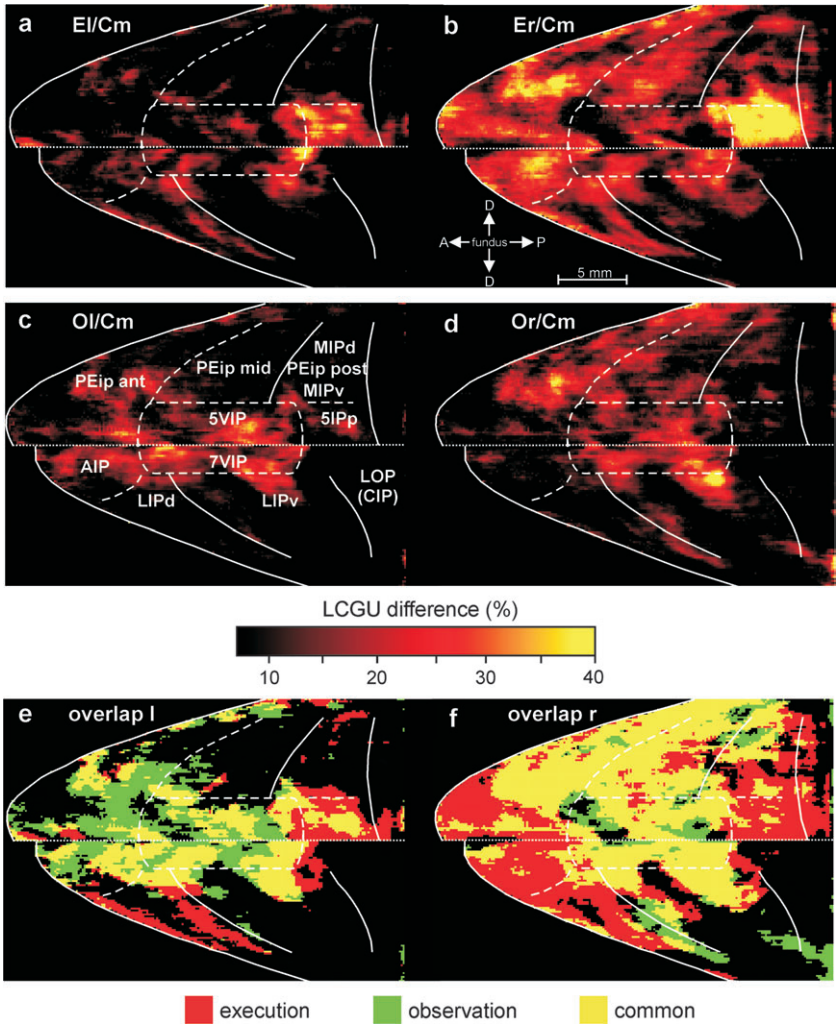

Figure 6. Intraparietal cortical maps of percent LCGU differences from the motion control. (*a*) Map of net execution-induced activations averaged from the left hemispheres of the 2 execution monkeys, El/Cm. (*b*) Map of corresponding activations averaged from the right hemispheres (contralateral to the moving forelimb) of the same monkeys, Er/Cm. (*c*) Map of net observation-induced activations averaged from the left hemispheres of the 3 observation monkeys, Ol/Cm. White lines correspond to the surface landmarks and the cytoarchitectonic borders of labeled areas, as in Figure 3. (*d*) Map of corresponding activations averaged from the right hemispheres of the 3 observation monkeys, Or/Cm. (*e*) Superimposition of panels (*a*) and (*c*). (*f*) Superimposition of panels (*b*) and (*d*). Other conventions as in Figure 5.

When spatially compared by superimposition, the observation-induced activations were found to overlap the execution-induced ones, partially in the parietal (Fig. 5*e,f*), largely in the intraparietal (Fig. 6*e,f*) and considerably in the parietoccipital cortex (Fig. 7*e,f*). In the above mentioned figures, red, green and yellow correspond to execution-induced, observation-elicited, and common activations, respectively. The distribution of activations for action execution differed from those for action observation in a more or less general pattern. To graphically illustrate the spatio-intensive (quantitative) distribution of metabolic activity within the affected regions, we plotted the differences between the experimental monkeys and the Cm (as % LCGU values and 95% confidence intervals per 100 μm) across the rostrocaudal extent in the reconstructed maps (Figs 8–10). The plots in these figures represent the percent differences between the E and the Cm monkeys (red lines) as well as between the O and the Cm monkeys (green lines). Baseline indicates 0% difference from the Cm. The plot in Figure 8 represents differences in the inferior parietal cortex along the ribbon highlighted in the schematic representation of the reconstructed cortex above the graph. In the left hemispheres of the 2 E monkeys ipsilateral to the grasping hand (dotted red line), activity is similar to that of the corresponding areas in the Cm (fluctuating around 0%). In contrast, significantly larger activations were found within areas PF, PFG, and PG (but not Opt) of the hemispheres contralateral to the grasping hand (Fig. 8, solid red line), resulting in a pronounced interhemispheric difference in the E monkeys. Interestingly, there is no interhemispheric difference in the activated PF of the O monkeys (Fig. 8, distance between the solid and the dotted green lines within PF). Consequently, the inferior parietal activations induced by action execution are contralateral to the grasping forelimb, in contrast to the PF activation elicited by action observation which is bilateral (see also Table 1).

The plots in Figure 9 represent differences from Cm in 4 subdivisions of the intraparietal cortex indicated by the ribbons of different gray-shades (Fig. 9*a*: ribbons b, c, d, and e), as highlighted in the schematic representation of the reconstructed cortex above the graphs. Graphs in panel b represent

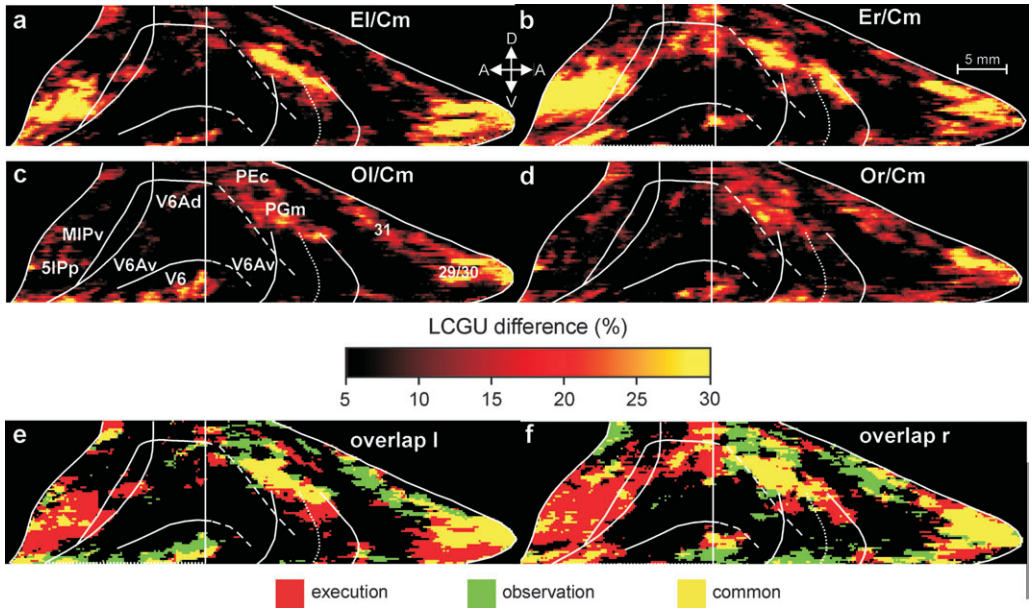

Figure 7. Medial parietal and parietoccipital cortical maps of percent LCGU differences from the motion control. (*a*) Map of net execution-induced activations averaged from the left hemispheres of the 2 execution monkeys, El/Cm. (*b*) Map of corresponding activations averaged from the right hemispheres (contralateral to the moving forelimb) of the same monkeys, Er/Cm. (*c*) Map of net observation-induced activations averaged from the left hemispheres of the 3 observation monkeys, Ol/Cm. White lines correspond to the surface landmarks and the cytoarchitectonic borders of labeled areas, as in Fig. 4. (*d*) Map of corresponding activations averaged from the right hemispheres of the 3 observation monkeys, Or/Cm. (*e*) Superimposition of panels (*a*) and (*c*). (*f*) Superimposition of panels (*b*) and (*d*). Other conventions as in Figure 5.

the 3 portions of area PEip (anterior, middle and posterior) in the medial bank of the IPs, as demarcated by the b-ribbon in panel (*a*). It is demonstrated that in the left hemispheres of the 2 E monkeys ipsilateral to the grasping hand (dotted red line) activity is similar to that of the corresponding areas in the Cm (fluctuating around zero), in contrast to the significant activations in the hemispheres contralateral to the grasping hand (solid red line), resulting in a pronounced interhemispheric difference in the E monkeys (distance between dotted and solid red lines). Interestingly, a much smaller interhemispheric difference is illustrated in the PEip of the O monkeys (Fig. 9*b*, distance between the solid and the dotted green lines smaller than that between the corresponding red lines). Moreover, in the O monkeys the PEip divisions are less activated than the corresponding areas of the affected hemisphere (contralateral to the grasping forelimb) of the E monkeys (Fig. 9*b*, Table 1). The plots in Figure 9*c* demonstrate the pattern of activations in areas 5VIP and 5IPp. The plots in Figure 9*d* demonstrate the 7VIP activation and the LOP/CIP inhibition. The plots in Figure 9*e* illustrate the activations in AIP and LIP. Finally, the plots in Figure 10 illustrate the activation of the contralateral V6A-dorsal in the E monkeys, the bilateral activations of the PGm/7m and the retrosplenial cortex in both the E and O cases, and the bilateral activation of area 31 in the O monkeys. In general, activations are higher in the E monkeys, and interhemispheric differences are smaller in the O monkeys (see also Table 1).

Discussion

The present quantitative neuroimaging study, combined with cytoarchitectonic identification of cortical areas, demonstrates the considerable overlap of the action execution and action observation networks in superior, inferior, and medial parietal cortical areas, which are thought to be involved in visuospatial attention, target selection for arm and eye movements, processing of visuomanual information, arm reaching, and object manipulation. At this point it should be noted that, although the activation of specific areas reflects their unequivocal involvement in action execution and/or in action observation in our study, the overlapping activations for execution and observation do not necessarily indicate involvement of the same cell populations in the 2 conditions.

Lateral Parietal Cortex

The lateralization of activation in the SI-forelimb representation of the SPL (corresponding to Brodmann's areas 1 and 2) contralateral to the moving forelimb of the E monkeys is compatible with classical knowledge and our previous reports (Savaki and Dalezios 1999; Raos et al. 2004; Gregoriou et al. 2005). The equivalent SI-forelimb activation in the SPL of the O monkeys mimics the results of previous reports demonstrating that the SI-forelimb activity within the Cs (corresponding mainly to areas 3a and 3b) was enhanced not only during manipulative hand actions but also during the observation of the same actions performed by another subject (Avikainen et al. 2002; Raos et al. 2004). The present results provide additional support to our earlier suggestion that overlapping somatosensory–motor neural correlates are responsible for motor program execution and motor percept creation (Raos et al. 2004, 2007). Moreover, the present results confirm that the activations induced by grasping execution and grasping observation in the SI-forelimb regions have similar patterns of distribution but different metabolic intensities. As we found for the SI-forelimb representation in the Cs (Raos et al. 2004), the activation of the SI-forelimb representation in the superior parietal convexity induced by observation of grasping is about 50% weaker in intensity than that induced by execution of

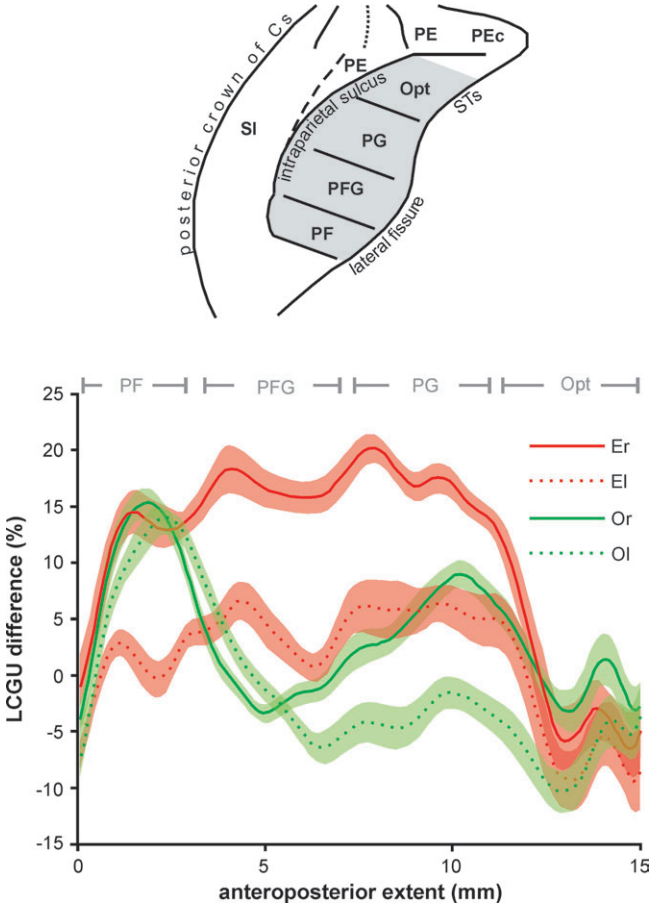

Figure 8. Plots of percent LCGU differences along the rostrocaudal extent of the reconstructed cortex of the inferior parietal convexity (along the ribbon highlighted in the drawing above the plots). The different areas corresponding to the various anteroposterior parts of the plots are labeled on top of the graphs. Red plots illustrate the differences between the 2 execution monkeys and the Cm. Green plots illustrate the differences between the 3 observation monkeys and the Cm. Plots with solid and dotted lines correspond to the right and the left hemispheres, respectively. Red and green shaded areas indicate 95% confidence intervals. Baseline corresponds to 0% LCGU difference from the Cm. Zero rostrocaudal extent represents the anterior border of PF. These plots illustrate the detailed spatio-intensive pattern of activation of PF, PFG and PG in the execution monkeys (activated only contralaterally to the moving forelimb), the bilateral activation of PF in the observation monkeys, and the smaller interhemispheric differences in the effects of the observation as compared with the execution monkeys. El, execution monkey left hemisphere; Er, execution right; Ol, observation left; Or, observation right.

grasping. As we have already suggested, the SI-forelimb activations during observation of actions may imply that subjects mentally rehearse the movements executed by others, and that the representation of movement is retrieved together with its somatosensory component. Indeed, in the absence of overt movement, EMG activation (Raos et al. 2004) and apparent sensory input, the SI-forelimb activation during observation of grasping may reflect the effects of mental simulation of this movement by the observer with prediction of the consequence of the movement (simultaneous recall of previous knowledge about the sensory effects). Finally, the fact that the SI-forelimb activation was found in the right superior parietal convexity of the O monkeys, that is, ipsilaterally to the experimenter's arm position and independently of the forelimb used in previous grasping experience of these monkeys (see Methods), is consistent with our previous results in the Cs (Raos et al. 2004) and with the right hemisphere dominance for visuospatial processes relative to movements (Chua et al. 1992; Decety 1996). Our findings that areas PE and PEc are involved in both execution and observation of grasping confirm previous reports demonstrating that the SPL contains a sensorimotor representation of the arm. On the sensory side, SPL receives somatosensory afferents from area 2 of the primary sensory cortex (Jones et al. 1978) and probably visual afferents from area MIP of the IPs (Caminiti et al. 1996), thus being able to integrate information about hand position and targets for reaching. On the motor side, SPL has connections with the primary motor cortex (Jones et al. 1978), the lateral premotor (Marconi et al. 2001) and the supplementary motor area (Pandya and Seltzer 1982) and is processing information about movement kinematics (Kalaska et al. 1990; Ashe and Georgopoulos 1994). Interestingly, all the above mentioned areas connected with the SPL were found to be activated for both execution and observation of grasping in our study (see also Raos et al. 2007). Finally, the bilateral involvement of the lateral PE (corresponding to the forelimb representation in area 5 of the SPL) in both experimental cases indicates that there is relatively smaller bias toward contralateral responses in PE than in SI and PEc, for example, that there are more bilateral visual and/or somatosensory receptive fields in the former than in the latter areas. Indeed, a substantial number of neurons with bilateral RFs on the hand digits have been found clustered adjacent to and/or within the medial bank of IPs (Iwamura et al. 1994) in contrast to the SI and PEc neurons which display mostly contralateral RFs (Nelson et al. 1980; Breveglieri et al. 2006).

In the IPL, the lack of involvement of Opt in reaching-to-grasp execution and the involvement of PF, PFG, and PG contralaterally to the grasping hand are findings compatible with previous reports demonstrating that area Opt receives mainly visual and eye-related input, whereas areas PG and PFG are connected with extrastriate visual, superior parietal somatosensory and premotor areas related to the control of arm movements, and area PF receives input from SI area 2 and projects to PG, PFG, and premotor arm-related areas (Pandya and Seltzer 1982; Petrides and Pandya 1984; Andersen et al. 1990; Rozzi et al. 2005; Gregoriou et al. 2006). The parallel activations measured in the superior and inferior parietal cortical areas during reaching-to-grasp execution in our study complement the recently reported strong similarity of firing patterns between hand manipulation neurons in SPL and IPL (Gardner et al. 2007) and support the suggestion that the former may supply arm movement–related information to the latter parietal areas. In fact, it was recently demonstrated that SPL neurons combining retinal, eye- and arm-movement information displayed discharges which were stronger and earlier than those displayed by IPL neurons processing the same information, and thus it was suggested that SPL can be the source of input signals to IPL (Battaglia-Mayer et al. 2007). Of the inferior parietal cortical areas we examined, only PF was involved in observation of grasping, and it was activated bilaterally. This finding confirms a previous report that PF neurons discharged not only during execution of hand actions but also during the observation of similar actions made by another individual, and therefore were defined as "PF-mirror neurons" in analogy with the F5-mirror neurons with corresponding properties (Gallese et al. 2002). Interestingly, PF neurons' discharge depends on the final goal of the action

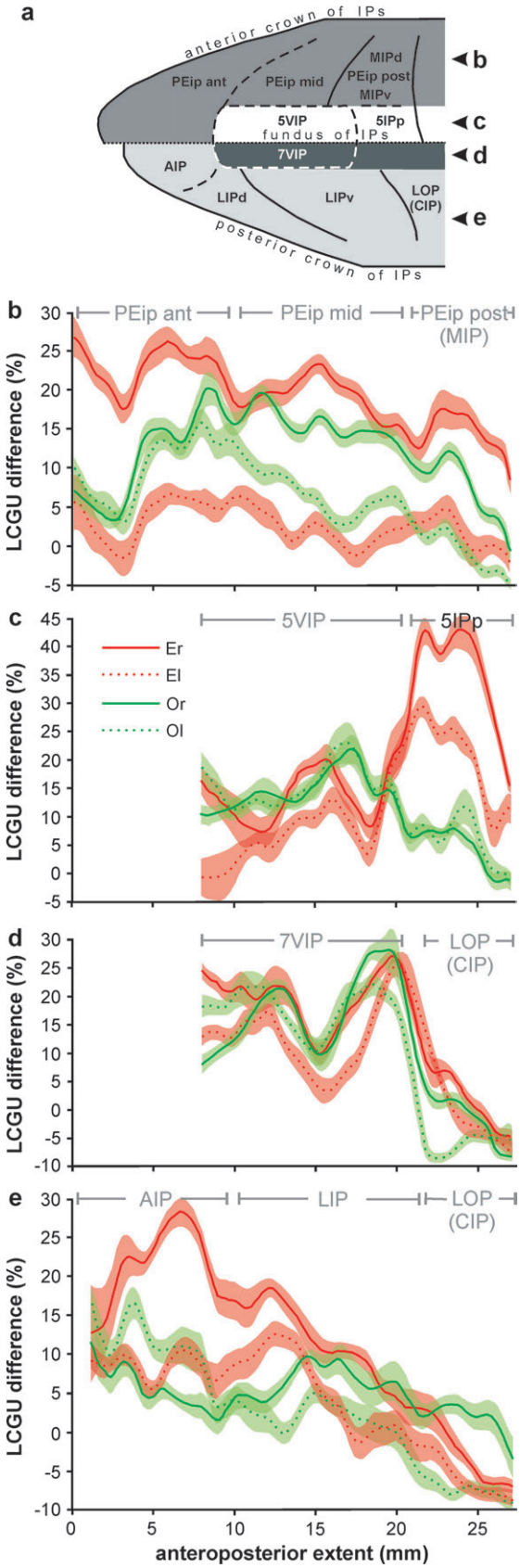

Figure 9. Plots of percent LCGU differences along the rostrocaudal extent of the reconstructed cortex in the IPs. Letters *b–e*, in the IPs drawing of the panel (*a*), label the different parts of cortex (differently shaded ribbons) which are plotted in the (*b–e*) panels, respectively. The different areas corresponding to the various anteroposterior parts of the plots are labeled on top of the graphs in each panel. Red plots illustrate the differences between the 2 execution monkeys and the Cm. Green plots illustrate the differences between the 3 observation monkeys and the Cm. Plots with solid and dotted lines correspond to the right and the left hemispheres, respectively. Red and green shaded areas indicate 95% confidence intervals. Baseline corresponds to 0% LCGU difference from the Cm. For example, the plots in panel b illustrate the detailed spatio-intensive pattern of activation of PEip contralaterally to the moving forelimb in the execution monkeys, the quantitatively less intense activation of PEip in the observation monkeys, and the smaller interhemispheric differences in the effects of the observation as compared with the execution monkeys. Other conventions as in Figure 8.

sequence in which grasping is embedded, thus probably encoding intention of movement (Fogassi et al. 2005). Additionally, in line with our finding that the PF is involved in action observation is the report that lesions of the IPL produced severe and selective impairments in motor imagery, that is, mental simulation of hand and finger movements (Sirigu et al. 1996).

All in all, our results confirm previous imaging studies of lower resolution which have demonstrated that superior and inferior parietal regions are involved in the observation of human actions (Bonda et al. 1996; Grafton et al. 1996; Decety et al. 1997; Grezes et al. 1998; Buccino et al. 2001). Moreover, they demonstrate the precise topography of these regions within the SPL and IPL of primates.

Intraparietal Cortex

The biggest part of the medial (or superior) bank of the IPs, corresponding to area 5, is occupied by area PEa (Pandya and Seltzer 1982) or PEip (Matelli et al. 1998). All the constituents of this area, that is, PEip anterior, PEip middle, and PEip posterior (the latter corresponding to area MIP) were activated in the E monkeys contralaterally to the grasping hand whereas areas 5IPp and 5VIP were bilaterally activated. The same medial intraparietal areas (with the single exception of 5IPp) were also activated in the O monkeys, demonstrating once again that there is an extensive overlap of the action execution and the action observation networks. Interestingly, areas PEip and VIP, herein documented to be involved in both action execution and action observation, are known to include proximal and distal forelimb representations with bimodal neurons characterized by visual receptive fields near the tactile ones (Jones et al. 1978; Colby and Duhamel 1991; Iriki et al. 1996; Duhamel et al. 1998) and to be connected with the premotor cortex (Matelli et al. 1998; Luppino et al. 1999; Lewis and Van Essen 2000a, 2000b; Marconi et al. 2001) which is also involved in execution and observation of grasping (Raos et al. 2007). It should be noted that the 2 activated bands across the anterior and middle portions of area PEip in our reconstructions resemble the distribution of S1-forelimb projections to the medial bank of IPs (Jones et al. 1978) as well as the distribution of the 2 neuronal populations in the PEip sending afferents to the dorsal premotor F2-arm field (Matelli et al. 1998). These bands also resemble the zones activated for arm reaching to visual targets and for memory-guided reaching in the dark, zones which were associated with somatosensory guidance of movement and/or efference copy of motor command (Gregoriou and Savaki 2001). Also, the herein documented involvement of area MIP in execution and observation of reaching-to-grasp is compatible with reports that this area responds to visual and somatosensory stimuli, especially when visual stimuli are within reaching distance of the monkey (Colby and Duhamel

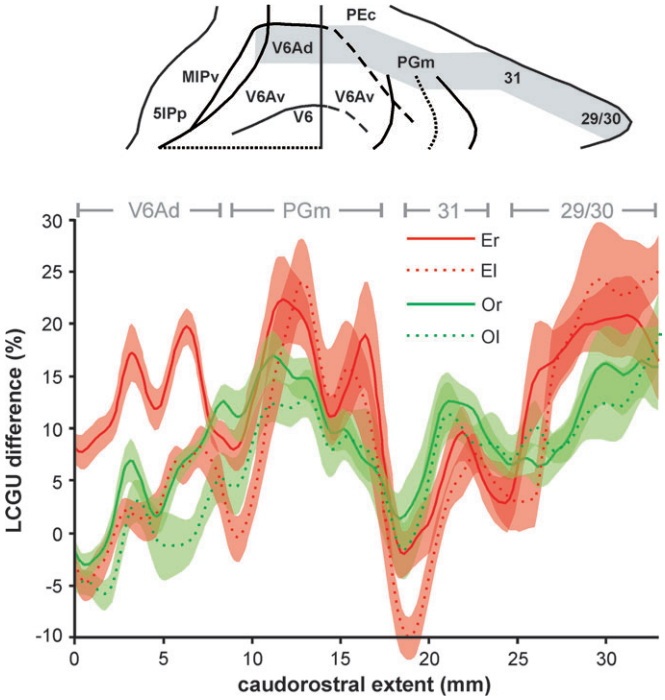

Figure 10. Plots of percent LCGU differences along the reconstructed cortex of the dorsal part of the anterior bank of POs and its adjacent medial parietal cortical field (along the ribbon highlighted in the drawing above the plots) including the dorsal part of V6A, areas PGm/7m, 31 and the retrosplenial cortical areas 29/30. Red plots illustrate the differences between the 2 execution monkeys and the Cm. Green plots illustrate the differences between the 3 observation monkeys and the Cm. Plots with solid and dotted lines correspond to the right and the left hemispheres, respectively. Red and green shaded areas indicate 95% confidence intervals. Baseline corresponds to 0% LCGU difference from the Cm. Zero rostrocaudal extent represents the anterior border of V6Ad. Other conventions as in Figure 8.

1991; Johnson et al. 1996), and receives a motor efference copy generated in relation to the preparation and/or execution of movement (for reviews see Andersen et al. 1997; Colby and Goldberg 1999). In general, the smaller activations that we found in the superior parietal convexity and the bigger and more bilateral activations in the medial bank of the IPs for action observation as compared with action execution are compatible with previous reports demonstrating that more dorsal SPL areas (around the convexity) are associated with movement- and position-related somatosensory activity whereas more ventral parts of the SPL (in the medial bank of the IPs) show more prominent visual activity (Colby and Duhamel 1991; Savaki et al. 1993; Johnson et al. 1996; Kalaska 1996; Graziano et al. 2000; Gregoriou and Savaki 2001). Area 5IPp in the caudalmost part of the medial bank of the IPs adjacent to the fundus, which displayed the strongest activation in the E monkeys and remained unaffected in the O monkeys, has not been previously reported. As explained in the Results section, this area may only partially correspond to the originally described area PIP (Colby et al. 1988) which is considered to be a motion sensitive area (Vanduffel et al. 2001; Durand et al. 2007) integrating shape information by cross-modal (tactile-visual) matching (Saito et al. 2003). Indeed, this cross-modal matching could take place only in the E monkeys.

In the lateral (or inferior) bank of the IPS, areas AIP and 7VIP are involved in both execution and observation of action whereas LIP dorsal is involved only in action execution. The bilateral involvement of area 7VIP in execution and observation of reaching-to-grasp supports our earlier suggestion that this region encodes visual information about the location of stimuli used as targets for motor acts, whatever the effector used (Gregoriou and Savaki 2001). The involvement of area AIP in both execution and observation of reaching-to-grasp is compatible with existing knowledge that its neurons are preferentially activated for various hand configurations during grasping of differently shaped objects (Sakata et al. 1995; Murata et al. 2000), and its pharmacological inactivation disrupts hand preshaping during grasping (Gallese et al. 1994). The AIP is a target of projections from area LOP/CIP (Nakamura et al. 2001) which was inhibited in our study, but it is also connected with area V6Ad (Borra et al. 2008) which was activated for execution, and with areas MIP and F5 (Petrides and Pandya 1984; Matelli et al. 1986; Luppino et al. 1999; Borra et al. 2008) which were activated for both execution and observation. Finally, our results confirm previous findings with imaging methods of lower resolutions, demonstrating that aIPS, the human equivalent of monkey AIP, is recruited on execution of grasping movements (Binkofski et al. 1998; Culham et al. 2003; Shmuelof and Zohary 2006), on an array of grasp observation tasks (Grafton et al. 1996; Hamilton et al. 2006; Shmuelof and Zohary 2006) and even on the perception of scripts of goal-directed hand actions (Bonda et al. 1996). As for area LIP, it is known that its neurons carry saccade-related signals (Gnadt and Andersen 1988; Duhamel et al. 1992) and their discharge is modulated by selective spatial attention (Duhamel et al. 1992; Gottlieb et al. 1998). Our finding that LIP dorsal but not LIP ventral is involved in visually guided reaching-to-grasp movements, is compatible with our recent report that the visual space is represented in LIP dorsal in contrast to the oculomotor space which is mainly represented in LIP ventral (Bakola et al. 2006). Furthermore, the bilateral involvement of 7VIP and 5VIP in action execution and observation complements a previous study demonstrating that there is an arm-reach-associated region which is located in 7VIP and extends to 5VIP (Gregoriou and Savaki 2001).

Our results confirm a recent imaging study of lower resolution, demonstrating that there is considerable overlap between areas activated for execution and observation of reaching movements in the SPL and the intraparietal sulcus in humans, and also that reaching activates these areas more than observation of reaching (Filimon et al. 2007). All existing data considered, the IPs cortex acts as a multifaceted behavioral integrator that binds information related not only to attention, visual and somatosensory space, oculomotor and skeletomotor activity but also to action recognition, thus operating at the interface of perception, action, and cognition.

Medial Parietal and Parietoccipital Cortex

The herein documented involvement of the visual area V6 in execution and observation of visually guided reaching-to-grasp movements is compatible with the knowledge that this area receives form- and motion-related visual inputs from the striate cortex and several extrastriate areas, and sends projections to arm-related areas such as MIP and V6A, as well as to areas encoding the spatial location of objects to be grasped such as VIP and V6A (Colby and Duhamel 1991; Duhamel et al. 1997; Galletti et al. 2001; Galletti et al. 2003). According to the retinotopic organization of its visual input, the peripheral field of V6 is represented medially and the central one laterally

(Galletti, Fattori, Gamberini, et al. 1999). Our finding that portions of both these fields of V6 are involved in reaching-to-grasp indicates that the monkeys were attending their arm approaching from the visual periphery to the center while fixating the object straight ahead. Interestingly, direction-selective (Galletti et al. 1996) and "real-motion" (Galletti and Fattori 2003) cells have been demonstrated in area V6. The dorsal part of the bimodal (visual/somatosensory) area V6A, herein found to be implicated in reaching-to-grasp execution, is known to contain more arm-related cells than its ventral counterpart (Fattori et al. 1999) which is not affected in our study. In fact, cells in V6A-dorsal modulate their activity during reaching to (Fattori et al. 2001, 2005) and grasping of (Fattori et al. 2004) objects in the peripersonal space. These cells are known to project to the dorsal premotor areas F2 and F7 (Matelli et al. 1998; Shipp et al. 1998; Marconi et al. 2001) and are thought to interact continuously with the premotor cortex in order to guide "on-line" the ongoing arm movement (Galletti et al. 2003).

In contrast to area V6A-dorsal involved only in execution, area PGm/7m which is the alternative visuomotor relay station receiving visual input and projecting to the dorsal premotor cortex (Petrides and Pandya 1984; Cavada and Goldman-Rakic 1989a, 1989b; Johnson et al. 1996; Matelli et al. 1998) was involved not only in the execution but also in the observation of reaching-to-grasp. Our results are in agreement with previous reports demonstrating that cell activity in PGm/7m relates to a combination of visuomanual and oculomotor information supposedly leading from target localization to movement generation (Ferraina, Johnson, et al. 1997), with the composition of motor commands based on kinesthetic and visual control signals (Ferraina, Garasto, et al. 1997). Also, our results support a previous imaging study demonstrating that execution and observation of action involve an area between the POs and the posterior end of the cingulate sulcus (Binkofski et al. 1999), which apparently corresponds to PGm/7m. Of interest is that area F7, which receives the main parietal input from PGm/7m, as well as other major projecting areas of PGm/7m such as the supplementary somatosensory area, the cingulate cortex, area VIP and the retrosplenial cortex (Petrides and Pandya 1984; Cavada and Goldman-Rakic 1989a, 1989b; Johnson et al. 1996; Matelli et al. 1998) are involved not only in execution but also in observation of reaching-to-grasp movements (see also Raos et al. 2007).

The bilateral involvement of the retrosplenial cortical areas 29 and 30 in both execution and observation of reaching-to-grasp is compatible with the suggestions that this region processes aspects of working memory (Petrides et al. 1993; Petrides 1995; Morris et al. 1999; Kobayashi and Amaral 2003) and is involved in the perception of visual objects associated with a specific context (Bar and Aminoff 2003). The bilateral involvement of area 31 in observation, is compatible with reports associating it with occulomotor activity in the service of the spatial analysis of visual input (Olson et al. 1996) and the motivational salience of visual and occulomotor events for orienting attention (Dean et al. 2004).

Mental Simulation of Action and Action Attribution

The overall finding that observing an action excites very similar parietal circuits used to execute that same action supports our earlier suggestion that observation of an action corresponds to simulation of its overt counterpart (Raos et al. 2007). Accordingly, to understand the action of another person the observer executes it "mentally." More specifically, the herein documented fact that the neural correlates of the action observation-driven system in the parietal cortex extend well beyond area PF where mirror neurons were found (Gallese et al. 2002), same way as those in the frontal cortex extend well beyond the F5-convexity (Raos et al. 2007) where the mirror neurons were originally discovered (Gallese et al. 1996; Rizzolatti et al. 1996), challenges the "mirror-neuron system" concept and supports the suggestion that a broader process such as "mental simulation of action" is responsible for action recognition (Goldman and Sebanz 2005). Hence, the present and our previous results (Raos et al. 2007) support the "mental simulation theory" which assigns the role of understanding others' actions to the entire distributed neural network responsible for the execution of actions, and not the concept of "mirroring" which reflects the function of a certain class of cells in premotor area F5 and parietal area PF.

A reasonable question is how we distinguish between the observer and the actor if we simulate the action when we observe it by recruiting the same circuits which are responsible for execution of the act. In a previous study, we argued that the attribution of an action to an agent is a function distributed within the action execution network rather than a function assigned to one or 2 areas on the side of this pathway. We also discussed, based on our results, how the primary motor and somatosensory, the premotor and supplementary somatosensory areas may contribute to the attribution of action to the other agent during action observation and to the self during action execution (Raos et al. 2007). In the parietal cortex, areas PG/PFG, LIPd, 5Ipp, and V6Ad which are involved only in action execution and not in action observation, as well as area 31 which is involved in observation but and not in execution, may contribute in attributing the action to the self and to the other agent, respectively. Moreover, the parietal activations induced by action observation were in general weaker than those induced by action execution, suggesting a possible subthreshold activation of the action execution circuits during action observation. Also, the effects induced by action observation displayed smaller interhemispheric differences (indicative of visual rather than hand identity specificity) as compared with those induced by action execution which were mostly contralateral to the moving forelimb (preserving hand identity specificity). These differential activations of parietal cortical areas could also play a role in attributing the action to the correct agent.

For example, in the forelimb-related areas of the parietal cortex, the higher level of activity for action execution may reflect the anticipated sensory consequence of the movement (based on efference copy of the motor command) and the actual afferent feedback (signal from the muscles), whereas the lower activity for action observation may reflect the anticipated consequence of the movement only. This interpretation of our results is compatible with previous suggestions such as that prediction (or anticipation) may turn motor commands into expected sensory consequences (Kilner et al. 2004, 2007), that prediction of the sensory consequences of an act may underlie our ability to distinguish between self-produced and externally generated actions (Blakemore and Frith 2003), and that the experience of ourselves or others as the cause of an action may be based on comparison of motor commands with the afferent feedback from the moving muscles and the external events

caused by these commands (Johnson and Haggard 2005), with the temporal attraction between self-produced actions and their sensory consequences binding them together and thus enhancing the experience of agency (Haggard et al. 2002).

There are several reports attributing to the parietal cortex a role in detecting conflicts between visual and somatomotor signals of motor acts (Fink et al. 1999; Farrer et al. 2003; Costantini et al. 2005), a role in action attribution (awareness of one's own movements versus movements of another agents) (Sirigu et al. 1999; Blakemore et al. 2003; Sirigu et al. 2004), and even more specifically assigning to the inferior parietal lobe and the intraparietal sulcus a role in the attribution of actions to external agents (Ruby and Decety 2001; Decety et al. 2002; Farrer and Frith 2002). However, our findings suggest that the parietal cortical areas associated with attribution of action in the above mentioned studies constitute central components of the execution/perception distributed network rather than extra machinery functioning on the side of this net.

In conclusion and all our results considered, observation of an action performed by another subject reflects the effects of our previous knowledge about the act and its predicted sensory consequences. During action observation, internally simulated experience of the specific movements recruits numerous parietofrontal sensory–motor cortical regions, mostly the same ones which are responsible for the execution of the same action. In addition, the parietal execution/perception system participates in the process of attribution of the action to the correct agent by integrating visual and effector-related somatosensory–motor inputs and thus by creating a coherent representation of the bodily self.

Funding

Greek Secretariat of Research and Technology (PENED grant 01ED111) supported Mina Evangeliou; and European Union (FP6 grant IST-027574).

Notes

We thank Helen Barbas, Michela Gamberini, Georgia Gregoriou, and Maya Medalla for advice and help regarding histology and Maria Kefaloyianni for help with the autoradiographic imaging. *Conflict of Interest:* None declared.

[AQ1] Address correspondence to Helen E. Savaki, Department of Basic Sciences, Faculty of Medicine, School of Health Sciences, University of Crete, P.O. Box 2208, GR-71003, Iraklion, Crete, Greece. Email: savaki@med.uoc.gr.

References

Andersen RA. 1989. Visual and eye movement functions of the posterior parietal cortex. Annu Rev Neurosci. 12:377–403.

Andersen RA, Asanuma C, Essick G, Siegel RM. 1990. Corticocortical connections of anatomically and physiologically defined subdivisions within the inferior parietal lobule. J Comp Neurol. 296:65–113.

Andersen RA, Snyder LH, Bradley DC, Xing J. 1997. Multimodal representation of space in the posterior parietal cortex and its use in planning movements. Annu Rev Neurosci. 20:303–330.

Ashe J, Georgopoulos AP. 1994. Movement parameters and neural activity in motor cortex and area 5. Cereb Cortex. 4:590–600.

Avikainen S, Forss N, Hari R. 2002. Modulated activation of the human SI and SII cortices during observation of hand actions. Neuroimage. 15:640–646.

Bakola S, Gregoriou GG, Moschovakis AK, Savaki HE. 2006. Functional imaging of the intraparietal cortex during saccades to visual and memorized targets. Neuroimage. 31:1637–1649.

Bar M, Aminoff E. 2003. Cortical analysis of visual context. Neuron. 38:347–358.

Battaglia-Mayer A, Mascaro M, Caminiti R. 2007. Temporal evolution and strength of neural activity in parietal cortex during eye and hand movements. Cereb Cortex. 17:1350–1363.

Binkofski F, Buccino G, Posse S, Seitz RJ, Rizzolatti G, Freund H. 1999. A fronto-parietal circuit for object manipulation in man: evidence from an fMRI-study. Eur J Neurosci. 11:3276–3286.

Binkofski F, Dohle C, Posse S, Stephan KM, Hefter H, Seitz RJ, Freund HJ. 1998. Human anterior intraparietal area subserves prehension: a combined lesion and functional MRI activation study. Neurology. 50:1253–1259.

Blakemore SJ, Frith C. 2003. Self-awareness and action. Curr Opin Neurobiol. 13:219–224.

Blakemore SJ, Oakley DA, Frith CD. 2003. Delusions of alien control in the normal brain. Neuropsychologia. 41:1058–1067.

Bonda E, Petrides M, Ostry D, Evans A. 1996. Specific involvement of human parietal systems and the amygdala in the perception of biological motion. J Neurosci. 16:3737–3744.

Borra E, Belmalih A, Calzavara R, Gerbella M, Murata A, Rozzi S, Luppino G. 2008. Cortical connections of the macaque anterior intraparietal (AIP) area. Cereb Cortex. 18:1094–1111.

Breveglieri R, Galletti C, Gamberini M, Passarelli L, Fattori P. 2006. Somatosensory cells in area PEc of macaque posterior parietal cortex. J Neurosci. 26:3679–3684.

Buccino G, Binkofski F, Fink GR, Fadiga L, Fogassi L, Gallese V, Seitz RJ, Zilles K, Rizzolatti G, Freund HJ. 2001. Action observation activates premotor and parietal areas in a somatotopic manner: an fMRI study. Eur J Neurosci. 13:400–404.

Caminiti R, Ferraina S, Johnson PB. 1996. The sources of visual information to the primate frontal lobe: a novel role for the superior parietal lobule. Cereb Cortex. 6:319–328.

Cavada C, Goldman-Rakic PS. 1989a. Posterior parietal cortex in rhesus monkey: I. Parcellation of areas based on distinctive limbic and sensory corticocortical connections. J Comp Neurol. 287:393–421.

Cavada C, Goldman-Rakic PS. 1989b. Posterior parietal cortex in rhesus monkey: II. Evidence for segregated corticocortical networks linking sensory and limbic areas with the frontal lobe. J Comp Neurol. 287:422–445.

Chua R, Carson RG, Goodman D, Elliot D. 1992. Asymmetries in the spatial localization of transformed targets. Brain Cogn. 20:227–235.

Colby CL, Duhamel JR. 1991. Heterogeneity of extrastriate visual areas and multiple parietal areas in the macaque monkey. Neuropsychologia. 23:517–537.

Colby CL, Duhamel J-R, Goldberg ME. 1993. Ventral intraparietal area of the macaque: anatomic location and visual response properties. J Neurophysiol. 69:902–914.

Colby CL, Gattass R, Olson CR, Gross CG. 1988. Topographical organization of cortical afferents to extrastriate visual area PO in the macaque: a dual tracer study. J Comp Neurol. 269:392–413.

Colby CL, Goldberg ME. 1999. Space and attention in parietal cortex. Annu Rev Neurosci. 22:319–349.

Costantini M, Galati G, Ferretti A, Caulo M, Tartaro A, Romani GL, Aglioti SM. 2005. Neural systems underlying observation of humanly impossible movements: an fMRI study. Cereb Cortex. 15:1761–1767.

Culham JC, Danckert SL, DeSouza JF, Gati JS, Menon RS, Goodale MA. 2003. Visually guided grasping produces fMRI activation in dorsal but not ventral stream brain areas. Exp Brain Res. 153:180–189.

Dalezios Y, Raos VC, Savaki HE. 1996. Metabolic activity pattern in the motor and somatosensory cortex of monkeys performing a visually guided reaching task with one forelimb. Neuroscience. 72:325–333.

Dean HL, Crowley JC, Platt ML. 2004. Visual and saccade-related activity in macaque posterior cingulate cortex. J Neurophysiol. 92:3056–3068.

Decety J. 1996. Do imagined and executed actions share the same neural substrate? Brain Res Cogn Brain Res. 3:87–93.

Decety J, Chaminade T, Grezes J, Meltzoff AN. 2002. A PET exploration of the neural mechanisms involved in reciprocal imitation. Neuroimage. 15:265–272.

Decety J, Grezes J, Costes N, Perani D, Jeannerod M, Procyk E, Grassi F, Fazio F. 1997. Brain activity during observation of actions. Influence of action content and subject's strategy. Brain. 120:1763–1777.

Duhamel J-R, Bremmer F, SB, Graf W. 1997. Spatial invariance of visual receptive fields in parietal cortex neurons. Nature. 389:845–847.

Duhamel J-R, Colby CL, Goldberg ME. 1992. The updating of the representation of visual space in parietal cortex by intended eye movements. Science. 255:90–92.
Duhamel J-R, Colby CL, Goldberg ME. 1998. Ventral intraparietal area of the macaque: congruent visual and somatic response properties. J Neurophysiol. 79:126–136.
Durand JB, Nelissen K, Joly O, Wardak C, Todd JT, Norman JF, Janssen P, Vanduffel W, Orban GA. 2007. Anterior regions of monkey parietal cortex process visual 3D shape. Neuron. 55:493–505.
Farrer C, Franck N, Georgieff N, Frith CD, Decety J, Jeannerod M. 2003. Modulating the experience of agency: a positron emission tomography study. Neuroimage. 18:324–333.
Farrer C, Frith CD. 2002. Experiencing oneself vs another person as being the cause of an action: the neural correlates of the experience of agency. Neuroimage. 15:596–603.
Fattori P, Breveglieri R, Amoroso K, Galletti C. 2004. Evidence for both reaching and grasping activity in the medial parieto-occipital cortex of the macaque. Eur J Neurosci. 20:2457–2466.
Fattori P, Gamberini M, Kutz DF, Galletti C. 2001. 'Arm-reaching' neurons in the parietal area V6A of the macaque monkey. Eur J Neurosci. 13:2309–2313.
Fattori P, Gamberini M, Mussio A, Breveglieri R, Kutz DF, Galletti C. 1999. A visual-to-motor gradient within area V6A of the monkey parieto-occipital cortex. Neurosci Lett Suppl. 52:S22.
Fattori P, Kutz DF, Breveglieri R, Marzocchi N, Galletti C. 2005. Spatial tuning of reaching activity in the medial parieto-occipital cortex (area V6A) of macaque monkey. Eur J Neurosci. 22:956–972.
Ferraina S, Garasto MR, Battaglia-Mayer A, Ferraresi P, Johnson PB, Lacquaniti F, Caminiti R. 1997. Visual control of hand-reaching movement: activity in parietal area 7m. Eur J Neurosci. 9:1091–1095.
Ferraina S, Johnson PB, Garasto MR, Battaglia-Mayer A, Ercolani L, Bianchi L, Lacquaniti F, Caminiti R. 1997. Combination of hand and gaze signals during reaching: activity in parietal area 7m of the monkey. J Neurophysiol. 77:1034–1038.
Filimon F, Nelson JD, Hagler DJ, Sereno MI. 2007. Human cortical representations for reaching: mirror neurons for execution, observation, and imagery. Neuroimage. 37:1315–1328.
Fink GR, Marshall JC, Halligan PW, Frith CD, Driver J, Frackowiak RSJ, Dolan RJ. 1999. The neural consequences of conflict between intention and the senses. Brain. 122:497–512.
Fogassi L, Ferrari PF, Gesierich B, Rozzi S, Chersi F, Rizzolatti G. 2005. Parietal lobe: from action organization to intention understanding. Science. 308:662–667.
Gallese V, Fadiga L, Fogassi L, Rizzolatti G. 1996. Action recognition in the premotor cortex. Brain. 119:593–609.
Gallese V, Fadiga L, Fogassi L, Rizzolatti G. 2002. Action representation and the inferior parietal lobe. In: Prinz W, Hommel B, editors. Common mechanisms in perception and action: attention and performance. Oxford: Oxford University Press. p. 334–355.
Gallese V, Murata A, Kaseda M, Niki N, Sakata H. 1994. Deficit of hand preshaping after muscimol injection in monkey parietal cortex. Neuroreport. 5:1525–1529.
Galletti C, Fattori P. 2003. Neuronal mechanisms for detection of motion in the field of view. Neuropsychologia. 41:1717–1727.
Galletti C, Fattori P, Battaglini PP, Shipp S, Zeki S. 1996. Functional demarcation of a border between areas V6 and V6A in the superior parietal gyrus of the macaque monkey. Eur J Neurosci. 8:30–52.
Galletti C, Fattori P, Gamberini M, Kutz DF. 1999. The cortical visual area V6: brain location and visual topography. Eur J Neurosci. 11:3922–3936.
Galletti C, Fattori P, Kutz DF, Gamberini M. 1999. Brain location and visual topography of cortical area V6A in the macaque monkey. Eur J Neurosci. 11:575–582.
Galletti C, Gamberini M, Kutz DF, Fattori P, Luppino G, Matelli M. 2001. The cortical connections of area V6: occipito- parietal network processing visual information. Eur J Neurosci. 13:1–18.
Galletti C, Kutz DF, Gamberini M, Breveglieri R, Fattori P. 2003. Role of the medial parieto-occipital cortex in the control of reaching and grasping movements. Exp Brain Res. 153:158–170.
Gardner EP, Babu KS, Reitzen SD, Ghosh S, Brown AS, Chen J, Hall AL, Herzlinger MD, Kohlenstein JB, Ro JY. 2007. Neurophysiology of prehension. I. Posterior parietal cortex and object-oriented hand behaviors. J Neurophysiol. 97:387–406.
Gnadt JW, Andersen RA. 1988. Memory related motor planning activity in posterior parietal cortex of macaque. Exp Brain Res. 70:216–220.
Goldman AI, Sebanz N. 2005. Simulation, mirroring, and a different argument from error. Trends Cogn Sci. 9:320.
Gottlieb JP, Kusunoki M, Goldberg ME. 1998. The representation of visual salience in monkey parietal cortex. Nature. 391:481–484.
Grafton ST, Arbib MA, Fadiga L, Rizzolatti G. 1996. Localization of grasp representations in humans by positron emission tomography. 2. Observation compared with imagination. Exp Brain Res. 112:103–111.
Graziano MSA, Cooke DF, Taylor CSR. 2000. Coding the location of the arm by sight. Science. 290:1782–1786.
Gregoriou GG, Borra E, Matelli M, Luppino G. 2006. Architectonic organization of the inferior parietal convexity of the macaque monkey. J Comp Neurol. 496:422–451.
Gregoriou GG, Luppino G, Matelli M, Savaki HE. 2005. Frontal cortical areas of the monkey brain engaged in reaching behavior: a (14)C-deoxyglucose imaging study. Neuroimage. 27:442–464.
Gregoriou GG, Savaki HE. 2001. The intraparietal cortex: subregions involved in fixation, saccades, and in the visual and somatosensory guidance of reaching. J Cereb Blood Flow Metab. 21:671–682.
Gregoriou GG, Savaki HE. 2003. When vision guides movement: a functional imaging study of the monkey brain. Neuroimage. 19:959–967.
Grezes J, Costes N, Decety J. 1998. Top-down effect of strategy on the perception of human biological motion: a PET investigation. Cogn Neuropsychol. 15:553–582.
Haggard P, Clark S, Kalogeras J. 2002. Voluntary action and conscious awareness. Nat Neurosci. 5:382–385.
Hamilton AF, Wolpert DM, Frith U, Grafton ST. 2006. Where does your own action influence your perception of another person's action in the brain? Neuroimage. 29:524–535.
Iriki A, Tanaka M, Iwamura Y. 1996. Coding of modified body schema during tool use by macaque postcentral neurons. Neuroreport. 7:2325–2330.
Iwamura Y, Iriki A, Tanaka M. 1994. Bilateral hand representation in the postcentral somatosensory cortex. Nature. 369:546–554.
Johnson H, Haggard P. 2005. Motor awareness without perceptual awareness. Neuropsychologia. 43:227–237.
Johnson PB, Ferraina S, Bianchi L, Caminiti R. 1996. Cortical networks for visual reaching: Physiological and anatomical organization of frontal and parietal lobe arm regions. Cereb Cortex. 6:102–119.
Jones EG, Coulter JD, Hendry HC. 1978. Intracortical connectivity of architectonic fields in the somatic sensory, motor and parietal cortex of monkeys. J Comp Neurol. 181:291–348.
Kalaska JF. 1996. Parietal cortex area 5 and visuomotor behavior. Can J Physiol Pharmacol. 74:483–498.
Kalaska JF, Cohen DAD, Prud'homme M, Hyde ML. 1990. Parietal area 5 neuronal activity encodes movement kinematics, not movement dynamics. Exp Brain Res. 80:351–364.
Kennedy C, Sakurada O, Shinohara M, Jehle J, Sokoloff L. 1978. Local cerebral glucose utilization in the normal conscious macaque monkey. Ann Neurol. 4:293–301.
Kilner JM, Friston KJ, Frith CD. 2007. The mirror-neuron system: a Bayesian perspective. Neuroreport. 18:619–623.
Kilner JM, Vargas C, Duval S, Blakemore SJ, Sirigu A. 2004. Motor activation prior to observation of a predicted movement. Nat Neurosci. 7:1299–1301.
Kobayashi Y, Amaral DG. 2003. Macaque monkey retrosplenial cortex: II. Cortical afferents. J Comp Neurol. 466:48–79.
Lewis JW, Van Essen DC. 2000a. Corticocortical connections of visual, sensorimotor, and multimodal processing area in the parietal lobe of the macaque monkey. J Comp Neurol. 428:112–137.
Lewis JW, Van Essen DC. 2000b. Mapping of architectonic subdivisions in the macaque monkey, with emphasis on parieto-occipital cortex. J Comp Neurol. 428:79–111.
Luppino G, Hamed SB, Gamberini M, Matelli M, Galletti C. 2005. Occipital (V6) and parietal (V6A) areas in the anterior wall of the parieto-occipital sulcus of the macaque: a cytoarchitectonic study. Eur J Neurosci. 21:3056–3076.

Luppino G, Murata A, Govoni P, Matelli M. 1999. Largely segregated parietofrontal connections linking rostral intraparietal cortex (areas AIP and VIP) and the ventral premotor cortex (areas F5 and F4). Exp Brain Res. 128:181–187.

Marconi B, Genovesio A, Battaglia-Mayer A, Ferraina S, Squatrito S, Molinari M, Laquaniti F, Caminiti R. 2001. Eye-hand coordination during reaching. I. Anatomical relationships between parietal and frontal cortex. Cereb Cortex. 11:513–527.

Matelli M, Camarda R, Glickstein M, Rizzolatti G. 1986. Afferent and efferent projections of the inferior area 6 in the macaque monkey. J Comp Neurol. 251:281–298.

Matelli M, Govoni P, Galletti C, Kutz DF, Luppino G. 1998. Superior area 6 afferents from the superior parietal lobule in the macaque monkey. J Comp Neurol. 402:327–352.

Medalla M, Barbas H. 2006. Diversity of laminar connections linking periarcuate and lateral intraparietal areas depends on cortical structure. Eur J Neurosci. 23:161–179.

Morecraft RJ, Cipolloni PB, Stilwell-Morecraft KS, Gedney MT, Pandya DN. 2004. Cytoarchitecture and cortical connections of the posterior cingulate and adjacent somatosensory fields in the rhesus monkey. J Comp Neurol. 469:37–69.

Morris R, Petrides M, Pandya DN. 1999. Architecture and connections of retrosplenial area 30 in the rhesus monkey (Macaca mulatta). Eur J Neurosci. 11:2506–2518.

Mountcastle VB, Lynch JC, Georgopoulos AP, Sakata H, Acuna C. 1975. Posterior parietal association cortex of the monkey: command function for operations within extrapersonal space. J Neurophysiol. 38:871–908.

Murata A, Gallese V, Luppino G, Kaseda M, Sakata H. 2000. Selectivity for the shape, size, and orientation of objects for grasping in neurons of monkey parietal area AIP. J Neurophysiol. 83:2580–2601.

Nakamura H, Kuroba T, Wakita M, Kusunoki M, Kato A, Mikami A, Sakata H, Itoh K. 2001. From three-dimensional space vision to prehensile hand movements: the lateral intraparietal area links the area V3A and the anterior intraparietal area in macaques. J Neurosci. 21:8174–8187.

Nelson RJ, Sur M, Fellman DJ, Kaas JH. 1980. Representations of the body surface in postcentral parietal cortex of *Macaca fascicularis*. J Comp Neurol. 192:611–643.

Olson CR, Musil SY, Goldberg ME. 1996. Single neurons in posterior cingulate cortex of behaving macaque: eye movement signals. J Neurophysiol. 76:3285–3300.

Pandya DN, Seltzer B. 1982. Intrinsic connections and architectonics of posterior parietal cortex in the rhesus monkey. J Comp Neurol. 204:196–210.

Pearson RCA, Powell TPS. 1985. The projection of the primary somatic sensory cortex upon area 5 in the monkey. Brain Res Rev. 9:89–107.

Petrides M. 1995. Impairments on nonspatial self-ordered working memory tasks after lesions of the mid-dorsal part of the lateral frontal cortex in the monkey. J Neurosci. 15:359–375.

Petrides M, Alivisatos B, Evans AC, Meyer E. 1993. Dissociation of human mid-dorsolateral from posterior dorsolateral frontal cortex in memory processing. Proc Natl Acad Sci USA. 90:873–877.

Petrides M, Pandya DN. 1984. Projections to the frontal cortex from the posterior parietal region in the rhesus monkey. J Comp Neurol. 228:105–116.

Pons TP, Garraghty PE, Cusick CG, Kaas JH. 1985. The somatotopic organization of area 2 in macaque monkeys. J Comp Neurol. 241:445–466.

Raos V, Evangeliou MN, Savaki HE. 2004. Observation of action: grasping with the mind's hand. Neuroimage. 23:193–201.

Raos V, Evangeliou MN, Savaki HE. 2007. Mental simulation of action in the service of action perception. J Neurosci. 27:12675–12683.

Rizzolatti G, Fadiga L, Gallese V, Fogassi L. 1996. Premotor cortex and the recognition of motor actions. Cogn Brain Res. 3:131–141.

Rozzi S, Calzavara R, Belmalih A, Borra E, Gregoriou GG, Matelli M, Luppino G. 2005. Cortical connections of the inferior parietal cortical convexity of the macaque monkey. Cereb Cortex. 16:1389–1417.

Ruby P, Decety J. 2001. Effect of subjective perspective taking during simulation of action: a PET investigation of agency. Nat Neurosci. 4:546–550.

Saito DN, Okada T, Morita Y, Yonekura Y, Sadato N. 2003. Tactile-visual cross-modal shape matching: a functional MRI study. Brain Res Cogn Brain Res. 17:14–25.

Sakata H, Taira M, Murata A, Mine S. 1995. Neural mechanisms of visual guidance of hand action in the parietal cortex of the monkey. Cereb Cortex. 5:429–438.

Savaki HE, Dalezios Y. 1999. ^{14}C-Deoxyglucose mapping of the monkey brain during reaching to visual targets. Prog Neurobiol. 58:479–540.

Savaki HE, Kennedy C, Sokoloff L, Mishkin M. 1993. Visually guided reaching with the forelimb contralateral to a "blind" hemisphere: a metabolic mapping study in monkeys. J Neurosci. 13:2772–2789.

Savaki HE, Raos VC, Dalezios Y. 1997. Spatial cortical patterns of metabolic activity in monkeys performing a visually guided reaching task with one forelimb. Neuroscience. 76:1007–1034.

Shipp S, Blanton M, Zeki S. 1998. A visuo-somatomotor pathway through superior parietal cortex in the macaque monkey: cortical connections of areas V6 and V6A. Eur J Neurosci. 10:3171–3193.

Shmuelof L, Zohary E. 2006. A mirror representation of others' actions in the human anterior parietal cortex. J Neurosci. 26:9736–9742.

Sirigu A, Daprati E, Ciancia S, Giraux P, Nighoghossian N, Posada A, Haggard P. 2004. Altered awareness of voluntary action after damage to the parietal cortex. Nat Neurosci. 7:80–84.

Sirigu A, Daprati E, Pradat-Diehl P, Franck N, Jeannerod M. 1999. Perception of self-generated movement following left parietal lesion. Brain. 122(Pt 10):1867–1874.

Sirigu A, Duhamel JR, Cohen L, Pillon B, Dubois B, Agid Y. 1996. The mental representation of hand movements after parietal cortex damage. Science. 273:1564–1568.

Sokoloff L, Reivich M, Kennedy C, Des Rosiers MH, Patlak CS, Pettigrew KS, Sakurada O, Shinohara M. 1977. The [^{14}C]-deoxyglucose method for the measurement of local cerebral glucose utilization: theory, procedure, and normal values in the conscious and anesthetized albino rat. J Neurochem. 28:879–916.

Tsutsui K, Jiang M, Sakata H, Taira M. 2003. Short-term memory and perceptual decision for three-dimensional visual features in the caudal intraparietal sulcus (area CIP). J Neurosci. 23:5486–5495.

Vanduffel W, Fize D, Mandeville JB, Nelissen K, Van Hecke P, Rosen BR, Tootell RB, Orban GA. 2001. Visual motion processing investigated using contrast agent-enhanced fMRI in awake behaving monkeys. Neuron. 32:565–577.